Abstract of the thesis titled

'NOISE ASSISTED PHENOMENA IN PHYSICAL SYSTEMS'

BY

SHANTU SAIKIA

DEPARTMENT OF PHYSICS,

NORTH-EASTERN HILL UNIVERSITY,

SHILLONG

Submitted in partial fulfillment of the requirement of the degree of Doctor of Philosophy in Physics of North-Eastern Hill University, Shillong.

Physics

Noise or fluctuations i.e. the minute and random variations in temperature to which any physical or biological system at a finite temperature are subjected to, are present in almost all systems. These fluctuations play a non negligible role in determining the system behaviour particularly in systems in the microscopic domain.

Though conventionally the presence of noise was always considered to be destructive and unwanted, many systems have now been discovered, where these random fluctuations play a counterintuitive and constructive role. Several noise-induced or noise-assisted non-equilibrium phenomena have been discovered in biological and physical systems. For example ratchet effect, Stochastic Resonance, resonant activation, noise-induced stability of states, noise-induced transitions etc. In the work presented in this thesis, we focus primarily on the phenomenon of ratchet effect and Stochastic Resonance.

Ratchet effect is the phenomenon in which a net unidirectional motion of particles in periodic potentials is obtained in the presence of noise (fluctuations), however, without the presence of any obvious external bias. Though the primary motivation for the study of ratchets was to understand the working of naturally occurring molecular motors (biological motors like motor protein kinesin etc.), the field of noise assisted transport have gone far beyond the biological domain leading to possible technological applications like particle separation techniques, designing of nano devices etc. We study various aspects of particle transport in a model inhomogeneous inertial ratchet having a symmetric and periodic potential with a space dependent friction coefficient which is similarly periodic, but has a phase difference with the potential.

The term Stochastic Resonance (SR) refers to a phenomenon of enhanced periodic response of a system to an external periodic drive in the presence of noise or fluctuations. The system shows an optimal response as a function of noise strength. Though primarily thought of as a phenomena exhibited by bistable systems, SR has also been proved to be there in monostable as well as multistate systems. The phenomenon has been experimentally verified in electronic circuits,

neuronal systems, nanomechanical devices etc. The main utility of SR is that it can be used to select and enhance a signal of a particular frequency out of a host of signals by tuning the noise strength. Different quantifiers for SR like signal to noise ratio, hysteresis loop area, input energy, area under the first peak in the residence time distribution etc. have been used as regards to its validity as a bonafide resonance. In our work, we study the phenomenon of SR in a bistable system and also in periodic potential system using input energy and hysteresis loop area as quantifiers.

The work presented in the thesis is organized in seven chapters.

Chapter I is the introduction where we give an introduction to the basic aspects of our work, the motivation behind it and also a brief layout of the thesis and its contribution.

In Chapter II, we present the results of our studies on deterministic dynamics of a periodically driven particle in the underdamped case in a spatially symmetric periodic potential. The system is subjected to a space dependent friction coefficient, which is similarly periodic as the potential but with a phase difference. We observe that frictional inhomogeneity in a symmetric periodic potential mimics most of the qualitative features of deterministic dynamics in a homogeneous system with an asymmetric periodic potential. We point out the need for averaging over the initial phase of the external drive at small frictional inhomogeneity parameter values or analogously low potential asymmetry regimes in obtaining ratchet current. We also show that at low amplitudes of drive, where ratchet current is not possible in the deterministic case, noise plays a significant role in realizing ratchet current.

In Chapter III we present the results of our work on ratchet effect in a square-wave driven inertial periodic potential system. We study the underdamped particle motion in a symmetric periodic potential and subjected to a periodic square wave forcing with zero mean, in the presence of random fluctuations. We show that the particle acquires a steady state mean velocity at asymptotically large timescales. This particle current is obtained just by exploiting the frictional inhomogeneity of the medium. We also study the dependence of the ratchet current on the various

parameters of the system like the amplitude of driving, the frequency of driving, phase difference of the friction coefficient with the potential etc. The current is found to have a peaking behaviour both with the amplitude and frequency of drive. The steady state diffusion coefficient is interestingly found to peak at exactly the same amplitude at which the ratchet current peaks. This means that the particle motion is highly diffusive in the amplitude regime at which the current peaks. We characterize the ratchet performance by calculating its efficiency, Peclet number etc. We show that the performance of the ratchet can be optimized by a proper choice of the different parameters.

In Chapter IV we present the results of our study on an interesting aspect of underdamped particle transport in a square wave driven periodic potential system. Underdamped particle transport in tilted periodic potential systems was earlier shown to exhibit dispersionless motion in intermediate time regimes. This is a counterintuitive result as the particles show coherent motion even in the presence of fluctuations. We show that using a square-wave drive of proper amplitude and frequency, instead of a constant tilt, as was done in an earlier work, coherent motion can be obtained repeatedly. Thus, the cumulative duration of coherent motion of the particles can be prolonged. Also, we show that by taking an appropriate combination of periods of the external field, one can postpone the beginning of coherent motion and can even have coherent motion at a lower value of position dispersion than in the constant tilt case. The inhomogeneous inertial ratchet model that we have used for these investigations can have exact correspondence to physical systems like the diffusion of Cooper pairs across a Josephson junction. Our results are amenable to experimental verifications and can have important implications.

Chapter V deals with the phenomenon of SR in a periodically driven bistable potential system. We use the average work done (or equivalently the average input energy) per period of external drive and the hysteresis loop area as quantifiers for SR. We also show that the hysteresis loop area, which gives a measure of the energy dissipated, exactly matches the input energy. We also study the distribution of average work done per period across the SR peak. In the second

part of our work, we study the role of the confining strength of the bistable potential on the nature of SR. Using average work done as a quantifier, we reproduce an earlier result that below a particular confining strength of the potential, the system does not show SR. We explain this behaviour by studying the nature of the distributions of the average work done.

The occurrence of Stochastic Resonance in periodic systems is a widely debated topic. In Chapter VI we present our investigations on the phenomenon of SR in periodic systems. Using average input energy per period of external drive and the hysteresis loop area as quantifiers for SR, we show that SR can indeed be observed in both homogeneous and inhomogeneous periodic systems. Both these (equivalent) quantifiers are found to peak as a function of temperature. We find that when the system is driven with a frequency near about the natural frequency, the particles can exists in two dynamical states of trajectories characterized by their phase and energy. We show that SR is due to the noise facilitated transitions that the particle make between the two dynamical states, synchronized with the external driving. We also investigate the nature of the variation of the amplitude and phase of the average particle response with temperature. The distributions of the input energy across the resonance peak are also studied. We find that our results conform to the earlier criteria of SR in bistable systems proving the genuineness of SR observed by us in periodic systems.

In Chapter VII we conclude by summarizing our results.

NOISE ASSISTED PHENOMENA IN PHYSICAL SYSTEMS

BY
SHANTU SAIKIA
DEPARTMENT OF PHYSICS,
NORTH-EASTERN HILL UNIVERSITY,
SHILLONG-793022

Submitted in partial fulfillment of the requirement of the degree of Doctor of Philosophy in Physics of North-Eastern Hill University, Shillong.
October, 2010.

Thesis

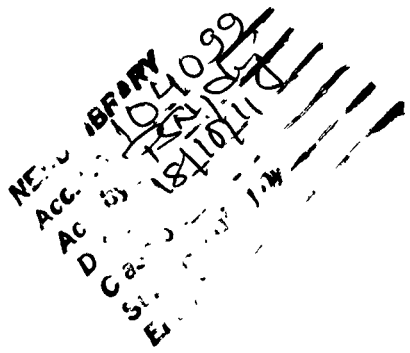

Declaration

North–Eastern Hill University,

Shillong,

October, 2010.

I, Shri Shantu Saikia hereby declare that the subject matter of this thesis is the record of work done by me, that the contents of this thesis did not form the basis of the award of any previous degree to me or to the best of my knowledge to anybody else, and that the thesis has not been submitted by me for any research degree in any other university / institute.

Shantu Saikia.

(Candidate)

22/11/2010

(Head)

Mangal

(Supervisor)

Certificate

This is to certify that the thesis entitled 'Noise Assisted Phenomena in Physical Systems', submitted by Shantu Saikia in partial fulfillment of the requirement of the degree of Doctor of Philosophy of North-Eastern Hill University, Shillong, is a record of his own research work carried out by him under my supervision. To the best of my knowledge, the matter embodied in the thesis has not been submitted for the award of any other degree by him or anybody else to any other university/institute.

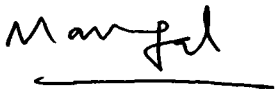

(Supervisor)
Dr. Mangal C. Mahato,
Department Of Physics,
North-Eastern Hill University,
Shillong.

Certificate

This is to certify that the thesis entitled 'Noise Assisted Phenomena in Physical Systems', submitted by Shantu Saikia in partial fulfillment of the requirement of the degree of Doctor of Philosophy of North-Eastern Hill University, Shillong, is a record of his own research work carried out by him under the supervision of Dr. Mangal C. Mahato, in the Department of Physics, North-Eastern Hill University, Shillong.

22/10/2010

Prof. P. N. Pandita,
Head of the Department,
Department Of Physics,
North-Eastern Hill University,
Shillong.

Acknowledgements

At the very beginning, I would like to dedicate this thesis to my parents who are everything behind what little I am today.

My sincere thanks and gratitude to my thesis supervisor, Dr.Mangal Chandra Mahato for his able guidance, inspiration and support through these years. I learnt lots from my association with him. His sincerity and dedication towards his work has been a leading example for me. I would also like to thank my collaborator Prof. Arun M. Jayannavar, Director, Institute of Physics, Bhubaneswar, who had always been a pillar of support and understanding. It was he who made my visits to IOP possible during which I completed a part of my work. Discussing Physics while walking around the IOP campus with him during my visits there was something special.

My heartfelt thanks to my wife Archana (Sumi), whose unconditional support and understanding went a long way in helping me complete my work. Thanks also to my little daughter Trikha, whose arrival in my life inspired me to work harder.

My thanks are due to my employer Fr. I Warpakma, Principal, St. Anthony's College, Shillong and the Department of Physics, North Eastern Hill University, Shillong, for allowing me to pursue my Ph. D. on a part time basis. My sincere thanks also to my fellow colleagues in the Department of Physics, St. Anthony's College for making this possible with their support, particularly Dr.Simanta Chutia for being there whenever I needed any help or advice.

This acknowledgement wont be complete without thanking my other collaborators Wandahoon L. Reenbohn, Dr. Ratnadeep Roy and Dr. Mamata Sahoo. Also my heartfelt thanks to Dr. Raishma Krishnan, Trilochan Bagarti and Saurabh Lahiri who have helped me with my research in some way or the other.

A special thanks to my colleague, friend and neighbour Dr. Anjan Das for just being there through these years and helping me in different ways. My thanks also goes to my brother, my sisters and my in-laws, for their love and support.

Last, but not the least, I would like to thank all who have directly or indirectly helped me in different ways during these years enabling me to complete my work.

Shantu Saikia.

(Shantu Saikia)

Contents

List of Figures

List of Tables

Chapter 1

Introduction

Noise or fluctuations, in this work, are considered as the minute random variations in temperature to which any physical or biological system at a finite temperature is subjected to. They have their origin in the coupling of these systems to the external environment and so are present in almost all systems.

Conventionally, the presence of noise (fluctuations) in a system was always thought to have a destructive, annoying role. But their presence in almost all systems led to efforts to discover systems, if any, where these random fluctuations may play a constructive role. As a result of these endeavours, over the past three decades, many pioneering works have revealed the constructive role of noise in different systems [1, 2, 3, 4, 5].

As the energy associated with these random fluctuations in the macroscopic domain is negligible compared to the mean energy, these fluctuations have insignificant effect. But as we go down to the microscopic regimes, the energy scales of these fluctuations become comparable to the mean energy scales of the system and they start playing a non-negligible, at times a dominant role in determining the nature of the system dynamics. The discovery of 'Brownian motion' by British botanist Robert Brown (1773-1858) in 1827 [6] and its subsequent analysis highlighted the role these random fluctuations can play in

the microscopic regime. Different theories came up to explain the phenomenon of 'Brownian Motion'. However, the first convincing theory was put forward by Albert Eintein (1879-1955) in his *annus mirabilis* 1905, in which he gave a theoretical explanation for Brownian motion [7]. He suggested the role of the thermal fluctuations in the random motion of the Brownian particles. The theoretical explanation was further consoliditated by extensive work of Smoluchowski. The same results were subsequently obtained by Langevin in a different manner.

As of now many systems have been discovered whose dynamics is governed by non-equilibrium fluctuations [8]. Several noise-induced or noise-assisted nonequilibrium phenomena have been discovered in physical and biological systems. For example, thermal ratchets (also called Molecular motors or Brownian motors) [5], Stochastic resonance (SR) [9, 10], resonant activation [11], noise induced stability of states [12], noise-induced transitions [13] and phase transitions [14], reaction rate theory [15], driven diffusive systems [16], etc., are a few of these systems and processes. The focus of this thesis is on the ratchet effect and the phenomenon of stochastic resonance.

1.1 Ratchet effect

Ratchet effect is the phenomenon in which a net unidirectional motion of particles in periodic potentials is obtained in the presence of fluctuations (noise), however, without any obvious external bias. Over the years there has been some notable works in the field of ratchets and Brownian motors (both theoretical and experimental) [17, 18, 19, 20, 21, 27, 28]. Nowadays, it is a significant part in the field of physical and biological research. Primary motivation for the study of ratchets was to understand the operation of biological motors or molecular machines occurring in nature [29]. For example, how to give a physical explanation of the motion of the motor protein (kinesin) along microtubules.

The proteins (actin, kinesin and dyenin) transport organelles (cargo) for

intracellular transport (kinesin and dyenin) and for muscle contraction (actin). They use energy generated from the hydrolysis of ATP to ADP. The dimensions of these molecular engines are in the nanometer range. They vary in size from 2 to 100 nm. The microtubules along which they move have a diameter of about 25 nm and length varying from 200 nm to 25 micrometer. Also, the operation of these systems deals with minute amounts of energy. For example, the stepsize of kinesin motor was measured to be 8 nm [30] with a step each in 10-15 milliseconds, during which a single ATP is hydrolysed. An energy of about 20 k_BT is released during each ATP hydrolysis and the motor does about 12 k_BT of work in each step (k_BT at body temperature $\simeq$ 4 x 10^{-21} Joules). Thus the efficiency of the motor is about 60 percent. It dissipates about $650k_BT$ of energy to the environment per second [31]. With the molecular dimensions being 10 nm, the characteristic forces of such motors are of the order of 10^{-11} N (10 piconewtons). At these dimensions and energy scales, the behaviour of these systems is influenced by fluctuations far away from equilibrium, as the energy of these fluctuations becomes comparable to the energy scales of the system. This leads to many observable and significant deviations from the system's average behaviour. The molecular motors, inspite of operating in a very noisy environment, have high efficiencies converting almost 20-90 percent of the energy to mechanical work and dissipating the rest into the environment.

Though the primary motivation for studying ratchet effect was to understand the underlying mechanism for the operation of molecular motors, the realm of noise assisted transport mechanism has gone far beyond the biological domain. The ability of the molecular motors to utilise non-equilibrium fluctuations for the generation of useful work and their high efficiencies has aroused the interest of the scientific community in small systems of molecular dimensions. The very presence of these naturally occurring molecular motors points to the possibility of fabricating artificial nanodevices for various technological applications. During the past decade, significant strides have been made in designing artificial

Brownian motors with successful experimental demonstrations and technological applications [32]. Inspired by naturally occuring ion pumps in biological systems which transport ions through nanopores in membranes against concentration gradients, artificial nanopores have been fabricated in polymer films and silicon materials. Nanofluidic diodes have been prepared which can rectify ion currents similar to a semiconductor diode rectifying electron current [33, 34]. Advanced high resolution particle separation techniques are being developed. For example, mesoscopic particles can be selectively filtered through asymmetric bottlenecklike pores pierced in silicon membranes. This is possible due to the sensitive dependence of the transport direction on the particle size [35]. Ratchet devices that control the motion of magnetic flux quanta in superconductors were predicted. This is possible by allowing these fluxons to move along asymmetric channels [36]. Subsequently, the findings were experimentally verified [37, 38]. These devices find applications in superconductivity [39, 40]. These are but only a few of the many potential applications of devices based on ratchet effect.

Any system in contact with a constant temperature bath is subjected to random thermal fluctuations. But the second law of thermodynamics forbids the utilisation of these fluctuations by the system to generate useful work as long as the system is in thermodynamic equilibrium. If that was possible, it would be like having a *perpetuum mobile* of the second kind, which will be able to extract thermal energy from a single temperature bath and convert it into mechanical energy. Hence rectification of the fluctuations is impossible in equilibrium. This is supported by the principle of detailed balance discovered by Onsager [41]. It states that at equilibrium, the rate of occurrence of any transition in a system equals the corresponding rate of occurrence of the reverse transition. Rectification is possible only when the system is driven away from thermodynamic equilibrium. Efforts were made to conceptualise a model to illustrate the phenomenon of ratchet effect [42]. This dates back to Curie [43] who stated that a locally asymmetric but globally symmetric system may induce

global transport if it is out of equilibrium. Feynman in a thought experiment [44] elucidated upon an idea originally proposed by Smoluchowski [45]. With his famous 'ratchet and pawl' experiment, Feynman was able to design a model which could utilise the random motion of Brownian particles to generate directed motion, by breaking the symmetry of the system. The system also has to be driven away from equilibrium. Smoluchowski-Feynman ratchet and pawl was subsequently experimentally verified by Kelly, Tellitu and Sestelo [46]. Its subsequent analysis [47, 48] contributed a lot to the theoretical formulation of the physics of ratchets and ratchet effect.

For ratchet effect to be realised, a system has to satisfy the following general conditions: (i) There should be an underlying spatially periodic potential in the system, (ii) The symmetry of the system has to be broken, (iii) All the forces and gradients present in the system has to average out to zero when averaged over time, space or ensembles, (iv) The system has to be driven permanently out of thermodynamic equilibrium, and (v) Random forces (of thermal, non-thermal, or even deterministic (chaotic) origin) should play a prominent role.

1.1.1 Types of Ratchets

There are different ways in which the above mentioned general conditions can be met. Based on these, diferent ratchet models are classified into categories [5]. Here we introduce three important models of ratchets - rocking ratchets, flashing ratchets and inhomogeneous ratchets. In the following we discuss the working of these three models of ratchets separately.

Flashing Ratchets

In a flashing ratchet, the underlying periodic potential or the 'Ratchet potential' $V(x)$, is spatially periodic and asymmetric as shown in figure (Fig.1.1). The potential regularly flips between two states V_{on} and V_{off}, i.e the potential is in the on state for a time τ_{on} and in the off state for a time τ_{off}. When the potential is in the on state, the particles sees a finite potential barrier and they dominantly are confined to the bottom of the wells of the potential. After a time τ_{on}, when the potential goes to the off state, the barriers to the particle motion disappear and the particles start diffusing out of the wells on both directions under the influence of the inherent thermal fluctuations in the system. When after time τ_{off}, the potential reverts back to the on state, the particles again slide to the potential well bottoms. If the time τ_{off} is adjusted properly, such that there is appreciable spread of the particles, because of asymmetry of the system, more particles accumulate in the adjacent well on the steeper slope side of the potential, as is clear from the figure (Fig. 1.1). Hence if the potential is flipped continuously for a number of times, the particles show appreciable motion towards the direction of the gentler slope.

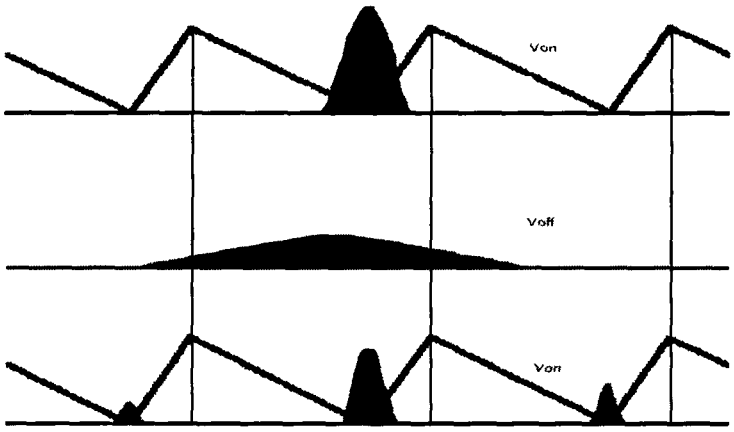

Figure 1.1: Scheme of a Flashing Ratchet. The horizontal axis gives the position while the vertical axis gives the the potential and the particle distribution. In the off state the particle does not see any potential barrier.

In this model, the system is driven out of equilibrium by the process of switching the potential between the two states. But there is no net external bias applied. Thus the Brownian particles show a directed motion without any external biasing force, aided, however, by the inherent random fluctuations.

The flashing ratchet can also be realised if the particles are exposed to two temperature baths periodically. When they are in contact with the high temperature bath, at which the effective energy possessed by the particles is higher than the potential barrier, then there would be no barrier to their motion and it would be like the off state of the potential. On the other hand when the particles are in contact with the low temperature bath, they see a finite barrier to their motion.

The on-off ratchet model or equivalently the flashing ratchet model was introduced in a theoretical context by Bug and Berne [49] in 1987. Ajdari and Prost [17] reinvented the model as a general theoretical concept in 1992. Since then his model has been verified experimentally in different contexts [21, 22].

Rocking Ratchets

In rocking ratchets, there is a periodic and asymmetric potential which is periodically modulated by an external force. During rocking, the slope of the potential changes within a positive maximum to a negative maximum value as shown in the figure (Fig. 1.2). This change of slope depends on the amplitude of the rocking force. The amplitude of this force is equal in the positive and the negative direction ensuring that it averages out to zero over a cycle.

In the case of the asymmetric potential shown in the figure, when a positive force is applied, the average slope of the potential is negative and vice versa. When a positive force is applied, the particles trapped in the potential minima tends to move in the positive direction and in the case of the negative force, they tend to move in the negative direction. If the amplitude of the rocking force

is such that even in the extremities, finite barrier to motion remains, then the

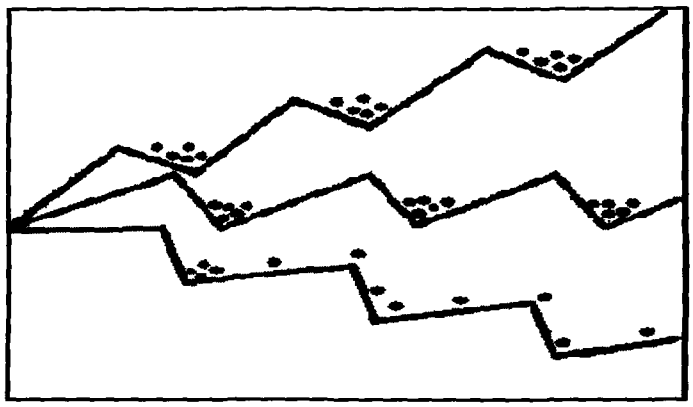

Figure 1.2: Scheme of a Rocking Ratchet; horizontal axis gives the position while the vertical axis represents the potential amplitude. The figure shows the potential in the unmodulated position (centre) and the two extreme positions of its modulation (top and bottom).

particles overcome these barriers under the influence of the thermal fluctuations. Because of the asymmetry of the potential, in case of the positive force, the particles sees a smaller barrier to motion as compared to the case when there is a negative force. Hence, if the potential is rocked continuosly, the particles on an average show a preferential motion in the positive direction.

The particle current obtained, which is a long time average, is a function mainly of the rocking amplitude and frequency, though it also depends on various other parameters, like the strength of the thermal noise etc., of the ratchet. Also, in the long time limit it is independent of the initial conditions [23]. It is seen that the current approches zero in the limits of very large and very small rocking amplitudes. So there is an optimal amplitude for which the current in the ratchet is maximised.

There has been many experimental realisations of the Rocking ratchet model in Josephson-junctions [24], SQUIDs [25], superconductors [26] etc.

Inhomogeneous Ratchets

Inhomogeneous ratchets are a class of ratchets in which the potential is periodic but symmetric unlike in the case of rocking and flashing ratchets. In these ratchets, the symmetry of the system is broken by subjecting the particles to a space dependent diffusion coefficient $D(x)$.

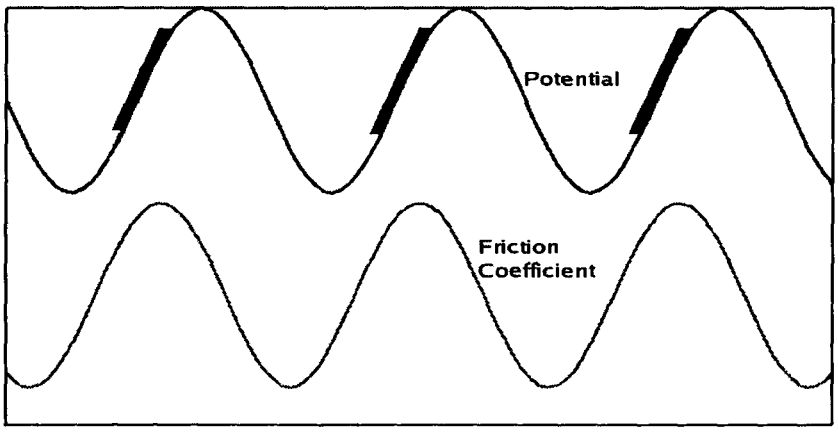

Figure 1.3: Scheme of an inhomogeneous ratchet; horizontal axis represents the position coordinate while the vertical axis represents the periodic potential (top) and the friction coefficient (bottom).

The space dependence of the diffusion coefficient is due to the presence of a space dependent temperature ($T(x)$) or friction ($\eta(x)$) or both. Because of the presence of a space dependent diffusion, the particles dissipate energy differently in different regions. The basic criteria for the realisation of this ratchet is the presence of a phase difference ϕ ($\neq 0, \pi$) between the periodic potential and the similarly periodic friction or temperature. In the figure above the basic scheme of an inhomogeneous ratchet is shown with a periodic and symmetric potential and a similarly periodic and symmetric space dependent friction coefficient, which is separated from the potential by a phase difference of ϕ. Owing to the phase difference ϕ between the potential and the friction coefficient it is clear from the figure that the overall friction is larger on the left of the potential peak position

than on the right. In the figure, the darkened regions are the regions having a high friction. Since in the static situation the position probability distribution is independent of the profile of the friction coefficient, the distribution will be Gaussian-like and symmetric about the minima of the potential. However, the situation changes in the dynamic case (when the system is driven by an external periodic forcing). Because of higher friction largely on the left (than on the right) side of the potential peak position the particle motion will be slower and hence it spends more time there (than in the corresponding region to the right of the peak) during its motion. Therefore, the effective position probability distribution is skewed with higher probability on the left than on the right of the potential peaks as though a static constant force has been applied in the left (negative) direction. With the above argument one can clearly obtain a ratchet current in the negative direction. The presence of a space dependent friction is thus analogous to that of a space dependent temperature. The possibility of a ratchet current in the reverse direction can also be envisaged, however. As the particles tend to spend more time on the left of the peak they will absorb more thermal energy from the bath and hence effectively they will be at a higher temperature. Higher temperature on the left leads to a higher probability of passage from the left of the potential peak to the right, giving rise to a net current in the right (or positive) direction. These two net current generating consequences of nonuniform friction in two opposing directions would naturally lead to competition in deciding the direction of net current, depending on the temperature of the system. The magnitude and direction of the particle current depend upon the phase difference ϕ between the friction and the periodic potential.

Apart from rocking, flashing and inhomogeneous ratchets, different other models have been proposed [5]. In all of these models there is a complex interplay of thermal noise, nonlinearity, asymmetry and unbiased driving which can lead to a rectification of noise resulting in a net motion of particles. In recent

years, an enormous amount of work has been devoted to the detailed theoretical exploration of all these numerous models. Moreover, an appreciable and growing number of experimental studies and biological and technological applications have been established [50] such as microscopic particle separation [51].

The field of deterministic ratchets pioneered by Jung et.al. [53] has also drawn substantial interest of the scientific community recently. These deterministic ratchets, unaided by 'thermal' noise, are shown to yield current in overdamped [19, 54], underdamped [52, 53, 55, 56, 57, 58, 59, 60, 61, 62, 63], as well as in Hamiltonian [65, 66, 67] periodic potential systems, and also in overdamped quenched disordered [68, 69] systems. In these systems net current results, without the presence of any external bias or asymmetric fluctuations, due to the presence of various regular transporting or chaotic attractors depending on the initial conditions for given system parameter values. In these ratchets, the deterministically induced chaos mimics the role of thermal noise [53].

1.1.2 Characterisation of Ratchets

A Brownian motor performs work by harnessing the random fluctuations. For optimizing the performances of such motors, their performance needs to be characterised. As the operations of these motors are dominated by the random fluctuations, their performances are measured by the fluctuating quantities [71] like position ($x(t)$), velocity (v) or work output (W). In the presence of fluctuations, the particle positions at any given time get spread out when being transported as an ensemble through a distance from a common initial position and time. A measure of this spread is given by the effective diffusion or dispersion $D_{eff} = \frac{\langle x^2(t)\rangle - \langle x(t)\rangle^2}{2t}$, where the average $< .. >$ is over an ensemble. But as D_{eff} does not distinguish between motors of different average velocities, we need a coherency parameter which incorporates both velocity and spread. This is given by the Peclet number [72] $P_e = \frac{\langle v\rangle l}{D_{eff}}$, where l is a characteristic length

of the system and $< v >$ is the time averaged velocity.

Apart from the Peclet number another important parameter for the characterisation of a Brownian motor is its efficiency. As these motors operate in a viscous environment, they can do work against an external load F, and against the viscous drag in the medium or both. The *efficiency of energy conversion* of a motor with respect to the work done against a load F [5, 73] is given as $\eta_E = \frac{|F\langle v\rangle|}{P_{in}}$, where P_{in} is the input power. Though this definition is thermodynamically correct, it becomes unsatisfactory in the case of Brownian motors which also works via the transport againts the viscous drag of the medium but in the absence of load. A definition of efficiency which takes into account the work done solely against the viscous drag is called the *Stokes efficiency*, $\eta_S = \frac{\langle v\rangle^2}{|\langle v^2\rangle - T|}$ [74]. Suzuki and Munakata [75] combined the above two efficiencies to give a more general definition of efficiency called the rectification efficiency given as $\eta_{rec} = \frac{\gamma\langle v\rangle^2 + F\langle v\rangle}{P_{in}}$.

Transport in almost all the models of molecular motors, is along tracks containing a periodic sequence of wells and barriers. The presence of the barriers significantly suppresses diffusion induced by presence of fluctuations. Noise also assists the particles to cross the barriers by providing a mechanism of thermal activation [15]. Presence of an optimal amount of noise in the system is thus necessary for particle transport in ratchets and it facilitates energy conversion by a ratchet [76].

1.2 Stochastic Resonance

Another physical phenomenon where the noise assisted activated barrier crossing plays a significant role is Stochastic Resonance (SR). This is a phenomenon in which a non-linear system shows an enhanced response to a small deterministic periodic forcing in the presence of an optimal amount of noise [9, 8]. The presence of noise enhances the systems response to the external signal. This,

seemingly counterintuitive phenomenon is due to a cooperative interplay between nonlinearity of the system, input signal and noise. The phenomenon of SR was first investigated as a possible explanation of one of the observed periodicities in the recurrence of the ice ages [77]. Since then there has been extensive theoretical and experimental investigations of this phenomenon [78, 79]. Different quantifiers of SR like signal to noise ratio, hysteresis loop area [80], input energy [81, 82], area under the first peak in the residence time distribution [83], etc. has been used as regards to its validity as a bonafide resonance. The phenomenon of SR has found wide applications in diverse fields like a global climate model [77, 84], electronic circuits, e.g. Schmitt triggers [85], and a bidirectional ring laser [86] to biological systems [87].

Though conventionally, Stochastic Resonance was thought to be a phenomenon exhibited by a bistable system with a coherent input signal, SR was found to be more widespread in nature. Recently, attempts have been made to apply the concepts of SR to multistate systems, particularly to diffusive transport in periodic potentials [134, 89, 90, 110]. In these systems, some of the transport properties like diffusion and mobility exhibit a peak at an optimum value of noise. Also, nonconventional SR has been reported in monostable wells where inertial effects are important [92]

Both Brownian ratchets (BR) and SR are nonlinear effects in which noise plays a constructive role. Hence efforts have been made to connect BR and SR [93]. Using a specific example of Brownian ratchets, it was shown that SR and BR share the same physical principles [94].

1.3 Fluctuation Theorems

The dynamics of non-equilibrium small systems are dominated by the random fluctuations. As a result of this, they continuously dissipate energy and make transitions between steady states. In such systems, as in nanoengines and bio-

logical motors, the energies of the thermal fluctuations become comparable with the energy scales of operation of these devices. Under such circumstances these fluctuations can lead to deviations from the average behaviour of the system. For instance the instantaneous energy transfer to such a system can be reversed by a large fluctuation, which can lead to instantaneous energy flow from a cold source to a hot one. Or in other words, the engine can work in the reverse order converting heat from the surroundings into useful work. These phenomena are rare in occurrence, however. Though these phenomena have finite probablity of occurrence and appear to violate the second law of thermodynamics, infact they do not violate the law which is a statement on average quantities. Recently, there has been a significant development in the realm of non-equilibrium thermodynamics [31]. Many general relations such as the fluctuation theorems [95, 96, 97, 98] have been discovered which are applicable to systems driven arbitrarily far from equilibrium. Fluctuation theorems (FTs) describe properties of the distribution of various quantities such as work, heat, entropy etc. in non-equilibrium processes. In such processes when a system is driven to a non-equilibrium state, certain apparently second law violating trajectories occur as stated earlier. The Fluctuation theorems quantify the probability of these '*transient second law violating*' trajectories. These theorems can be extremely useful in analyzing the role of fluctuations on the performance characteristics of systems at nanoscale (such as molecular motors).

1.4 Contribution of this thesis

In modern day scientific pursuits, substantial interest is being devoted to the understanding of the working of micro and nano sized systems like molecular motors. This is inspired by the possibility of controlling and fabricating nano devices which can have tremendous technological applications [50]. At these dimensions the systems are non-negligibly influenced by the fluctuations that are

inherent. Also they are found to use these fluctuations constructively. Different models have been made to study these systems, emphasis being on understanding the constructive role played by fluctuations in these systems giving rise to phenomenon like ratchet effect, stochastic resonance etc. (as introduced above).

Inspired by a need for a better understanding of such systems, we try to address a few aspects of the phenomenon of ratchet effect in inhomogeneous underdamped systems and also stochastic resonance in a bistable as well as periodic system in the Brownian regime.

Particle transport in inhomogeneous systems driven away from equilibrium has been an active field of research in the past few decades [19, 99, 100, 102, 103, 104, 105, 106, 107, 108, 109, 110, 111, 112, 113, 114, 115]. In these systems, the particle experiences a non uniform diffusion. This may be either due to a space dependent temperature in the system [99, 100, 102, 104] or due to a space dependent friction [108, 109, 110, 111, 112, 113, 114, 115, 116]. Systems having a space dependent friction are not uncommon in nature. For example, Brownian motion in confined geometries shows a space dependent friction [118]. Particles diffusing close to the surface have a space dependent friction coefficient [118, 119]. Also molecular motor proteins moving close along the periodic structure of microtubules experiences a friction which is space dependent [107]. Frictional inhomogeneities are also common in superlattice structures. In Josephson Junction equation, terms analogous to space-dependent friction appear [103]. The model form of a periodically varying friction coefficient also is justified by the mode-coupling theory of adatom motion on the surface of a crystal of identical atoms [120]. For our work we consider a model inhomogeneous system with a space dependent friction coefficient.

The various aspects of particle transport in overdamped inhomogeneous systems with a space dependent friction coefficient has been extensively studied [108, 109, 110, 111, 112, 113, 114]. It was shown that it is possible to obtain directed particle transport aided by noise even with a perfectly symmetric and

periodic potential in the presence of a similarly periodic friction coefficient, but with a phase difference ϕ ($\phi \neq 0, \pi$) with the potential; the system being driven away from equilibrium. The various parameters characterising the transport and particle current, like the particle velocity, efficiency and coherence of transport, diffusion etc. have been studied. Also it has been shown that forced inhomogeneous ratchets exhibit current reversals. The mobility of a particle in such a system is found to exhibit Stochastic Resonance in the presence of a finite tilt [112].

Though overdamped approximation is valid for many physical and biological processes and systems [5] - for example molecular motor movement in the Brownian regime - inertial effects can, however, play an important role in many other situations [53, 52, 56, 57, 58, 61, 70, 74, 121, 122, 115, 116, 120, 117]. Examples being the diffusion of adatoms on a crystal surface [123], dissipation in threshold devices [124], dislocation of defects in metals [125] and Josephson junctions [126].

Inertial inhomogeneous system with a space dependent temperature has been [99, 100, 101, 102, 104] shown to yield directed transport of particles in the absence of any external bias. These results make us curious as to the nature of inertial inhomogeneous systems with a space dependent friction coefficient. In this work we present the results of our studies on a model inhomogeneous inertial system with a symmetric and periodic potential. The particles moving on this system experience a similarly periodic friction coefficient, but with a phase difference with the potential [109, 115, 116]. Although such systems have been extensively studied in the overdamped regime [108, 109, 110, 111, 112, 113, 114] the presence of inertia promises to throw up new and interesting results [115, 116]. Such a model inhomogeneous system can have analogies in physical systems like Josephson Junctions [103, 115].

In an earlier work [115], it was shown that the average mobility of an underdamped particle in a tilted periodic and symmetric potential is enhanced upon

periodic modulation of the average slope of the potential, in the presence of a space dependent friction. This implies that the effective friction is reduced just by modulating the potential periodically. This, infact, has analogies in tribiology [127]. Further the particle mobilities were found to be different for positive and negative average slopes of the periodic potential keeping the other paramaters fixed. The difference was found to be dependent on the average slope of the potential and the phase difference between the periodic potential and the similarly periodic space dependent friction coefficient [116] . This hints at the possibilty of obtaining directed transport in such a system by periodically modulating the average slope of the potential without any bias on the average which gives us a direction for our work, the results of which are presented in the following chapters.

Though most of the studies on particle transport in the Brownian regime is in the presence of noise, recently the study of deterministic ratchets have contributed a lot to the understanding of the subject [52, 53, 55, 54, 56, 57, 58, 59, 61, 60, 65, 66, 67, 68, 70, 69]. In these systems directed particle transport is obtained in the absence of noise and any external average bias. The transport can be either regular or chaotic depending upon the initial conditions. This sensitivity of the nature of the particle dynamics, and hence the current, to the initial conditions has been studied [52, 55, 65]. Also, the phase locking behaviour of the particle trajectories [57] due to the presence of velocity attractors [61] and the nature and cause of the observed current reversals [55, 56] in these systems have been studied. The transport properties of inertial systems were shown to be sensitively dependent on the (constant) friction parameter [64, 62, 63]. In most of these works (barring a few [52, 66, 67]), the underlying potential was asymmetrical.

We study deterministic particle transport in a driven inertial inhomogeneous ratchet, the results of which are presented in Chapter II. We show that frictional inhomogeneity in a symmetric periodic potential mimics most of the qualitative

features of deterministic dynamics in a homogeneous system with an asymmetric periodic potential. The role of the initial phase of the external drive has been hinted at for Hamiltonian systems [65, 67]. We point out the need of averaging over the initial phase of the external drive at small frictional inhomogeneity parameter values or analogously low potential asymmetry regimes in obtaining ratchet current. We also show that noise plays an important role in obtaining ratchet current at low amplitudes of drive, where there is no current in the deterministic regime. The presence of noise does even lead to the occurrence of current reversals for some parameter values of the system.

Going a step further from the deterministic regime, the addition of noise to the driven system leads to a well defined particle current even at low amplitudes of drive as was hinted in reference [116]. In ref. [116] it was shown that there was a difference in the average mobility of the particle for positive and negative slopes of the potential. Thus the periodic modulation of the slope of the potential could lead to particle current. In Chapter III, *we present the results of our work in which we study a zero-mean square wave driven inertial inhomogeneous ratchet system in the presence of noise. We obtain particle current in both the adiabatic limit and finite time period of drive just by exploiting the frictional inhomogeneity of the medium. The current is found to have a peaking behaviour both as a function of the driving amplitude and frequency. The steady state diffusion coefficient is interestingly found to peak at exactly the same amplitude at which the current peaks. This means that the particle motion in the amplitude regime at which the current peaks is highly diffusive. But a calculation of the Péclet number shows that the motion is greatly coherent too. We also calculate the Stoke's efficiency for the particle transport. Though this system gives very small efficiency of transport, an optimal choice of the parameters can improve the efficiency.*

Particle transport in a ratchet system under the influence of noise or fluctuations is invariably associated with diffusive spread. Hence a measure of the

diffusion coefficient becomes an important parameter in characterising the particle transport. Studies have been made to investigate the steady state diffusion in ratchet systems [128, 129, 130, 131]. But the intermediate time scales during transport can become interesting throwing up unexpected results [117]. In ref. [117] the dispersionless behaviour of an underdamped particle moving in a tilted periodic potential at intermediate time scales is reported. In Chapter IV *we present the results of our work to study the intermediate time dispersionless regime of particle transport in our model inertial inhomogeneous ratchet system. We consider the system to be driven by a zero-mean square wave drive. Unlike in [117] where it was shown that dispersionless motion persists for a finite length of time before it becomes diffusive again, we show that such coherent motion can be obtained repeatedly by applying an external zero mean square wave drive of a proper amplitude and frequency instead of a constant tilt. Thus the cumulative duration of coherent motion of particles can be prolonged. Moreover we show that taking an appropriate combination of periods of the external field, one can postpone the beginning of coherent motion and can even have coherent motion at a lower value of position dispersion than in the constant tilt case. This model can have an exact correspondence to physical systems like the diffusion of Cooper pairs across a Josephson junction [103]. So our results are amenable to experimental verification and have important implications.*

Apart from particle transport in ratchet systems, noise assisted barrier crossing plays an important role in the phenomenon of Stochastic Resonance (SR). Substantial work has been done to study the phenomenon of Stochastic Resonance in bistable systems [9] and different quantifiers have been used. In Chapter V, *we present our studies on the motion of a Brownian particle in a double-well potential driven by an ac force.* Earlier studies on the work done in a periodically driven bistable system by an external agent has established that the average work peaks around the resonance, as expected [81, 137]. *We not only calculate the average work done (or equivalrntly the average input energy) per*

period of external drive, but also the hysteresis loop area and compare both. We show that in these systems, the hysteresis loop area, which gives a measure of the energy dissipated, exactly matches the input energy and it can also be used as a quantifier for Stochastic Resonance. We study the distribution of work done on the system over a drive period across the SR peak, in the time asymptotic regime.

In the second part of the work we study the role of the confining strength of the bistable potential on the nature of SR. In an earlier work [136], it was shown that the nature of SR varies with the confining strength of the potential. The amplitude of interwell hoppings of the particle was taken as a quantifier of SR. *In our work by using the average input energy per period as a quantifier of SR, we too find that below a particular confining strength of the potential, the system does not show SR. We explain this behaviour by studying the nature of the distributions of the the input energy per period into the system.*

Though the phenomenon of SR was originally studied in bistable systems, recently some investigations has been done for multistate systems [89, 90, 110, 134]. Particularly, there has been lots of controversy as to whether or not the phenomenon of SR can be observed in periodic systems. In an earlier work, there was a suggestion that SR can be observed in the drift velocity of an overdamped Brownian particle in a tilted periodic potential [132]. Though this suggestion was contradicted for overdamped systems [133], it was argued to be correct for underdamped systems [134] where friction can act as a surrogate for the external periodic drive. The mobility of an overdamped particle in an inhomogeneous system with a tilted periodic and symmetric potential was shown to exhibit Stochastic Resonance in the presence of a space dependent friction [135]. In Chapter VI *we present our studies on the phenomenon of SR in underdamped periodic systems.* Whether or not SR occurs in periodic systems has been a question which is inconclusive [138]. *We show that SR can indeed be observed in periodic systems. For our investigation we use the average input energy per*

period and the hysteresis loop area as quantifiers for SR. Both these quantities shows a peaking behaviour as a function of temperature. This peaking is due to the noise facilitated transistions that the particles make between two dynamical states, synchronised with the external driving. The particles can exist in either of these states, characterised by their phase and energy. We also investigate the nature of variation the amplitude and phase difference of the response function with the external drive, with the temperature.

In Chapter VII *we will conclude by summarising our results.*

Bibliography

[1] F. Julicher, A. Ajdari and L. Prost, Rev. Mod. Phys. 69, 1269 (1997); R. D. Astumian, Scientific American 285, 56 (2001).

[2] *Special issues on "Ratchets and Brownian motors: Basics, Experiments and applications"*, Ed. H. Linke, Appl. Phys. A 75(2), 167 (2002).

[3] R. D .Astumian and P. Hanggi, Phys. Today 55, 33 (2002).

[4] M. C. Mahato and A. M. Jayannavar, Resonance 8 (7), 33 (2003); *ibid* M. C. Mahato, and A. M. Jayannavar, Resonance 8 (9), 4 (2003).

[5] P. Reimann, Phys. Rep. 361, 57 (2002).

[6] R. Brown, Philos. Mag. 4, 161 (1828).

[7] J. Stachel, *Eintein's miraculous year: Five papers that changed the face of Physics* (Princeton University Press, 1998).

[8] J. Maddox, Nature 369, 271 (1994); *ibid* 369, 181 (1994).

[9] L. Gammaitoni, P. Hanggi, P. Jung, F. Marchesoni, Rev. Mod. Phys. 70, 223 (1988).

[10] A. Simon and A. Lichaber, Phys. Rev. Lett. 68, 3375 (1992).

[11] C. R. Doering and J.C. Gadoua, Phys. Rev. Lett. 69, 2318 (1992).

[12] I. Dayan, M. Gitterman and G.H. Weiss, Phys. Rev. A 46, 757, (1992); R. N. Mantegna and B. Spagnolo, Phys. Rev. Lett. 76, 563 (1996); P. Reimann and P. Hanggi, *Lecture Notes in Physics* 484 (Springer Verlag, Berlin, 1997).

[13] W. Horsthemke, R. Lefever, *Noise-induced Transistion*, Springer, Berlin, Heidelberg, New York, 1984.

[14] C. Van den Broeck, J.M.R. Parrondo, R. Toral, R. Kawai, Phys. Rev. E 55, 4084 (1997).

[15] P. Hanggi, P. Talkner, M. Borkovee, Rev. Mod. Phys. 62, 251 (1990).

[16] B. Schmittmann, R. K. P. Zia, *Phase Transistions and Critical Phenomena*, Vol.17, ed. by C. Domb and J. L. Lebowitz (Academic, London, 1995).

[17] A. Ajdari, J. Prost, C. R. Acad. Sci. Paris t. 315, Série II (1992) 1635.

[18] R.D. Astumian, M. Bier, Phys. Rev. Lett. 72, 1766 (1994).

[19] R. Bartussek, P. Hänggi, J. G. Kissner, Europhys. Lett. 28, 459 (1994).

[20] M. O. Magnasco, Phys. Rev. Lett. 71, 1477 (1993).

[21] J. Rousselet, L. Salone, A. Ajdari, J. Prost, Nature 370, 446 (1994).

[22] L .P. Faucheux, A. Libchaber, J. Chem. Soc. Faraday Trans. 91, 3163 (1995).

[23] A. Ajdari, D. Mukamel, L. Peliti, J. Prost, J. Phys. I France 4, 1551 (1994).

[24] E. Trias, J. J. Mazo, F. Falo, T. P. Orlando, Phys. Rev. E 61, 2257 (2000); E. Golobin, A, Sterck, D. Koelle, cond-mat/0008237.

[25] I. Zapata, R. Bartussek, F. Sols, P. Hanggi, Phys. Rev. Lett. 76, 1968 (1996).

[26] C. S. Lee, B. Janko, I. Derenyi, A. L. Barabasi, Nature 400, 5106 (1999).

[27] C. R. Doering, W. Horsthemke, and J. Riordan, Phys. Rev. Lett. 72, 2984 (1994).

[28] M. M. Millonas, and M. I. Dykman, Phys. Lett. A. 185, 65 (1994).

[29] J. A. Spudich, Nature 372, 515 (1994).

[30] K. Svoboda, C. F. Schmidt, B. J. Schnapp and S. M. Block, Nature 365, 721 (1993).

[31] C. Bustamante, J. Liphardt, F. Ritort, Phys. Today 58, 45 (2005).

[32] P. Hanggi and F. Marchesoni, Rev. Mod. Phys. 81, 387 (2009).

[33] Z. Siwy and A. Fulinski, Phys. Rev. Lett. 89, 198103 (2002); *ibid* Am. J. Phys. 72, 567 (2004); Z. Siwy, I. D. Kosinska, A. Fulinsky, and C. R. Martin, Phys. Rev. Lett. 94, 048102 (2005).

[34] H. Daiguji, Y. Oka and K. Shirono, Nano Lett. 5, 2274 (2005).

[35] C. Kettner, P. Reimann, P. Hanggi and F. Muller, Phys. Rev. E 61, 312 (2000).

[36] J. F. Wambaugh, C. Reichhardt, C. J. Olson, F. Marchesoni and F. Nori, Phys. Rev. Lett. 83, 5106 (1999).

[37] Y. Togawa, K. Harada, T. Akashi, H. Kasai, T. Matsuda, F. Nori, A. Maeda, and A. Tonomura, Phys. Rev. Lett. 95, 087002 (2005).

[38] K. Yu, T. W. Heitmann, C. Song, M. P. DeFeo, B. L. T. Plourde, M. B. S. Hesselberth, and P. H. Kes, Phys. Rev. B. 76, 220507 (2007).

[39] S. Savelev, F. Nori, Nature Mater. 1, 179 (2002).

[40] J. E. Villegas, S. Savelev, F. Nori, E. M. Gonzales, J. V. Anguita, R. Garcia, and J. L. Vincent, Science 302, 1188 (2003); S. Savelev, F. Marchesoni, and F. Nori, Phys. Rev. Lett. 91, 10601 (2003); B. Y. Zhu, F. Marchesoni and F. Nori, Phys. Rev. Lett. 92, 180602 (2004).

[41] L. Onsager, Phys. Rev. 37, 405 (1931); *ibid* 38, 2265 (1931).

[42] J. Maddox, Nature 365, 203 (1993); *ibid* 368, 287 (1994).

[43] P. Curie, J. Phys. (Paris), 3, 393 (1894).

[44] R. P. Feynman, R. B. Leighton and M. Sands. *The Feynman Lectures on Physics*, Addison-Wesley, Reading, MA, Vol 1 (1963).

[45]

[46] T. R. Kelly, I. Tellitu, J. P. Sestelo, Angew. Chem. Int. Ed. Engl. 36, 1866 (1997); *ibid* J. Org. Chem. 63, 3655 (1998).

[47] M. O. Magnasco and G. Stolovitzky, J. Stat. Phys. 93, 165 (1998).

[48] J. M. R. Parrondo and P. Espanol, Am. J. Phys. 64, 1125 (1996).

[49] A. L. R. Bug, B.J. Berne, Phys. Rev. Lett. 59, 948 (1987).

[50] P. Hanggi and F. Marchesoni, Rev. Mod. Phys. 81, 387 (2009).

[51] D. Erlas, Phys. Rev. Lett. 80, 1552 (1998); B. Lindner, L. Schimansky-Geier, P. Reimann, P. Hanggi, AIP Conf. Proc. 411, 309 (1997).

[52] S. Flach, O. Yevtushenko, and Y. Zolotaryuk, Phys. Rev. Lett. 84, 2358 (2000).

[53] P. Jung, J. G. Kissner and P. Hänggi, Phys. Rev. Lett. 76, 3436 (1996).

[54] J. F. Chauwin, A. Ajdari and J. Prost, Europhys Lett. 27, 421 (1994); *ibid* 32, 373 (1995).

[55] A. Kenfack, S. M. Sweetnam and A. K. Pattanayak, Phys. Rev. E 75, 056215 (2007).

[56] J. L. Mateos, Phys. Rev. Lett. 84, 258 (2000).

[57] M. Barbi and M. Salerno, Phys. Rev. E 62, 1988 (2000).

[58] C. M. Arizmendi, F. Family and A. L. Salas-Brito, Phys. Rev. E 63, 061104 (2001).

[59] M. Borromeo, G. Constantini and F. Marchesoni, Phys. Rev. E 65, 041110 (2002).

[60] L. Cai, Physica A 389, 362 (2010).

[61] H. A. Larrondo, F. Family and C. M. Arizmendi, Physica A 303,67 (2002).

[62] F. Marchesoni, S. Savelev and F. Nori, Phys. Rev. E 73, 021102 (2006).

[63] M. F. Carusela, A.J. Fendrik and L. Romanelli, Physica A 388, 4017 (2009).

[64] H. Risken, *The Fokker-Planck Equation*, (Springer- Verlag, Berlincl), 1996.

[65] O. Yevtushenko, S. Flach, and K. Richter, Phys. Rev. E 61, 7215 (2000).

[66] S. M. Soskin, O. M. Yevtushenko, and R. Mannella, Phys. Rev. Lett. 95, 224101 (2005).

[67] D. Hennig, L. Schimansky-Geier and P. Hänggi, Eur. Phys. J. B 62, 493 (2008).

[68] M. N. Popescu, C. M. Arizmendi, A. L. Salas-Brito and F. Family, Phys. Rev. Lett. 85, 3321 (2000).

[69] F. Family, H. A. Larrondo, D. G. Zarlenga and C. M. Arizmendi, J. Phys. Cond. Matter 17, S3719, (2005).

[70] H. A. Larrondo, C. M. Arizmendi and F. Family, Physica A 320, 49 (2003).

[71] H. Linke, M. T. Downton, and M. J. Zuckermann, Chaos 026111 (2005).

[72] L. D. Landau and E. M. Lifshitz, *Fluid Mechanics*, (Pergamon Press, New York, 1959) p.203.

[73] K. Sekimoto, J. Phys. Soc. Jpn. 66, 1234 (1997).

[74] L. Machura, M. Kostur, F. Marchesoni, P. Talkner, P. Hänggi and J. Luczka, J. Phys.: Condens. Matter 17, S3741 (2005); L. Machura, M. Kostur, P. Talkner, J. Luczka, F. Marchesoni and P. Hänggi, Phys. Rev. E 70, 061105 (2004).

[75] D. Suzuki and T. Munakata, Phys. Rev. E 68, 021906 (2003).

[76] F. Takagi and T. Hondou, Phys. Rev. E. 60, 4954 (1999).

[77] A. R. Benzi, A. Sutera, and A. Vulpiani, J.Phys. A 14, L453 (1981).

[78] L. Gammatoni, P. Hanggi, P. Jung, F. Marchesoni, Rev. Mod. Phys. 70, 223 (1998); B. McNamara and K. Wiesenfeld, Phys. Rev. A 39, 4894 (1989); T. Zhou, F. Moss, and P. Jung, Phys. Rev. A 42, 3161 (1990); P. Jung and P. Hanggi, Phys. Rev. A 44, 8032 (1991).

[79] R. N. Mantegna and B. Spagnolo, Phys. Rev. E 49, R1792 (1994).

[80] M. C. Mahato and S. R. Shenoy, Phys. Rev. E 50, 2503 (1994); M. C. Mahato and A. M. Jayannavar, Phy. Rev. E 55, 6266 (1997); *ibid* Mod. Phys. Lett. B 11, 815 (1997); *ibid* Physica A 248, 138 (1998); J. C. Philips and K. Schulten, Phys. Rev. E 52, 2473 (1994); .

[81] T. Iwai, Physica A 300, 350 (2001); T. Iwai, J. Phys. Soc. Jon. 70, 353 (2001).

[82] D. Dan and A. M. Jayannavar, Physica A 249, 88 (1998).

[83] L. Gammaitoni, F. Marchesoni, S. Santuchi, Phys. Rev. Lett, 74, 1052 (1995); M. H. Choi, R. F. Fox, P. Jung, Phys. Rev. E 57, 6335 (1998); F. Marchesoni, L. Gammatoni, F. Apostolico, S. Santucci, Phys. Rev. E 62, 146L (2000).

[84] C. Nicolis, Tellus 34, 1 (1982); R. Benzi, G. Parisi, A. Sutera and A. Vulpiani, Tellus 34, 10 (1982).

[85] S. Fauve and F. Heslot, Phys. Lett. 97A, 5 (1983).

[86] B. McNamara, K. Wiesenfeld and R. Roy, Phys. Lett. 60, 2626 (1988).

[87] K. Wiesenfeld and F. Moss, Nature (London) 373, 33 (1995).

[88] F. Marchesoni, Phys. Lett. A 231, 61(1997).

[89] H. Gang, A. Daffertshofer and H. Haken, Phys. Rev. Lett 76, 4874 (1996).

[90] W. Y. Kim and W. Sung Phys. Rev. E 57, 6237 (1998).

[91] D. Dan, M. C. Mahto and A. M. Jayannavar Phys. Rev. E 60, 6421 (1999).

[92] M. I. Dykman, D. G. Luchinsky, R. Mannella, P. V. E. McClintock, N. D. Stein and N. G. Stocks, J. Stat. Phys. 70, 479 (1993).

[93] M. Bier, Contemp. Phys. 38, 371 (1997); V. Berdichevsky and M. Gitterman, Physica A 249, 88 (1998); R. D. Astumian and F. Moss, Chaos, 8, 533 (1998).

[94] A. Allison and D. Abbot, Fluc. and Noise Letters, 1(4), L239 (2001).

[95] D. J. Evans, E. G. D. Cohen and G. P. Morriss, Phys. Rev. Lett. 71, 2401 (1993).

[96] G. Gallavotti and E. G. D .Cohen, Phys. Rev. Lett. 74, 2694 (1995); J. Stat. Phys. 80 (5-6), 931 (1995).

[97] D. J. Evans and D. J. Searles, Phys. Rev. E 50, 1645 (1994); *ibid* Advances in Physics, 51 (7), 1529 (2002); *ibid* Phys. Rev. E. 71 (5), 056120 (2005).

[98] R. van Zon and E. G. D. Cohen, Phys. Rev. Lett. 91 (11), 110601 (2003); *ibid* Phys. Rev. E 67, 046102 (2003); *ibid* Phys. Rev. E. 69, 056121 (2004).

[99] R. Landauer, J. Stst. Phys. 53, 233 (1988).

[100] M. Buttiker, Z. Phys. B 68, 161 (1987).

[101] P. Reimann, R. Bartussek, R. Haubler, and P. Hanggi, Phys. Lett. A 215, 26 (1996).

[102] Ya. M. Blanter and M. Büttiker, Phys. Rev. Lett. 81, 4040 (1988).

[103] C. M. Falco, Am. J. Phys. 44, 733 (1976); A. Barone and G. Patterno *Physics and applications of the Josephson effect*, John Wiley, New York, 1982.

[104] R. Benjamin and R. Kawai, Phys. Rev. E 77, 051132 (2008).

[105] M. M. Millonas, Phys. Rev. Lett. 74, 10 (1995).

[106] N. G. van Kampen, IBM. J. Res. Dev. 32, 107 (1988).

[107] R. H. Luchsinger, Phys. Rev. E. 62, 272 (2000).

[108] A. M. Jayannavar, Phy. Rev. E. 53, 2957 (1996).

[109] M. C. Mahato, T. P. Pareek and A. M. Jayannavar, Int. J. Mod. Phys. B 10, 3857 (1996).

[110] D. Dan, M. C. Mahato and A. M. Jayannavar, Int. J. Mod. Phys. B 14, 1585 (2000); *ibid* Phys. Lett. A 258, 217 (1999); *ibid* Phys. Rev. E 60, 6421 (1999).

[111] A. M. Jayannavar and M. C. Mahato, Pramana J. Phys. 45, 369 (1995).

[112] D. Dan and A. M. Jayannavar, Int. J. Mod. Phys. B 14, 1585 (2000). *ibid* Phys. Rev. E 60, 6421 (1999).

[113] M. C. Mahato and A. M. Jayannavar, Phys. Rev. E 63, 056307 (2001).

[114] R. Krishnan, M. C. Mahato and A. M. Jayannavar, Phys. Rev. E 70, 021102 (2004); R. Krishnan, D. Dan and A. M. Jayannavar, Indian J. Phys. 78, 747 (2004).

[115] M. C. Mahato and A. M. Jayannavar, Physica A 318, 154 (2003).

[116] M. C. Mahato, Indian J. Phys. 78 (8), 693 (2004).

[117] K. Lindenberg, J. M. Sancho, A. M. Lacasta and I. M. Sokolov, Phys. Rev. Lett. 98, 020602 (2007).

[118] L. P. Faucheux and A. J. Libchaber, Phys. Rev. E 49, 5158 (1994).

[119] H. Brenner, Chem. Eng. Sci. 16, 242 (1962).

[120] G. Wahnstrom, Surf. Sci. 159, 311 (1985).

[121] C. Constantini and F. Marchesoni, Europhys. Lett. 48, 491 (1999).

[122] B. Lindner et. al. Phys. Rev. E 59, 1417 (1999).

[123] E. Pollak, J. Bader, B. J. Berne and P. Talkner, Phys. Rev. Lett. 70, 3299 (1993); M. Borromeo and F. Marchesoni, Phys. Rev. Lett. 84, 203 (2000); O. M. Braun and R. Ferrando, Phys. Rev. E 65, 061107 (2002).

[124] M. Borromeo, G. Constantini and F. Marchesoni, Phys. Rev. Lett. 82, 2820 (1999); G. Constantini and F. Marchesoni, Europhys. Lett, 48, 491 (2000).

[125] O. M. Braun, A. R. Bishop and J. Roder, Phys. Rev. Lett. 79, 3692 (1997); C. Cattuto and F. Marchesoni, Phys. Rev. Lett. 79, 5070, (1997).

[126] E. Ben-Jacob, D. J. Bergman, B. J. Matkowsky and Z. Schuss, Phys. Rev. A 26, 2805 (1982); E. Ben-Jacob, D. J. Bergman and Z. Schuss, Phys. Rev. B 25, 519 (1982).

[127] S. Grahick, Phys. Today 52, 26 (1999).

[128] J. A. Freund and L. Schimansky-Geier, Phys. Rev. E 60, 1304 (1999)

[129] T. Harms and R. Lipowsky, Phys. Rev. Lett. 79, 2895 (1997).

[130] B. Lindner and L. Scimansky-Geier, Phys. Rev. Lett. 230602 (2002).

[131] R. Krishnan, D. Dan and A. M. Jayannavar, Indian J. Phys. 78, 747 (2004); *ibid* Cond-mat 0409287v1.

[132] G. Hu. Phys. Lett. 174, 247 (1993).

[133] M. Gitterman, I. B. Khalfin and B. Ya. Shapiro, Phys. Lett. A 184, 339 (1994); J. M. Casada, J. J. Mejias and M. Marilla, Phys. Lett. A 197, 365 (1994).

[134] F. Marchesoni, Phys. Lett. A 231, 61 (1997).

[135] D. Dan, M. C. Mahato and A. M. Jayannavar, Phys. Rev. E 60, 6421 (1999).

[136] E. Heinsalu, M. Patriarca and F. Marchesoni, Eur. Phys. J. B, 69, 19 (2009). 70 (2001) 353.

[137] D. Dan and A.M. Jayannavar, Physica A 345 (2005) 404.

[138] Y. W. Kim and W. Sung, Phys. Rev. E 57, R6237 (1998).

Chapter 2

Deterministic Inhomogeneous inertia Ratchets

2.1 Introduction

In this chapter we present the results of our studies on the various facets of particle transport in an underdamped inhomogeneous ratchet system in the deterministic regime i.e. in the zero temperature limit [1].

Ratchet effect, the occurrence of directed particle transport in asymmetric periodic (ratchetlike) potentials without the application of any obvious external bias in the presence of noise, has been widely studied both in overdamped and underdamped conditions [2, 3, 4, 5, 6]. The same effect, has also been obtained in underdamped symmetric periodic (non-ratchetlike) potential systems, by considering either the temperature [7, 8, 9, 10] or the friction coefficient [11, 12] to be space dependent. It can also result in a symmetric periodic potential when the system is driven by an externally applied zero-mean temporally asymmetric forcing aided by Gaussian white noise [13] or by the explicit application of non-thermal noise [14, 15]. The ratchet effect is being studied intensively for about two decades and its applications envisaged in periodic systems that are common in many areas of natural sciences [16].

All the above ratchet models use the presence of (Gaussian or colored) noise (fluctuations) to obtain directed transport. In these models noise is essential. However, the study of deterministic ratchets, pioneered by Jung et. al. [17], has also contributed significantly to the understanding of the subject. These deterministic ratchets, unaided by noise, are shown to yield current in overdamped [18, 19], underdamped [15, 17, 20, 21, 22, 23, 24, 25, 26, 28, 29], as well as in Hamiltonian [30, 31, 32] periodic potential systems, and also in overdamped quenched disordered [33, 35] systems. In these systems net current results, without the presence of applied nonzero average forcing or asymmetric fluctuations, due to the presence of various regular transporting or chaotic attractors depending on the initial conditions for given system parameter values. In Ref. [15] the symmetry criteria for the realization of ratchet current have been discussed in detail.

Owing to the complexity of the dynamics, for example the simultaneous presence of periodic and chaotic attractors, there is a need for unbiased choice of initial conditions and ensemble averaging over them to obtain realistic averages [15, 20, 30]. This fact has been exemplified in an (zero mean) ac modulated periodic Hamiltonian system [32]. It has been shown there that slower modulations of the symmetric periodic potential lead to asymmetric access (in momentum) of chaotic regimes in the phase space resulting in a giant net particle transport in one direction. The direction and magnitude of the current depends on the initial phase of the modulating ac drive. Ofcourse, the net current must disappear if averaged over the initial phase.

The driven deterministic systems show frequent ensemble-averaged current reversals as the drive parameters are changed. Mateos identified bifurcation from a chaotic to a periodic regime as the mechanism for the average-current reversals [21] in these systems. However, the change in direction of individual single particle trajectories could be related to phase locking phenomena [22] due to the presence of various velocity attractors [25]. The average current directions

are thus sensitive to initial conditions [39] which allow to explore these attractors selectively in the phase space. In a recent further investigation [20] it has been conjectured that, in general, bifurcations from chaos to periodic behaviour could be associated with abrupt changes (and not necessarily reversals) in the ensemble averaged currents.

In Ref. [35], the effect of different control parameters were analysed in the inertial limit. It was found that the control mechanisms were associated with the fractal nature of the basins of attraction of the mean velocity attractors and that small perturbations of the control variable could produce drift reversals. However, the effect of the presence of a weak subharmonic component in the ac drive field on the phase locked dynamics of a ratchet is to suppress chaos and stabilize regular orbits over large range of driving amplitudes [38].

The transport properties of inertial systems depend sensitively on the (constant) friction parameter [27, 28, 29]. The addition of noise to the system in the low damping regime makes the system dynamics robust against initial conditions [28]. Moreover, in a well defined damping window the efficiency of ratchet current generation becomes appreciable even for small applied periodic field amplitudes. In Ref. [29] the effect of noise on individual transporting deterministic trajectories is analysed. A small noise seem to have little effect on some trajectories in one direction whereas it destroys trajectories in the opposite direction resulting in a robust finite ratchet current.

In most of the above works (barring a few, for instance [15, 30, 32]), particle motion in periodic but asymmetric potentials is considered; for example a system with potential $V(x) = V_0(\cos x + b\cos 2x)$ driven by a periodic field, $F(t) = a\cos(\omega t + \phi_0)$ in uniform friction media. In these studies the potential asymmetry ($b \neq 0$) is the primary cause of net particle drift. In the present work, we consider a *symmetric* periodic potential, for example $V(x) = -V_0 \sin x$, but in the presence of a space dependent friction coefficient $\gamma(x) = \gamma_0(1 - \lambda \sin(x + \phi))$ (as in [11]). A massive charged particle moving in a periodic ionic lattice and in

a medium with material density (friction) profile created by a stationary pressure wave can be thought of as a mechanical illustration of such systems [11, 12]. However, such systems have been studied earlier in a resistively and capacitatively shunted junction circuit model of small Josephson junctions [40, 41]. The frictional inhomogeneity term emulating there the "$\cos\theta$" term representing the coupling between the quasiparticle tunneling and Cooper pair tunneling across the Josephson junction. In Ref. [40] the phase space trajectories of this system are presented in detail.

In this work we show that all the features of deterministic inertia ratchets with asymmetric periodic potential can be observed even in the symmetric periodic potential system in an inhomogeneous medium. The frictional nonuniformity of the medium with phase shift $\phi(\neq 0, \pi)$ essentially emulates the effect of the asymmetry of the potential considered in earlier cases. Moreover, we show in our present inhomogeneous dissipative system that, for small inhomogeneity (roughly $\lambda \leq 0.6$), in order to get sensible ratchet current one also needs to average over the initial phase ϕ_0 of the drive as in the Hamiltonian system[30, 32]. Though ratchet current is a steady state ($t \to \infty$) phenomenon one is likely to obtain a finite ratchet current, an obvious erroneous result, even at zero potential asymmetry in a uniform medium without this averaging. Interestingly, the bifurcation diagrams with and without the frictional inhomogeneity are qualitatively indistinguishable. However, the stroboscopic Poincaré plots differ qualitatively in the driven system as the inhomogeneity parameter λ is varied. The presence of noise (which is ubiquitous in natural environments) smooths out the current fluctuations so numerously present in the deterministic case [29, 42]. In Ref. [42] a matrix continued fraction method is presented to obtain ratchet current in noisy periodically driven inertial systems. We further show in our inhomogeneous system that at low drive amplitudes noise plays a crucial role in getting ratchet (mean) current, that is conspicuously absent in the deterministic drive case, though at larger drive amplitudes one obtains ratchet current without the

presence of noise.

2.2 The model

As mentioned earlier, in this chapter, we consider the motion of a particle in a periodic potential $V(x) = -V_0 \sin(kx)$ which is symmetric in space (about $kx = (2n+1)\pi/2$, $n = 0, \pm 1, \pm 2, ...$). The friction coefficient $\gamma(x) = \gamma_0(1 - \lambda \sin(kx + \phi))$ is periodic with the same periodicity as the potential but has a phase difference. The system is driven periodically by an external periodic forcing $F(t)=a\ \cos(\omega t + \phi_0)$. We study the system in the deterministic regime i.e. in the absence of noise and also at the end in the presence of noise.

The one dimensional equation of motion of a particle of mass m is given by the Langevin equation,

$$m\frac{d^2x}{dt^2} = -\gamma(x)\frac{dx}{dt} - \frac{\partial V(x)}{\partial x} + F(t). \tag{2.1}$$

The corresponding equation of motion in the presence of noise is given by

$$m\frac{d^2x}{dt^2} = -\gamma(x)\frac{dx}{dt} - \frac{\partial V(x)}{\partial x} + F(t) + \sqrt{\gamma(x)T}\xi(t). \tag{2.2}$$

In Eq. 2.2, T is the temperature in units of the Boltzmann constant k_B. The Gaussian distributed fluctuating forces $\xi(t)$ satisfy the statistics: $< \xi(t) >= 0$, and $< \xi(t)\xi(t') >= 2\delta(t - t')$. For convenience, we write down Eq. 2.1 and Eq. 2.2 in dimensionless units. In terms of the reduced variables denoted again now by the same symbols, the two equations can be written as

$$\frac{d^2x}{dt^2} = -\gamma(x)\frac{dx}{dt} + \cos x + F(t), \tag{2.3}$$

and

$$\frac{d^2x}{dt^2} = -\gamma(x)\frac{dx}{dt} + \cos x + F(t) + \sqrt{\gamma(x)T}\xi(t), \tag{2.4}$$

where $\gamma(x) = \gamma_0(1 - \lambda \sin(x + \phi))$. Thus the periodicity of the potential $V(x)$ and also the friction coefficient γ is 2π . The potential barrier between any two consecutive wells of $V(x)$ persists for all field amplitudes a, $(0 < a < 1)$ and it just disappears at the critical field value $a = a_c = 1$. Notice that for $\phi = n\pi$, $n = 0, \pm 1, \pm 2, ...$ the deterministic Eq.2.3 should yield exactly the same trajectory but in the opposite direction on letting $x \to x - \pi/2$ and $t \to -t$ and in the presence of a thermal noise Eq. 2.4 should give the same ensemble averaged current but again in the opposite direction [15]. Thus in order that a ratchet current appears the symmetry of the system must be broken using $\phi \neq n\pi$.

The noise variable, ξ in Eq. 2.4, satisfies exactly similar statistics as earlier. We solve equation Eq. 2.3 and Eq. 2.4 numerically using the Heun's method for solving differential equations. The particle trajectories are obtained for given initial conditions for fixed values of a and γ_0. Also, the steady state mean velocity of the particles are calculated.

For the deterministic case the average velocity for a single particle (with a given initial condition) is obtained by the relation [25]

$$\langle v \rangle = \frac{x(t_{max}) - x(t_{tran})}{(t_{max} - t_{tran})}, \tag{2.5}$$

where t_{max} is the maximum time for which the particle is allowed to evolve and t_{tran} is the duration of initial transients that we remove.

Also the mean velocity averaged over an ensemble of N particles is defined as

$$\langle \langle v \rangle \rangle = \frac{1}{N} \sum_{i=1}^{N} \langle v \rangle_i, \tag{2.6}$$

For the particle trajectory in the presence of noise, the steady state mean velocity $\bar{v}$ of the particle is obtained as

$$\bar{v} = \langle \lim_{t \to \infty} \frac{x(t)}{t} \rangle, \tag{2.7}$$

where the average $\langle ... \rangle$ is evaluated over a large number of trajectories.

2.3 Numerical results

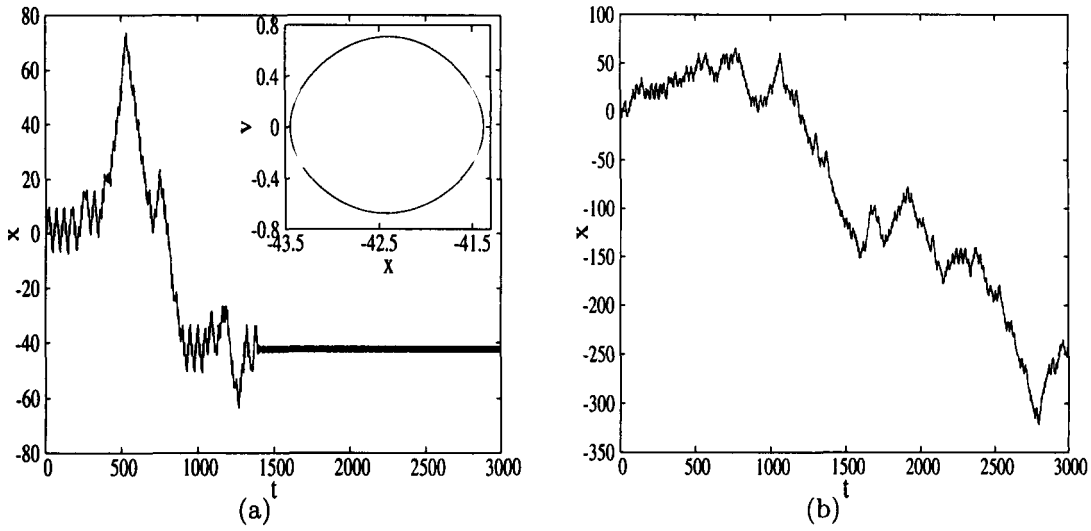

Figure 2.1: Plot of particle trajectory for $a = 0.5$ (main figure) and the corresponding phase space trajectory at large t(inset of fig. a) and particle trajectory for $a = 0.8$ (fig.b) with $\tau = 10$, $x(0) = \pi/2$, $v(0) = 0$, $\gamma_0 = 0.12$, $\phi = 0.35$, $\lambda = 0.9$.

In this work, we let the particle evolve for a long time so that the system reaches a steady state condition to investigate ratchet effect. Eq. 2.3 (for the deterministic case) and Eq. 2.4 (when noise is included) are solved using the second order Heun's method with time step size $\Delta t = 0.001$. For the calculation of deterministic average velocity (Eq. 2.5) we take $t_{max} = 10^6$ and $t_{tran} \approx 10^4$. We study the particle trajectories, the average velocities and the bifurcation diagrams. Similar studies were done earlier [21, 22, 25] for asymmetric periodic potentials. But in our work we consider a perfectly symmetric periodic potential. But instead of a uniform-friction-medium we consider a periodically varying friction coefficient.

2.3.1 Particle trajectories

The nature of the dynamics of the particle in a deterministic system is critically dependent on the amplitude a and frequency ω of the zero-mean external periodic drive [35]. For a dissipative system without any external drive, it goes to the only fixed point attractor at $v = 0$ and $x = (2n - 1)\pi/2$. However for a given (non-zero) amplitude and frequency of the drive the individual particle trajectories depend sensitively on the initial conditions. In the low amplitude regime (below a particular critical amplitude depending on the frequency) the particle, after initial transients, gets invariably trapped to a periodic attractor in some potential minima $x = (2n + 1)\pi/2$ $(n = 0, \pm 1, \pm 2, ...)$ and executes periodic motion within the potential well (Fig. 2.1a). On the average these cases give zero net current as is evident from the phase space trajectory (Inset, Fig. 2.1). Only beyond certain amplitude a (for a given initial condition and drive frequency ω), the particle starts evolving giving rise to either periodic or chaotic dynamics (Fig. 2.1b).

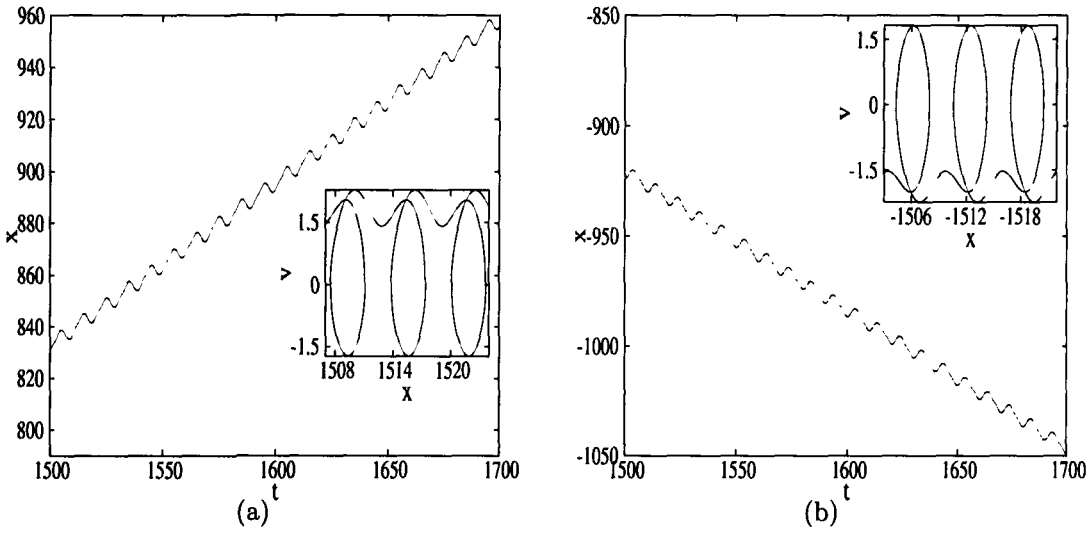

Figure 2.2: Particle trajectories (main figures) and the corresponding phase space plots (insets) showing different locking behaviour of the particle. For $a = 0.5926$ (a), the particle gets locked in the positive sense giving $< v >= v_\omega$ while for $a = 0.5925$ (b), the particle gets locked in the negative sense giving $< v >= -v_\omega$, with $\tau = 10$, $x(0) = \pi/2$, $v(0) = 0$.

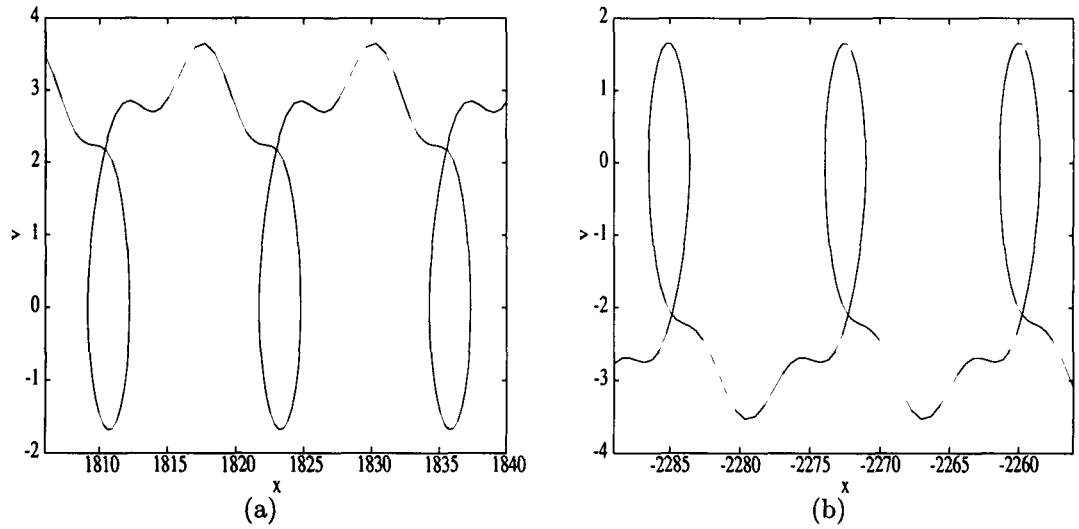

Figure 2.3: Particle locking giving rise to $< v >= +2v_\omega$ for $a = 1.183$ (Fig. 2.3a) and $< v >= -2v_\omega$ for $a = 1.16$ (Fig. 2.3b), $\tau = 10$, $x(0) = \pi/2$, $v(0) = 0$.

2.3.2 Phase locking

The deterministic dynamics of a particle in a driven system exhibits a phenomenon of phase locking in which the particle gets locked to the external drive [22, 25]. This phenomenon is sensitively dependent on the amplitude of driving all the other parameters like the frequency etc. being kept fixed. For some values of driving amplitude, the particle gets locked to the external drive in the positive sense giving rise to a positive average velocity, whereas for some other amplitudes, the particle may get trapped to the drive in the negative sense giving rise to a negative velocity (Fig. 2.2). For example, $a = 0.5926$ leads to phase locking in the positive sense giving rise to positive $< v >$ (Fig. 2.2a), while $a = 0.5925$ for the same initial conditions leads to locking in the negative sense giving a mean velocity $-< v >$ (Fig. 2.2b). The mean velocity $< v >$ for these phase locked trajectories can be $\pm v_\omega$ or multiples of it, where $v_\omega = T_{pot}/T_\Omega$ is the fundamental velocity and (T_{pot} is the spatial period of the potential and T_Ω is the time period of the external drive) [22]. Depending upon the number of spatial periods of the potential the particle traverses in one period of drive, the resulting velocity can be v_ω or multiples of that. For $a = 0.5931$ and $a = 0.592$,

the particle traverses one spatial period per period of drive as can be seen from the phase space trajectories (insets of Fig. 2.2 a and b). So the corresponding $< v >= \pm v_\omega$. Whereas for $a = 1.183$ and $a = 1.16$ the particle traverses two spatial periods per period of drive (Fig. 2.3a and b) giving $< v >= \pm 2v_\omega$ (Fig. 2.4). This locking behaviour is reflected in the variation of the mean velocity $< v >$ for a typical single particle trajectory (with the same initial condition ($x(0) = \pi/2$ and $v(0) = 0$) as a function of drive amplitude a (Fig. 2.4). As is seen from the figure there are a large number of current reversals as the driving amplitude a is varied. This is due to the different locking behaviour of the particle. As the border between the basins of the different attractors are very fine, slight change of the amplitude of the drive can lead the particle to a different basin of attraction giving rise to different $< v >$ (either $< v >= \pm v_\omega$ or multiples of that (Fig. 2.4). For our problem $T_{pot}=2\pi$, and for Fig. 3.4, $T_\Omega = 10$. So the fundamental velocity, $v_\omega = 0.6283$.

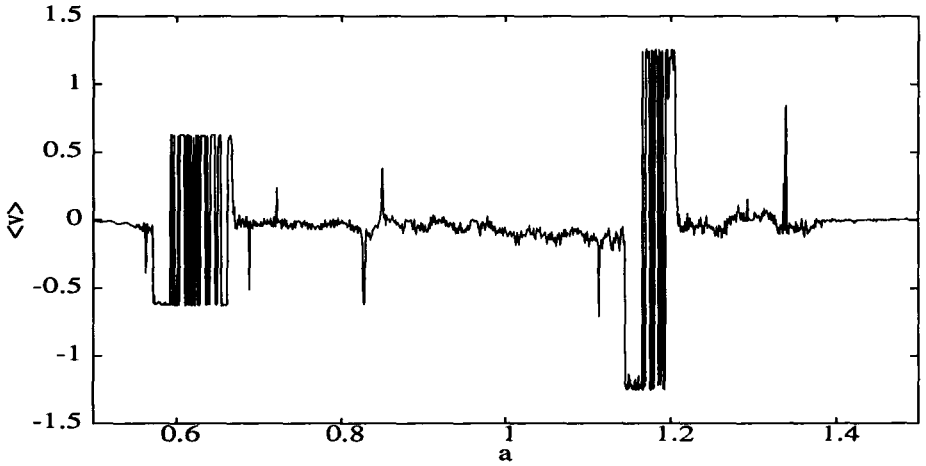

Figure 2.4: Variation of mean velocity $\langle v \rangle$ with amplitude a for a single particle; $v(0) = 0$, $x(0) = \pi/2$, $\gamma_0 = 0.12$, $\phi = 0.35$, $\lambda = 0.9$.

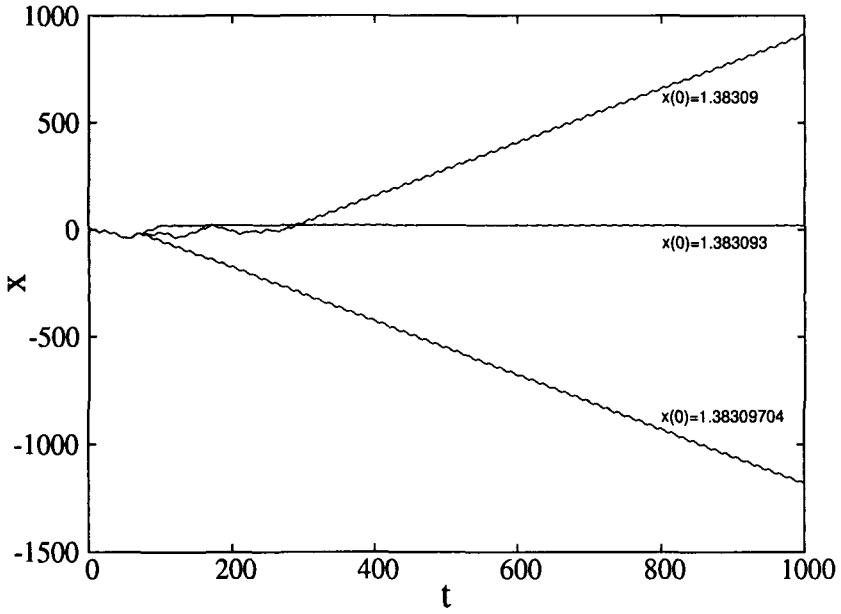

Figure 2.5: Particle trajectory for slightly different values of initial position $x(0) = 1.38309$ (top), $x(0) = 1.383093$ (middle) and $x(0) = 1.38309704$ (bottom); $v(0) = 0$, $\tau = 10$, $\gamma = 0.12$, $\phi = 0.35$.

2.3.3 Sensitivity to initial conditions and the need for ensemble averaging

The nature of the dynamics of a particle in the deterministic regime is extremely sensitive to the initial conditions. A slight variation in the initial conditions can lead to a totally different nature of the particle dynamics. This can be illustrated by the following observations. For $a = 0.7$ and $\tau = 10$, the initial condition $v(0) = 0$, $x(0) = 1.38309$ gives a transporting phase locked trajectory in the positive direction, whereas $v(0) = 0$, $x(0) = 1.383093$ gives locked periodic nontransporting trajectory and $v(0) = 0$, $x(0) = 1.38309704$ results in a transporting phase locked trajectory in the negative direction (Fig. 2.5). This is because of the the complex structure of the basins of attraction of the different attractors present. This sensitivity of the nature of the dynamics to the initial conditions demands that for physically meaningful net particle velocity for a given a and ω, there is a need of averaging over a large number of particle

trajectories corresponding to various initial conditions.

2.3.4 Ratchet current and bifurcation diagrams

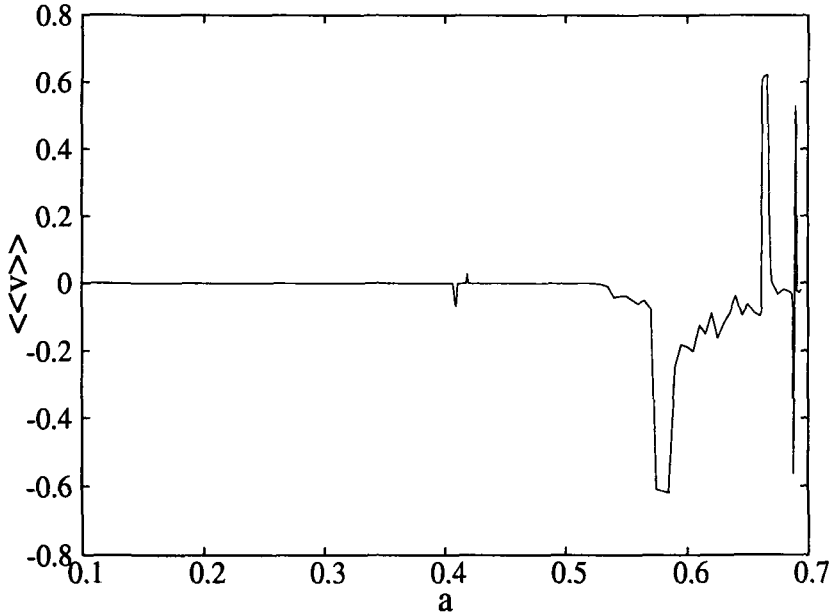

Figure 2.6: Variation of ensemble averaged velocity $\langle\langle v\rangle\rangle$ with amplitude of drive a, $\tau = 10$, $\gamma = 0.12$, $\lambda = 0.9$, $\phi = 0.35$.

As the nature of the particle trajectory depends critically on the chosen initial condition, for obtaining the ratchet current for the determinsitic ratchets we calculate the velocity (Eq. 2.6), averaged over an ensemble of N (typically equal to 500) particles. The particles are taken with identical initial velocities ($v_{ini} = 0$), but with initial positions uniformly distributed between two consecutive potential maxima [21]. We obtain ensemble averaged ratchet currents (Fig. 2.6) in the deterministic inertial inhomogeneous system with a symmetric and periodic potential. Also, we observe that the system shows current reversals as a function of the amplitude of the drive. On comparing with the single particle result, Fig. 2.4 (which has the same set of parameters as in Fig. 2.6) the numerous current reversals occurring in Fig. 2.4 disappears. This is due to the fact that different initial conditions select different attractors for a particular

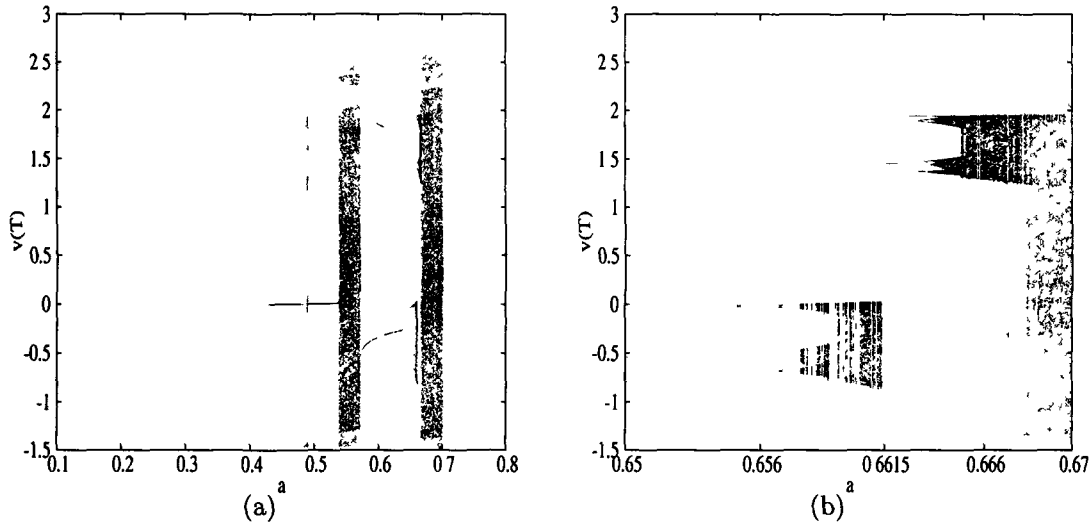

Figure 2.7: Bifurcation diagram corresponding to Fig. 2.6 (a). Fig. 2.7b is an amplified representation of Fig. 2.7a showing the amplitude at which the current reversal occurs in Fig.2.6; $\tau = 10$, $\gamma = 0.12$, $\lambda = 0.9$, $\phi = 0.35$.

amplitude, all the other parameters remaining the same. So, at a particular amplitude of drive, some particles of the ensemble may move in the positive direction and some may move in the negative direction with different multiples of the fundamental locking velocity v_ω. Others may show a chaotic dynamics giving rise to either zero velocity or some non-zero velocity on an average.

The deterministic dynamics of a particle in the underdamped regime has a complex nature due to the presence of multiple attractors and the intricate structure of the basins of attraction of these attractors, as has been hinted above. As a result depending upon the parameters, the particles may show either a chaotic or a periodic dynamics. The presence of both chaotic and regular dynamics can be seen from the bifurcation diagram which are obtained by recording the values of $\dot{x}(t_p)$ at times $t_p = n_p T$, for each value of the control parameter (the amplitude of the external drive), where T is the period of the external drive and n_p is an integer. Fig. 2.7a shows that the particle exhibits regimes of periodic and chaotic dynamics as a function of the control parameter a.

The ratchet current is found to undergo reversals as a function of the amplitude of drive a. The single particle showing multiple current reversals (Fig. 2.4) can be attributed to the different locking behaviour of the particle to the external drive [22]. For slight change of the driving amplitude, keeping all the other parameters fixed, the nature of locking may change (Fig. 2.2a and Fig. 2.2b) leading to a current reversal. On averaging over different initial condition, these many reversals disappear as discussed above. However there are reversals in the ensemble averaged ratchet current also for example at $a = 0.6615$ for the parameters as in Fig. 2.6. A comparision with the corresponding bifurcation diagram shows that the amplitude at which the current reversal occurs, there is a bifurcation in the dynamics of the particle from a chaotic to a periodic regime (Fig. 2.7b). This observation agrees with Mateo's conjecture [21] which atributes the current reversals in a deterministic system to such a bifurcation. Though the occurrence of a reversal in the ensemble averaged ratchet current can be attributed to the bifurcation from chaotic to regular dynamics, the mere presence of such a bifurcaton does not gurantee a current reversal [20]. There could be many such bifurcations (for example at $a = 0.57$ in Fig. 2.7a), but without an accompanying current reversal.

2.3.5 Frequency dependence of particle dynamics

The nature of the particle dynamics in deterministic ratchets is found to be dependent on the frequency of external driving $\omega = 2\pi/\tau$. We studied the dynamics of the particle in the deterministic inhomogeneous ratchet system for three values of the driving frequency, i.e for $\tau = 10$ (Fig. 2.6), $\tau = 100$ and 1000 (Fig. 2.8). The nature of the particle current and its magnitudes are found to change with the driving frequency. This can be inferred from a comparision of the variation of the ensemble averaged current as a function of the amplitude of driving a for the three values of the driving frequency, $\tau = 10$ (Fig. 2.6), $\tau = 100$ and 1000 (Fig. 2.8). It is observed that for different frequencies,

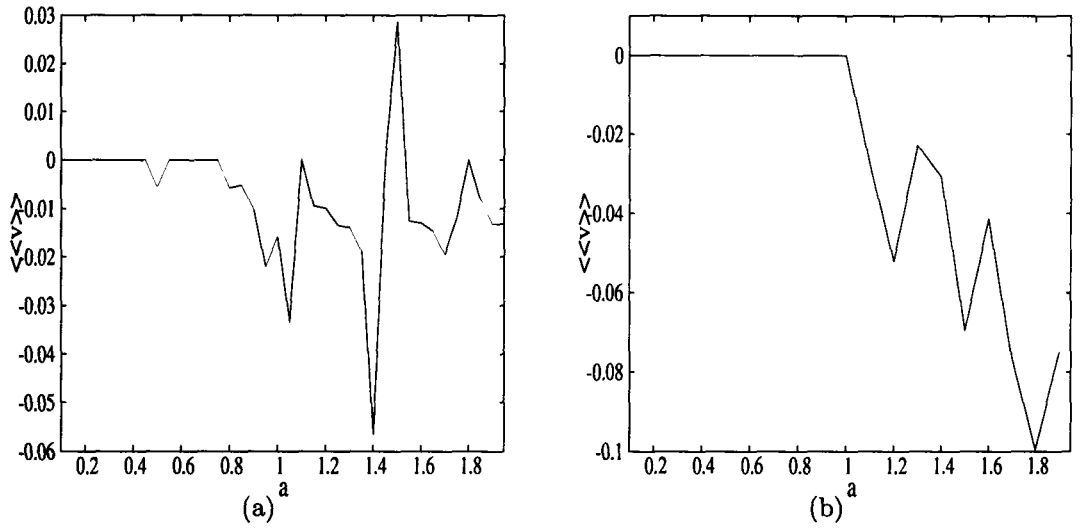

Figure 2.8: Variation of ensemble averaged velocity $\langle\langle v \rangle\rangle$ with amplitude of drive a for $\tau = 100$ (a) and $\tau = 1000$ (b); $\gamma = 0.12$, $\lambda = 0.9$, $\phi = 0.35$.

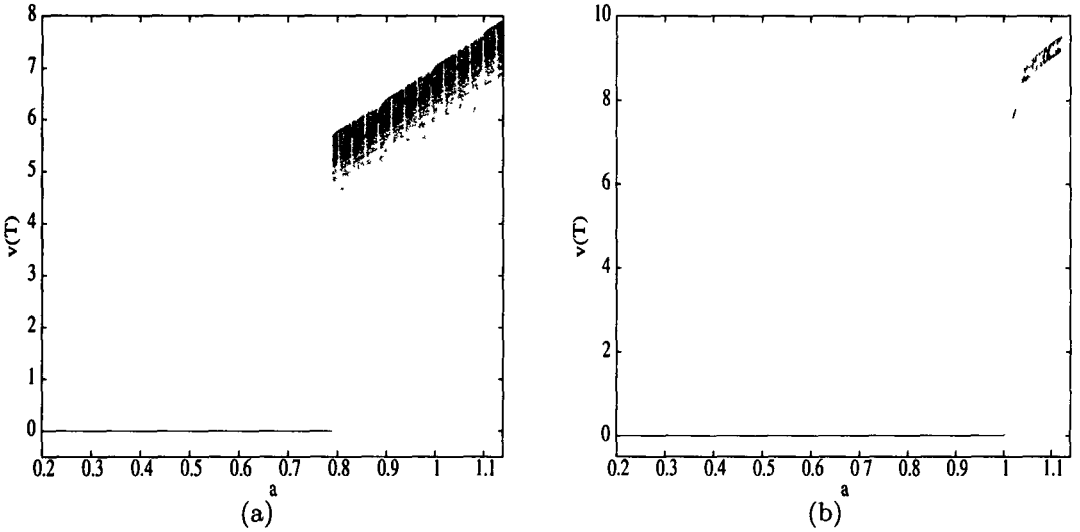

Figure 2.9: Bifurcation diagram for $\tau = 100$ (a) and $\tau = 1000$ (b); $x(0) = \pi/2$, $v(0) = 0$, $\gamma = 0.12$, $\lambda = 0.9$, $\phi = 0.35$.

particle current starts developing at different amplitudes. This is because the amplitude of the drive at which the particle starts evolving out of a single-well trapped-state differs with frequency. At higher frequencies, the particle gets out of the well at smaller amplitudes leading to particle current and vice versa. From the bifurcation diagrams for different frequencies (Fig. 2.7 and Fig. 2.9) we observe that the amplitude at which the particle develops chaotic dynamics is different for different frequencies. At lower frequencies, chaos develops at a higher amplitude of drive than that for higher fequencies. For example, for $\tau = 10$, 100 and 1000, chaotic dynamics appears at amplitudes $a = 0.5$ (Fig. 2.7a), $a = 0.8$ (Fig. 2.9a) and $a = 1.02$, respectively (Fig. 2.9b). As these deterministically induced chaos can play a role analogous to that of thermal noise, the occurrence of chaos can aid the particle in moving out of the potential wells. Hence for very low frequencies of the drive $\tau = 1000$ (Fig. 2.9b), particle currents are obtained only beyond the critical tilt ($a = 1.0$ for our case) whereas for $\tau = 10$ current starts developing essentially around $a = 0.55$. Also, whereas for the slower drive $\tau = 1000$ there is no current reversal in the range of drive amplitudes shown, for $\tau = 10$ and 100 there are several reversals of the direction of current in the same range of a. Thus, the mean velocity is expected to show a very complex behaviour in the $(a - \omega)$ space [35].

2.3.6 Role of frictional inhomogeneity and dependence on initial driving phase

We studied the role of the frictional inhomogeneity in shaping the nature of the particle dynamics in the deterministic ratchet system under consideration. In our work, we consider particle motion in a symmetric periodic potential in the presence of a space dependent friction coefficient $\gamma(x) = \gamma_0(1 - \lambda \sin(kx + \phi))$. Asymmetry is introduced into the system via the space dependent friction. So in our case, the frictional inhomogeneity, characterised by the parameters λ

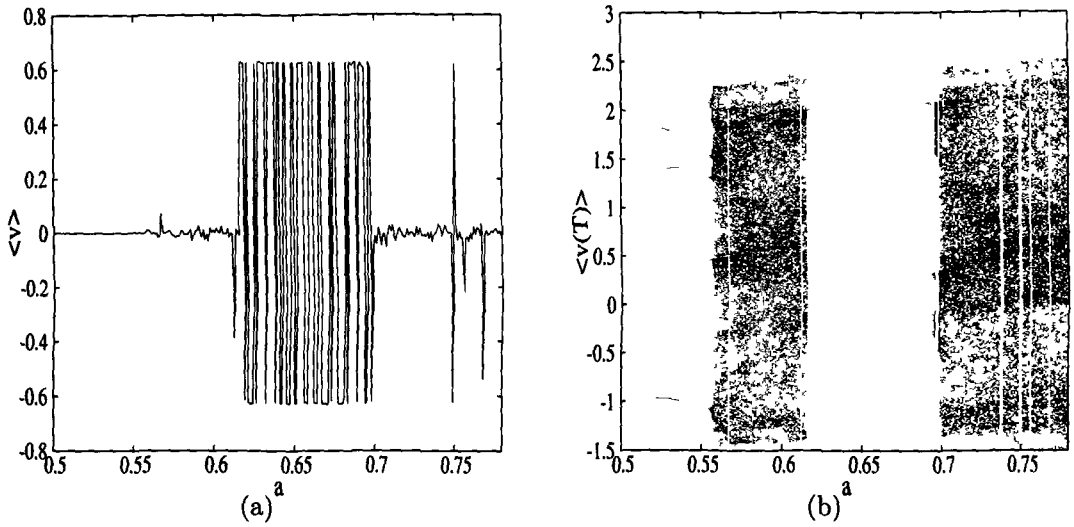

Figure 2.10: $\langle v \rangle$ versus a plot for a single particle with $\lambda = 0$ (a) and the corresponding bifurcation diagram (b); $\tau = 10$, $x(0) = \pi/2$, $v(0) = 0$, $\gamma = 0.12$, $\phi = 0.35$. .

and ϕ, is the cause of the asymmetry in the problem. We studied the particle transport taking into consideration different degrees of asymmetry by taking different values of the frictional inhomogeneity parameter λ, with $\phi = 0.35$, starting with $\lambda = 0$. For our case λ (with $\phi \neq n\pi$, $n = 0, \pm 1, ...$) plays a role analogous to the potential asymmetry in the uniform friction case. The variation of the steady state ($t \to \infty$) velocity with the driving amplitude both for a single particle, namely $\langle v \rangle$ (Fig. 2.10a), as well as when averaged over a large number of realizations, $\langle\langle v \rangle\rangle$ (Fig. 2.11) was studied. It is observed that even with zero asymmetry, finite particle current is obtained for a large range of driving amplitudes for both cases. For the single particle case, the particle velocity $\langle v \rangle$, undergo large number of reversals as a function of the driving amplitude (Fig. 2.10(a)) but are finite. The ensemble averaged velocity $\langle\langle v \rangle\rangle$ are not only finite but they vary smoothly with drive amplitude. The presence of particle current in a symmetric system is obviously an erroneous result. Also the bifurcation diagrams with inhomogeneity (Fig. 2.7a) and without inhomogeneity (Fig. 2.10(b)) on comparison appear very similar and do not provide any clue to

the error. The error could only come from lack of averaging over the initial phase ϕ_0 of the zero-mean external periodic drive $F(t)$. The relevance of averaging over initial phase has earlier been discussed for Hamiltonian systems [30, 32].

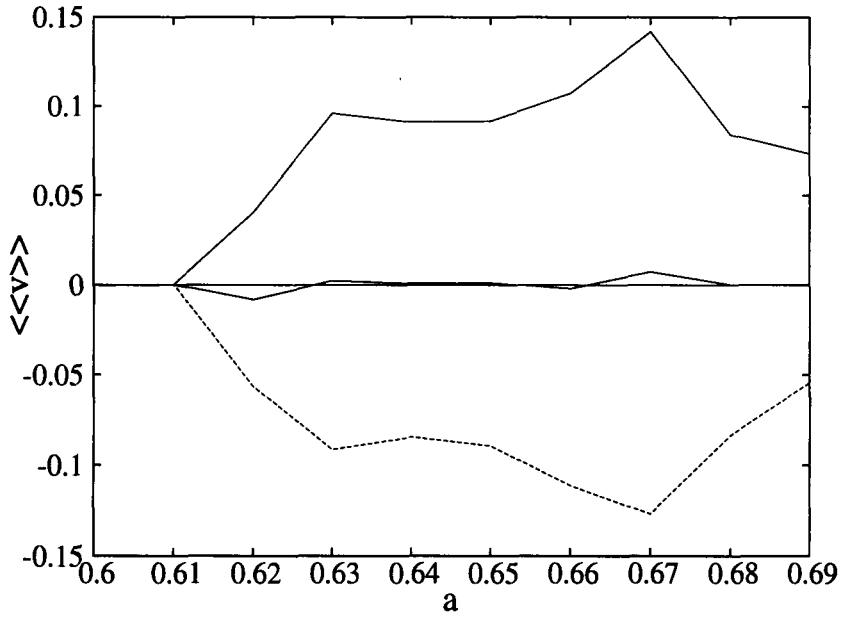

Figure 2.11: Plot of $\langle\langle v\rangle\rangle$ versus a with zero inhomogeneity ($\lambda = 0$) for initial phase of the external drive $\phi_0 = 0$ (lower dotted line) and $\phi_0 = \pi$ (upper solid line). Middle line shows $\langle\langle v\rangle\rangle$ after averaging over initial phases. Zeroline is drawn for reference; $\tau = 10$, $\lambda = 0.9$, $\gamma = 0.12$, $\phi = 0.35$.

In order to examine the role of the initial phase of the drive in determining the particle current, we calculated the ensemble averaged velocity $\langle\langle v\rangle\rangle$ as a function of the driving amplitude for two values of the initial phase $\phi_0 = 0$ and π of the external drive $F(t)$ of period $\tau = 10$ with zero inhomogeneity ($\lambda = 0$) (Fig. 2.11). It can be clearly seen that the initial bias due to a fixed value of ϕ_0 determines the steady state current giving non-zero current even with zero asymmetry. For $\phi = 0$ and π, the velocities are equal and opposite. Hence when averaged over the initial phase, we get zero current for the symmetric situation (Fig. 2.11) which is a physically viable result. So in order to get a sensible ratchet current one needs, therefore, to average over the initial phase ϕ_0 of the drive too. The figure also indicates that averaging should be carried out over at

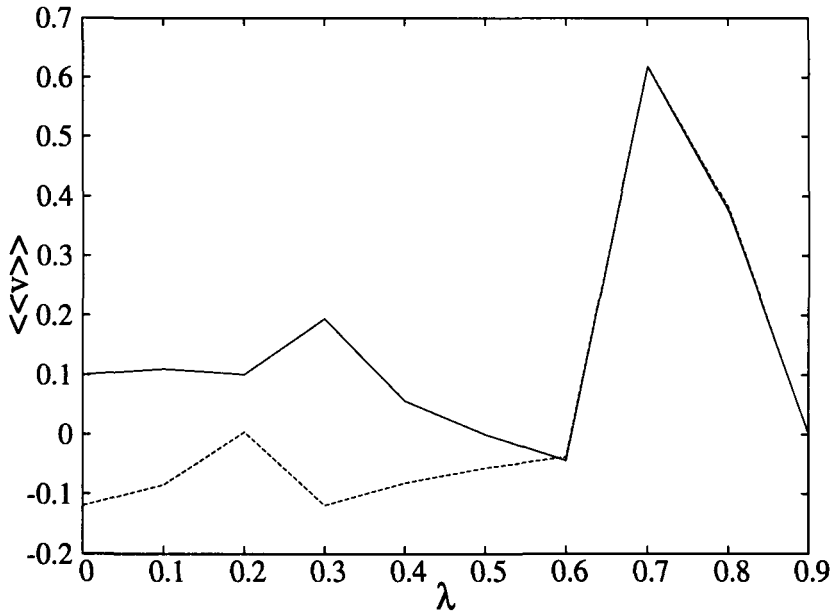

Figure 2.12: Variation of $\langle\langle v\rangle\rangle$ with the asymmetry parameter λ for initial phase of the external drive $\phi_0 = 0$ (lower dotted line) and $\phi_0 = \pi$ (upper solid line); $\tau = 10$, $a = 0.67$, $\gamma = 0.12$, $\phi = 0.35$.

least two values of ϕ_0 which differ by π .

The dependence of the current on the initial phase of the drive was found to be dependent on the degree of asymmetry. The ensemble averaged particle currents are found to be same irrespective of the initial phase beyond a particular value of the inhomogeneity parameter λ (=λ_c) (Fig. 2.12). Thus the averaging over initial phase is required only for small inhomogeneities whereas for large asymmetries, $\langle\langle v\rangle\rangle$ does not seem to depend on the initial phase ϕ_0. For our case the critical inhomogeneity $\lambda = \lambda_c \approx 0.6$ (Fig. 2.12). In the case of uniform friction the critical potential-asymmetry $b \approx 0.25$ which is what has been used incidentally by Mateos [21] and others corresponding to their parameter values.

For a qualitative explanation of this dependence of the nature of the dynamics on the inhomogeneity parameter, we studied the nature of the particle trajectories which were found to be different for different values of λ.

The nature of the variation of the ensemble averaged velocity $\langle\langle v\rangle\rangle$ with the inhomogeneity parameter can be understood by looking at the corresponding

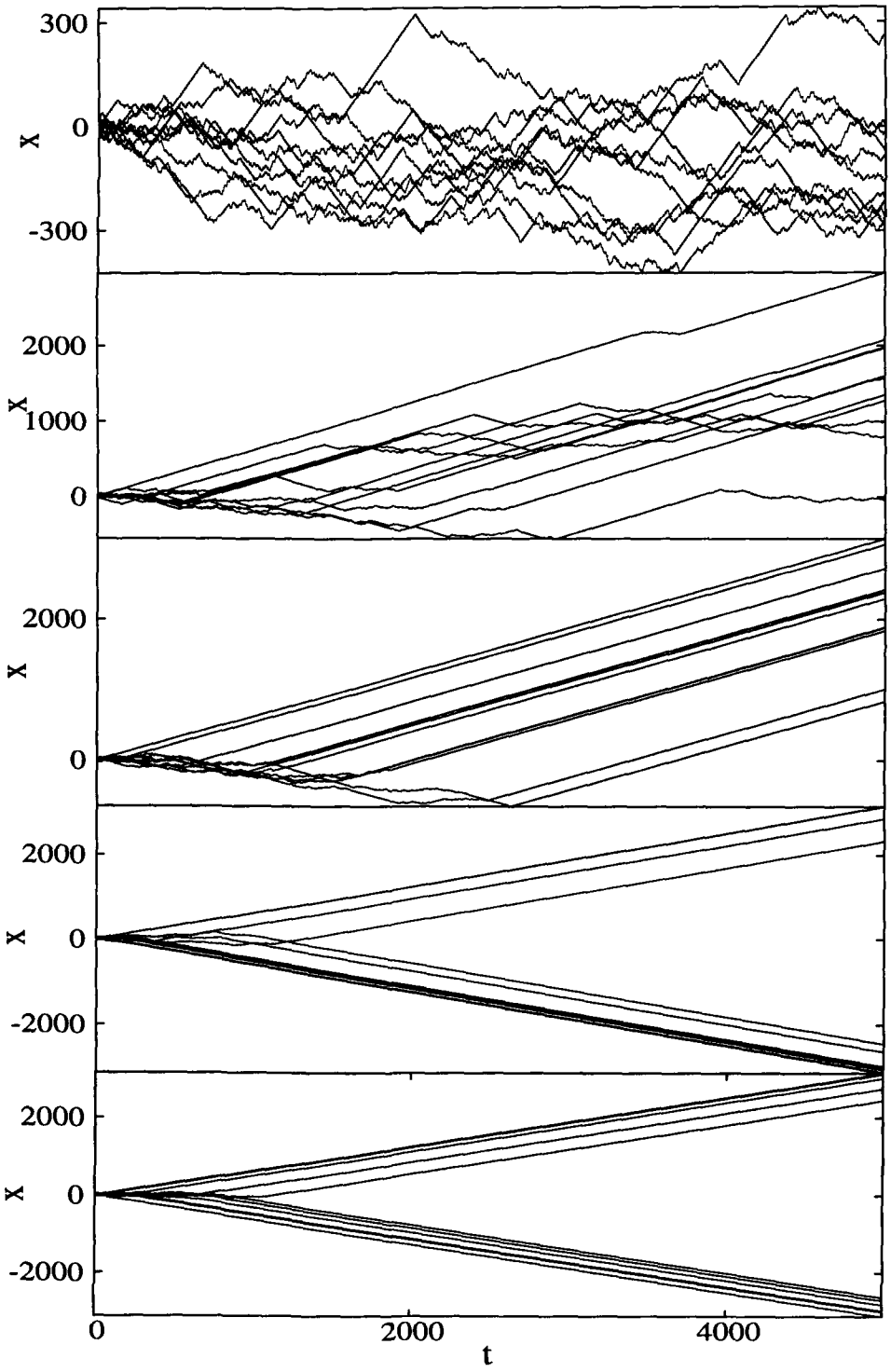

Figure 2.13: Particle trajectories for different values of inhomogeneity parameter λ ($\lambda = 0.9$ (a) to $\lambda = 0.5$ (e)); $\tau = 10$, $a = 0.67$, $\gamma = 0.12$, $\phi = 0.35$. Trajectories are shown for ten different sample initial conditions. Though the trajectories appear to be straight line in the scale of the figures, they are oscillatory as can be seen in Fig. 2.15 where a magnified single particle trajectory for the same parameters is shown.

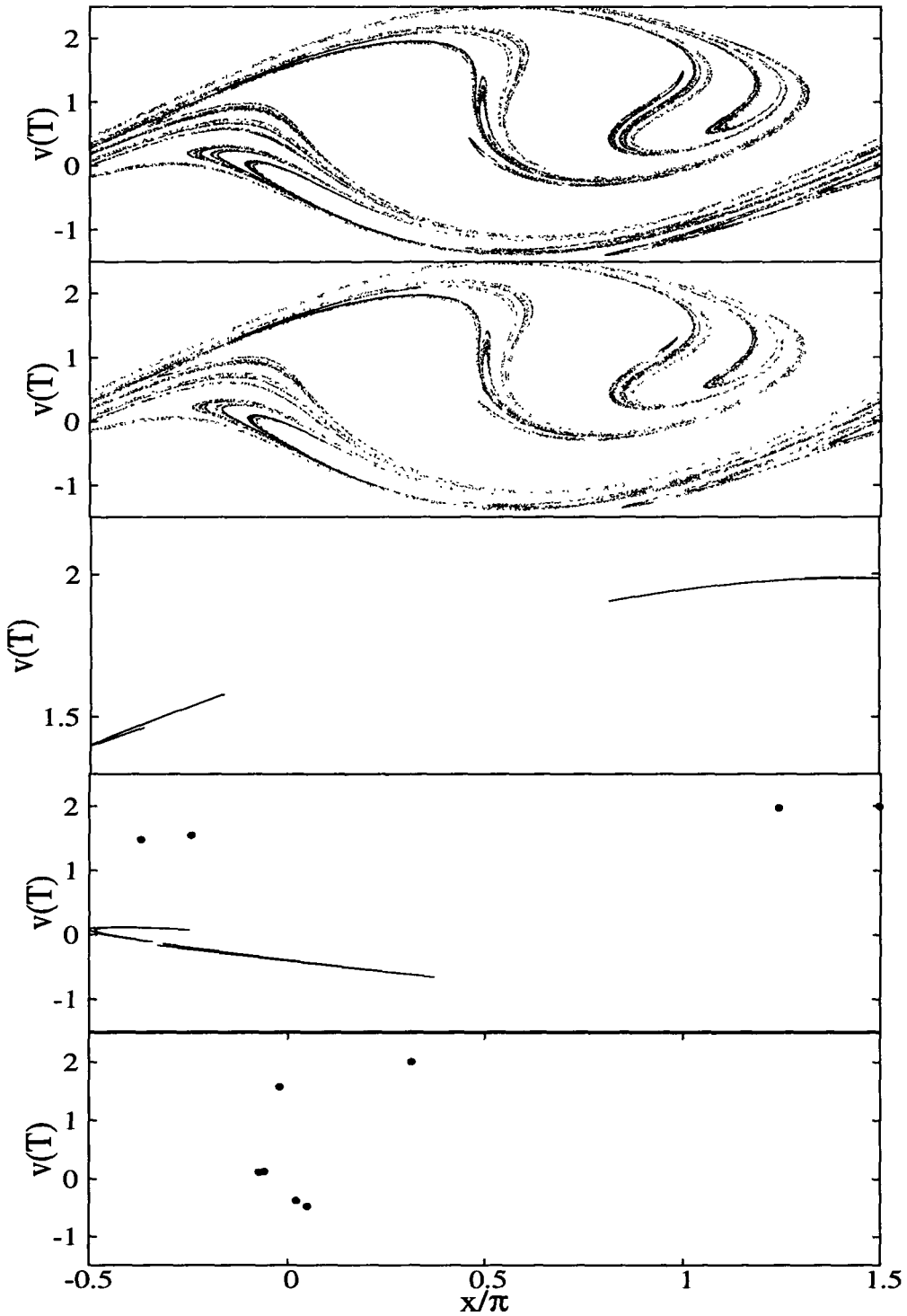

Figure 2.14: Stroboscopic plots corresponding to Fig. 2.13 for different values of inhomogeneity parameter λ ($\lambda = 0.9$ (top) to $\lambda = 0.5$ (bottom); $\tau = 10$, $a = 0.67$, $\gamma = 0.12$, $\phi = 0.35$.

particle trajectories $x(t)$ (Fig. 2.13) and the the stroboscopic phase points at regular time intervals $t = n\tau, n = 1, 2, 3, ..$ (Fig. 2.14) for various values of the inhomogeneity parameter λ, keeping the other parameters same as those used for obtaining Fig. 2.12 - amplitude $a = 0.67$, period $\tau = 10$ and initial phase $\phi_0 = 0$ of the external field $F(t)$. The nature of the particle trajectories are found to vary with the inhomogeneity parameter. For $\lambda = 0.9$ and 0.8 the trajectories are a mixture of quasiperiodic transporting regimes and chaotic regimes as in Fig. 2.15a. For $\lambda = 0.9$ quasiperiodic transporting regions are in both positive and negative directions. They persist for short duration and on averaging again give way to chaotic transport resulting in no net transport.

For $\lambda = 0.8$, the quasiperiodic transporting trajectories in the positive direction are longer interrupted by shorter such trajectories in the negative direction and chaotic trajectories giving finite ratchet current in the positive direction. For $\lambda = 0.7$ all the trajectories (after some initial time depending upon the initial conditions) become quasiperiodic transporting in the same positive direction as in Fig. 2.15b. This gives rise to $\langle\langle v \rangle\rangle$ which is close to the maximum ($=2\pi/\tau$) corresponding to the fundamental velocity. The corresponding stroboscopic plot shows their chaotic nature. As the value of λ is lowered from 0.7 to 0.6 we obtain a mixture of transporting quasiperiodic trajectories and transporting regular periodic trajectories (as can be seen from the stroboscopic plots). However, as the value $\lambda = 0.6$ is reached their directions of average motion gradually become equal giving zero current at $\lambda = 0.6$. As mentioned earlier, $\langle\langle v \rangle\rangle$ is independent of ϕ_0 for the considered parameters. For values of $\lambda \leq 0.5$ all the trajectories are transporting regular periodic with same average slope but differing in direction. For $\phi_0 = 0$ there are more negative-slope trajectories and vice-versa for $\phi_0 = \pi$. The five-paneled figures Fig. 2.13 and Fig. 2.14 gives a qualitative mechanism for the explanation of Fig. 2.12 and underlines the importance of averaging over the initial phase ϕ_0 at smaller inhomogeneities.

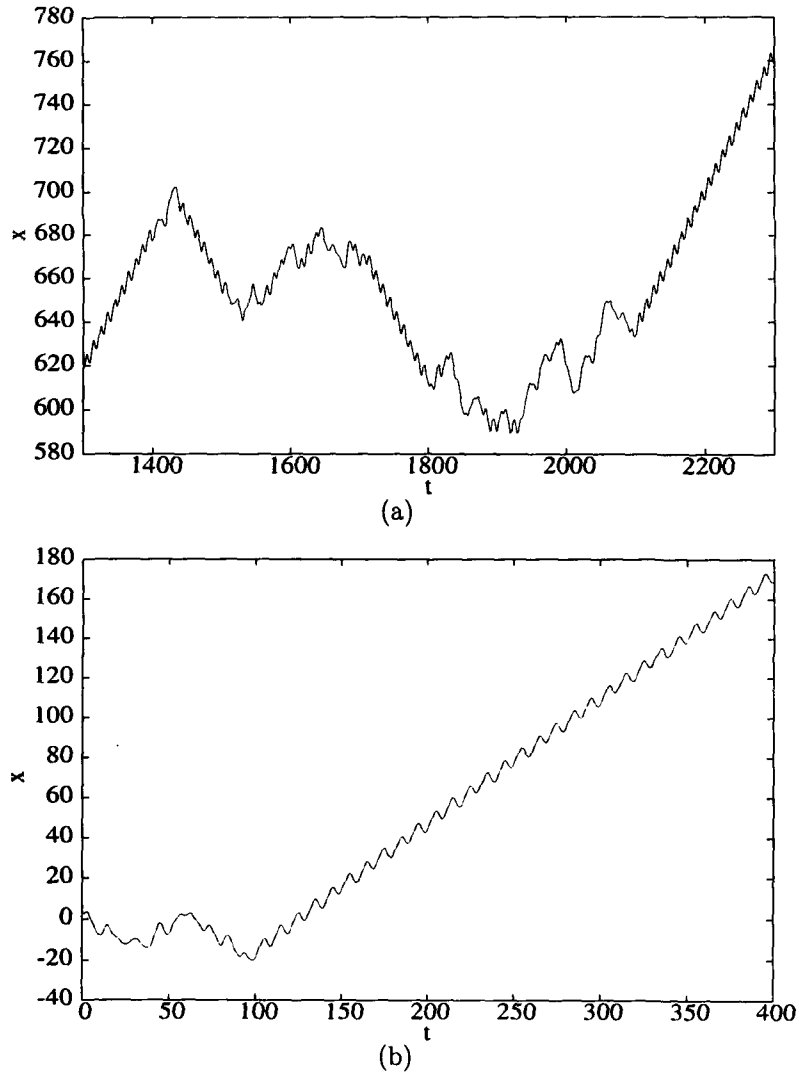

Figure 2.15: Particle trajectory for a single initial condition showing the presence of transporting trajectory segments in positive and negative direction interrupted by chaotic regime as for $\lambda = 0.9$ and 0.8 (a). (b) shows a transporting trajectory in the positive direction as for $\lambda = 0.7, 0.6$ and 0.5. Other parameters are same as in Fig. 2.13.

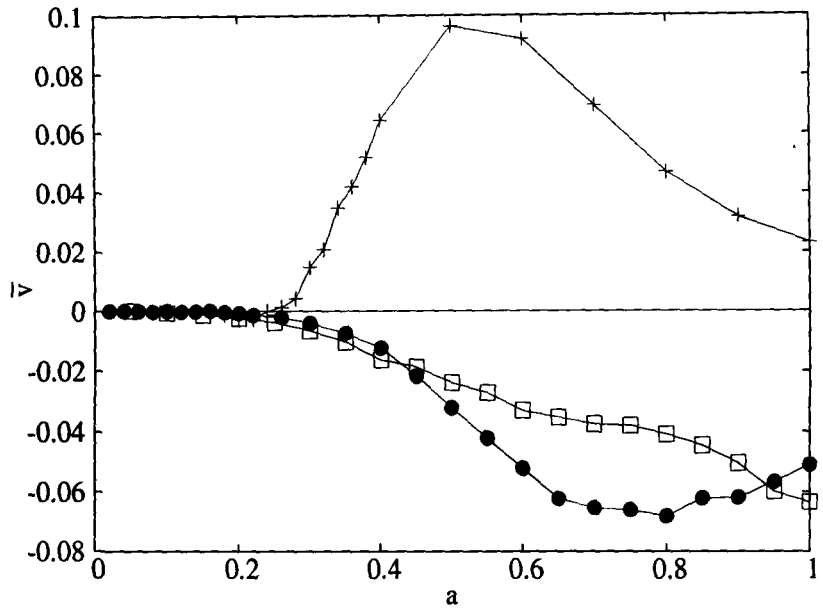

Figure 2.16: Plot of $\bar{v}$ versus a in the presence of noise, for three values of τ, $\tau = 1000$ (line with crosses), $\tau = 100$ (line with circles) and $\tau = 10$ (line with squares) with $T = 0.4$, $\gamma = 0.12$, $\lambda = 0.9$, $\phi = 0.35$.

2.3.7 Role of noise and low amplitudes of drives

In deterministic ratchets, because of the complex structure of the basins of attraction and the presence of multiple attractors in phase space [39], the nature of the current is sensitively dependent on the initial conditions. The presence of noise in the system, however, makes the particle dynamics independent of the initial conditions allowing the particle to explore all the existing attractors. As a result the chaotic behaviour of the system disappears. The average velocity shows a relatively smoother variation with the amplitude of external drive than in the deterministic case. In Fig. 2.16, the variation of $\bar{v}$ with a is shown for three different values of drive frequencies, keeping all the other parameters fixed.

With noise, appreciable ratchet current is obtained even at low amplitudes, where there was no current in the deterministic case (Fig.2.16). This is because, the presence of noise aids the particles to overcome the potential barrier which it could not have done otherwise. Hence the presence of noise plays a non-negligible

role in obtaining ratchet current in the low amplitude regime, contrary to what has been mentioned by others [21]. The same effect of noise has been shown in a different system using the matrix continued fraction method [42].

2.4 Conclusion

In this work the deterministic ratchet current was obtained in a periodically driven symmetric potential in the presence of frictional inhomogeneity (most of the earlier works were with a driven asymmetric potential). The particle dynamics shows similar characteristic as in an asymmetric potential. Initial conditions and the control parameters play a major role in shaping the nature of the dynamics. For low amplitudes of drive with low values of asymmetry in the system, the initial phase of the drive is found to play a non-negligible role. At these regimes, we show that averaging over initial conditions and initial phases of the external drive is essential to obtain realistic averages. With noise, ratchet current is obtained at amplitude regimes where there is no current in the deterministic systems.

Bibliography

[1] Shantu Saikia, Mangal C. Mahato, Physica A 389, 4052 (2010).

[2] P. Reimann, Phys. Rep. 57, 361 (2002).

[3] R. D. Astumian, Science, 276, 917 (1997); R. D. Astumian and P. Hänggi, Phys. Today 55, 33 (2002).

[4] R. P. Feynmann, R. B. Leighton and M. Sands, The Feynmann Lectures in Physics, Vol.1 (Phillipines: Addison-Wesley) Chapter 46.

[5] L. Machura, M. Kostur, F. Marchesoni, P. Talkner, P. Hänggi and J. Łuczka, J. Phys. Cond. Matter 17, S3741 (2005)'

[6] A. Ajdari and J. Prost, C. R. Acad. Sci. Paris 315, 4635 (1992).

[7] R. Landaurer, J. Stat. Phys. 53, 233 (1988).

[8] M. Büttiker, Z. Phys. 68, 161 (1987); M. C. Mahato, T. P. Pareek and A. M. Jayannavar, Int. J. Mod. Phys. B 10, 3857 (1996); M. C. Mahato, Indian J. Phys. 78, 693 (2004).

[9] Ya. M. Blanter and M. Büttiker, Phys. Rev. Lett. 81, 4040 (1988).

[10] R. Benjamin and R. Kawai, Phys. Rev. E, 77, 051132 (2008).

[11] S. Saikia and M. C. Mahato, J. Phys. Cond. Matter 21, 175409 (2009); W. L. Reenbohn, S. Saikia, R. Roy and M. C. Mahato, Pramana J. Phys. 71, 297 (2008).

[12] W. L. Reenbohn and M. C. Mahato, J. Stat. Mech. P03011 (2009).

[13] M. C. Mahato and A. M. Jayannavar, Phys. Lett. A 209, 21 (1995); D. R. Chiavlo, and M.M. Millonas, Phys. Lett. A 209,26 (1995).

[14] I. Zapata, J. Łuczka, F. Sols, and P. Hänggi, Phys. Rev. Lett. 80, 829 (1998).

[15] S. Flach, O. Yevtushenko and Y. Zolotaryuk, Phys. Rev. Lett. 84, 2358 (2000).

[16] P. Hänggi and F. Marchesoni, Rev. Mod. Phys. 81, 387 (2009).

[17] P. Jung, J. G. Kissner and P. Hänggi, Phys. Rev. Lett. 76, 3436 (1996).

[18] R. Bartussek, P. Hänggi and J. G. Kissner, Europhys Lett. 28 (7), 459 (1994).

[19] J. F. Chauwin, A. Ajdari and J. Prost, Europhys Lett. 27, 421 (1994); *ibid* 32, 373 (1995).

[20] A. Kenfack, S. M. Sweetnam and A. K. Pattanayak, Phys. Rev. E 75, 056215 (2007).

[21] J. L. Mateos, Phys. Rev. Lett. 84, 258 (2000).

[22] M. Barbi and M. Salerno, Phys. Rev. E 62, 1988 (2000).

[23] C. M. Arizmendi, F. Family and A. L. Salas-Brito, Phys. Rev. E 63, 061104 (2001).

[24] M. Borromeo, G. Constantani and F. Marchesoni, Phys. Rev. E 65, 041110 (2002).

[25] H. A. Larrondo, F. Family and C. M. Arizmendi, Physica A 303, 67 (2002).

[26] L. Cai, Physica A 389, 362-366 (2010).

[27] H. Risken, *The Fokker-Planck Equation*, Springer-Verlag, Berlin, 1989.

[28] F. Marchesoni, S. Savelev and F. Nori, Phys. Rev. E 73, 021102 (2006).

[29] M. F. Carusela, A. J. Fendrik and L. Romanelli, Physica A 388, 4017 (2009).

[30] O. Yevtushenko, S. Flach, and K. Richter, Phys. Rev. E 61, 7215 (2000).

[31] S.M. Soskin, O.M. Yevtushenko, and R. Mannella, Phys. Rev. Lett. 95, 224101 (2005).

[32] D. Hennig, L. Schimansky-Geier and P. Hänggi, Eur. Phys. J. B62, 493 (2008).

[33] M. N. Popescu, C. M. Arizmendi, A. L. Salas-Brito and F. Family, Phys. Rev. Lett 85, 3321 (2000).

[34] H. A. Larrondo, C. M. Arizmendi and F. Family, Physica A 320, 49 (2003).

[35] F. Family, H. A. Larrondo, D. G. Zarlenga and C. M. Arizmendi, J. Phys. Cond. Matter 17, S3719, (2005).

[36] L. Gorre-Talini, J. P. Spatz, and P. Silberzan, Chaos 8, 650 (1998); I. Derenyi and R. D. Astumian, Phys. Rev. E 58, 7781, 1998; D. Ertas, Phys. Rev. Lett. 80, 1548 (1998).

[37] T. Hondou, and Y. Sawada, Phys. Rev. Lett. 75, 3269 (1995).

[38] M. Barbi and M. Salerno, Phys. Rev. E 63, 066212, (2001).

[39] J. L. Mateos, Physica A 325, 92-100, (2003).

[40] C. M. Falco, Am. J. Phys. 44, 733 (1976).

[41] A. Barone, and G. Paternó, *Physics and Applications of the Josephson Effect*, John Wiley & Sons, New York, Inc., 1982.

[42] S. Denisov, P. Hänggi, and J. L. Mateos, Am. J. Phys. 77, 602606 (2009).

[43] B. A. Huberman, J. P. Crutchfield, and N. H. Packard, Appl. Phys. Lett. 37, 750 (1980); D. D'Humieres, M. R. Beasley, B. A. Huberman, and A. Libchaber, Phys. Rev. A 26, 3483 (1982).

Chapter 3

Ratchet effect in a driven inertial periodic potential system.

3.1 Introduction

The investigation of particle motion in periodic potentials has obvious relevance in condensed matter studies, for example the motion of ions in a crystalline lattice. Due to the finite non-zero temperatures, this motion, becomes stochastic in nature due to the presence of inherent fluctuations. In this chapter we present the results of our studies on underdamped particle motion in periodic and symmetric potentials with space dependent friction coefficient in the presence of noise [1]. This work is a logical extension of the work presented in the previous chapter where particle motion in the deterministic regime was studied and the role of noise in determining the ratchet current was hinted at.

The stochastic particle motion can be approximately described by a Langevin equation with suitable model potentials. Depending on the problem at hand the motion is either considered heavily damped, almost undamped, or in the intermediate situation mildly damped (or underdamped). In many a situations in the former two extreme cases analytical solution of the Langevin equation (or the corresponding Fokker-Planck equation) becomes possible. However, in the un-

derdamped situation, barring a few special cases, numerical methods are used to solve the equation of motion of the particle [2]. Owing to various kinds of errors and approximations involved in these (numerical) methods, exact quantitative solutions are not possible. However, the method can reveal useful qualitative trends in the behaviour of the particle motion. For instance, recently it was shown [3] that a Brownian particle, moving in an asymmetric but periodic potential and subjected to a symmetric periodic external drive (which adds to zero when averaged over a period), acquires a net motion when the parameters of the problem are chosen suitably. Such a net particle current without the application of any net external bias or potential gradient in the presence of thermal noise is called thermal ratchet current and the system giving such a current is termed as thermal ratchet [4]. Here the equilibrium condition of detailed balance is not applicable because the system was driven far away from equilibrium by rocking it periodically in the presence of noise. It was further shown that this system can even exhibit absolute negative mobility [5]. This prediction has already been found to be true experimentally [6]. It shows that in underdamped conditions or in the inertial regime diverse possibilities can be (qualitatively) uncovered by (numerically) solving the appropriate equations of motion.

In the above important examples [3, 5] the potential asymmetry was one of the necessary conditions for realization of ratchet current. The particle had to surmount the same potential barrier on either direction; only the slopes leading to the top of the barrier differed. A sinusoidal potential, for example, having no such asymmetry would not have yielded the ratchet current. In the present work, we consider similar particle motion in a sinusoidal potential $V(x) = -V_0 sin(kx)$. However, instead of a uniform friction coefficient of the medium we consider a model nonuniform space-dependent friction coefficient $\gamma(x)$ of the medium. In particular, we consider a sinusoidally varying $\gamma(x) = \gamma_0(1-\lambda sin(kx+\phi))$ exactly similar to the potential but with a phase lag, ϕ. A simple illustrative example of the model can be imagined as a stationary pressure wave established in air

giving a periodic $\gamma(x)$ for particle motion along x. An array of ions with the periodicity of $\gamma(x)$ but shifted a little to give a phase lag ϕ will just fit our model for a charged particle motion along x. Here the potential is symmetric and periodic. However, the directional symmetry of the system is broken by a phase shift in the similarly periodic $\gamma(x)$. The model form of a periodically varying friction $\gamma(x)$ has been justified earlier from mode-coupling theory of adatom motion on the surface of a crystal of identical atoms [7]. Also, the equation of motion has a direct correspondence with the resistively and capacitatively shunted junction (RCSJ) model of Josephson junctions; the term describing the nonuniformity of friction having an one-to-one correspondence with the '$\cos\phi$' term in the RCSJ model [8]. Apart from the close analogy with RCSJ model of Josephson junctions, the inhomogeneous systems with nonuniform diffusion coefficients have been investigated earlier by Landauer [9] and Büttiker [10]. Büttiker has shown that a particle moving in a one dimensional periodic potential with a similarly periodic diffusion coefficient, but with a phase difference will experience an effective constant force in one direction. Blanter and Büttiker obtained ratchet effect [11] in a system with similarly varying nonuniform temperature and hence nonuniform diffusion coefficient. The same has been obtained later in a detailed work by Benjamin and Kawai [12] who consider similarly and simultaneously varying periodic temperature and friction in space in the overdamped limit. However, as stated earlier, in this work we consider friction coefficient to be nonuniform keeping the temperature uniform. Since the diffusion coefficient is determined by the friction coefficient either seperately or together with the temperature, the arguments of Büttiker [10] holds equally in the present case too. There is a difference, however, between the role played by friction inhomogeneity and temperature inhomogeneity. Through the pioneering 'blow-torch' work of Landauer, temperature inhomogeneity giving current is a natural consequence [9, 11]. But in case of friction inhomogeneity, no such obvious inference can be drawn. Temperature along with the potential function determines the static

(equilibrium) particle density distribution irrespective of the spatial variation of friction. In other words, frictional inhomogeneity has no effect in determining the static density distribution of particles. Temperature nonuniformity can result in unidirectional net particle current even without the application of external forcings as has been clearly shown in [11], whereas the effect of frictional nonuniformity can be envisaged only in the dynamic situation [13]. The effect of frictional inhomogeneity can manifest in two ways. Wherever the friction is large in each period, particle movement gets damped and hence the particles spend more time there. This effectively changes the density distribution. For instance, for $\phi \neq 0,\pi$, the friction coefficient will be different immediately on the left side of the potential peak than on the corresponding immediate right of the peak. Hence, in the periodic (potential) situation it will appear (in the dynamic situation) as though a static force has been applied in order to bring about the change in the distribution [10]. On the other hand, since the particle spends more time in the regions where friction is large, they become more prone to absorb the thermal energy of the immediate environment and hence will effectively have higher probabiltiy to surmount the potential barrier for motion [11]. These two competing aspects can give rise to interesting complex behaviour of the particle currents in periodic potential systems. In the present work, we investigate a number of interesting phenomena exhibited by ratchet current in these inhomogeneous periodic systems [1] . We drive the system with a square-wave periodic field. The reason for choosing square-wave field as opposed to a sinusoidal field will become clear as we proceed. The resulting Langevin equation is solved numerically. We obtain particle current and properties associated with it in the parameter space of external-field-amplitude F_0, the average friction coefficient γ_0, the phase lag ϕ, and the temperature T. Since it is a formidable task to explore the entire parameter space, we present results for only some regions of a few sections of this space where appreciable ratchet current is obtained.

The ratchet current $\bar{v}$ is obtained for $\phi(\neq n\pi$, with integral $n)$ in the steady

state situation which is achieved in the asymptotic time limit. In our case we observe particle motion for a long time t such that the position dispersion $\langle(\Delta x(t))^2\rangle$ averaged over many similar trajectories approach $\sim t$. Thus, we calculate the diffusion constant D using the relation $\langle(\Delta x(t))^2\rangle = 2Dt$ for given γ_0, T, and ϕ. D shows nonmonotonic behaviour with the field amplitude F_0 and it peaks around a value of F_0 where $\bar{v}$ attains maximum. That is to say the ratchet current is maximised when the system is most diffusive. To compare the extent of this diffusive spread with the directional average displacement, a quantity Péclet number, $P_e = \frac{\bar{x}^2}{Dt}$, the ratio of square of mean displacement $\bar{x}$ in time t to half the square of diffusive spread in the same time interval t [15] is calculated. Our calculation shows that in the region where the ratchet current is appreciable and in particular where $\bar{v}$ peaks P_e is much larger than 2, indicating that the transport is coherent.

The current in the explored parameter region, however, is not large enough to obtain (practically) useful work; when a small load is applied against current the current either reduces to a small level or starts flowing in the direction of the applied load. Thus, in the given circumstances, no appreciable useful work can be extracted from this inhomogeneous (frictional) ratchet. However, even in the absence of any external load the particle keeps moving against the frictional resistance. Leaving out the symmetric diffusive part of the motion the particle's unidirectional (ratchet) current $\bar{v}$ is maintained against the average frictional force. The *Stokes efficiency*, η_S, which is the ratio of this work (that the ratchet performs against the frictional drag) to the total energy pumped into the system from the source of the external forcings, is also calculated.

An expression for η_S has been derived earlier [3, 15, 16] as $\eta_S = \frac{\langle v\rangle^2}{|\langle v^2\rangle - T|}$, which involves $\langle v\rangle$ as well as the second moment of the velocity v calculated from the probability distribution $P(v)$ of the velocity $v(t)$ recorded all through the trajectory of the particle. We have calculated η_S as a function of the amplitude of the applied forcing. η_S shows a peak, not coinciding with that of the ratchet

current. The distribution $P(v)$ is almost symmetric about $v = 0$ and the velocity dispersion grows monotonically approaching to be linear in F_0 at large F_0.

Recently, it has been reported [17] that in a tilted periodic potential an underdamped particle motion shows a remarkable dispersionless behaviour in the intermediate time regime for a range of constant tilt values, F_0. In this regime the majority of particles appear to move coherently with a constant speed roughly equal to $\frac{F_0}{\gamma_0}$. In the present work we show that when the system is driven by a square-wave forcing of appropriate amplitude and frequency, such dispersionless behaviour with added richness can be observed. The dispersionless behaviour corresponding to the constant tilt periodic potential, gets punctuated and oscillatory behaviour of dispersion of different kinds, depending on the frequency of the periodic drive, naturally emerges. Interestingly, however, contrary to expectations, the transient coherent particle motion does not contribute positively to the largely coherent steady state ratchet current in this system.

In section 3.2 the basic equation of motion used in this model calculation will be presented. The section 3.3 will be devoted to the presentation of the detailed results of our numerical calculation. In the last section (sec. 3.4) we shall conclude with a discussion.

3.2 The model

In this work we drive the system periodically by a symmetric square-wave forcing. The choice of square-wave forcing, instead of a sinusoidal forcing, is to make a direct contact with the adiabatically driven case. In the adiabatic drive case the particle motion was studied keeping the tilt of the periodic potential constant and the net current for two opposing directions of the same magnitude of tilt was calculated. The calculation of current for a constant tilt was carried out using the matrix continued fraction method (MCFM) as well as using the

numerical Langevin dynamics [14].

The matrix continued fraction method was developed by Risken and coworkers [2]. The method involves solving the Fokker-Planck equation governing the time evolution of the probability density function $W(x,v,t)$ of particle position x with velocity $v(=\frac{dx}{dt})$ at time t. The distribution function $W(x,v,t)$ is expanded in series in terms of Hermite functions $\psi_n(v)$ with expansion coefficients $C_n(x,t)$, as $W(x,v,t) = \psi_0 \sum_{n=0}^{\infty} C_n(x,t)\psi_n(v)$. The Fokker-Planck equation, is thus transformed into an infinite system of coupled differential equations for the expansion coefficients. The infinite system of equations is truncated and is put in the form of a vector recurrence relation of the expansion coefficients. This recurrence relation is solved by a continued fraction method for matrices in the steady state approximation to obtain the Fourier components of the expansion coefficients C_n, from which the different physical quantities of interest are calculated. The MCFM is extended to suit the present problem in references [13, 14].

The constant tilt case shows dispersionless motion in the intermediate regime as represented earlier [17]. Thus the square-wave drive provides an opportunity to study the dispersionless motion at finite frequencies. In the present case we consider the forcing $F(t)$ as,

$$\begin{aligned} F(t) &= \pm F_0, \quad (2nT_\Omega \leq t < (2n+1)T_\Omega), \\ &= \mp F_0, \quad ((2n+1)T_\Omega \leq t < 2(n+1)T_\Omega), \end{aligned}$$

where T_Ω is the half period of forcing (and which corresponds to a time interval after which the sign of F_0 is changed) and $n = 0, 1, 2, \ldots$. The motion of a particle of mass m moving in a periodic potential $V(x) = -V_0 sin(kx)$ in a medium with friction coefficient $\gamma(x) = \gamma_0(1 - \lambda sin(kx + \phi))$ with $0 \leq \lambda < 1$ and subjected

to a square-wave forcing $F(t)$ is described by the Langevin equation,

$$m\frac{d^2x}{dt^2} = -\gamma(x)\frac{dx}{dt} - \frac{\partial V(x)}{\partial x} + F(t) + \sqrt{\gamma(x)T}\xi(t). \tag{3.1}$$

Here T is the temperature in units of the Boltzmann constant k_B. The Gaussian distributed fluctuating forces $\xi(t)$ satisfy the statistics: $< \xi(t) >= 0$, and $< \xi(t)\xi(t') >= 2\delta(t-t')$. For convenience, we write down Eq. 3.1 in dimensionless units by setting $m = 1$, $V_0 = 1$, $k = 1$ so that $T = 2$ corresponds to an energy equivalent equal to the potential barrier height at $F_0 = 0$. The Langevin equation, with reduced variables denoted again now by the same symbols, is written as

$$\frac{d^2x}{dt^2} = -\gamma(x)\frac{dx}{dt} + cosx + F(t) + \sqrt{\gamma(x)T}\xi(t), \tag{3.2}$$

where $\gamma(x) = \gamma_0(1 - \lambda sin(x + \phi))$. Thus the periodicity of the potential $V(x)$ and also the friction coefficient γ is 2π [18]. The potential barrier between any two consecutive wells of $V(x)$ persists for all $F_0 < 1$ and it just disappears at the critical field value $F_0 = F_c = 1$. The noise variable, in the same symbol ξ, satisfies exactly similar statistics as earlier.

The Eq. 3.2 is solved numerically (with given initial conditions) to obtain the trajectory $x(t)$ of the particle for various values of the parameters F_0, γ_0, and T. Also, the steady state mean velocity $\bar{v}$ of the particle is obtained as

$$\bar{v} = \langle \lim_{t\to\infty} \frac{x(t)}{t} \rangle, \tag{3.3}$$

where the average $\langle ... \rangle$ is evaluated over many trajectories. The mean velocity is also calculated alternatively from the numerically obtained distribution $P(v)$ of velocities giving almost identical result.

3.3 Numerical results

The Langevin equation (3.2) is solved numerically using two methods: 4^{th}-order Runge-Kutta [19] and Heun's method (for solving ordinary differential equations). We take a time step interval of 0.001 during which the fluctuating force $\xi(t)$, obtained from a Gaussian distributed random number appropriate to temperature T, is considered as constant and the equation solved as an initial value problem. In the next interval another random number is called to use as the value of ξ and the process repeated. A careful observation of the individual trajectories of the particle shows that by $t = 10^4$ the particle completely loses its memory of the initial condition it had started with. When we look for steady state solutions the trajectory is generally allowed to run for a maximum time $t = 10^7$. Therefore, for steady state evaluation for $\bar{v}$, etc., the results become independent of initial conditions. The (Runge-Kutta) method had earlier been used and obtained correct results [20] in a similar situation. Also, the Runge-Kutta and Heun's methods were checked against results obtained earlier for the adiabatic case (using matrix continued fraction method) and found to compare closely (Fig. 3.2). Heun's method when applied in similar situations take much less time than the Runge-Kutta method and yields qualitatively as good result (Fig.3.2). With this confidence in our numerical procedures, we apply either one or the other of these two numerical schemes as the situation demands. We take $\lambda = 0.9$ all through our calculation in the following.

The motion of the particle is governed by the applied square-wave forcing $F(t)$. As $F(t)$ changes periodically so does the position of the particle. In view of this effect we start our simulation at $t = 0$ alternately with $F(0) = +|F_0|$(first, third, fifth....) and $-|F_0|$ (second, fourth, sixth.....) trajectories. This gives a nice nonoscillating(and initial condition independent) variation of overall average position when finally averaged over a large even number of trajectories. However, while calculating the position dispersions or velocity dispersions at a

given time t, the even (beginning with $F = -|F_0|$) and odd (beginning with $F = +|F_0|$) numbered trajectories are treated separately to calculate the deviations from their respective mean values.

3.3.1 Particle trajectories

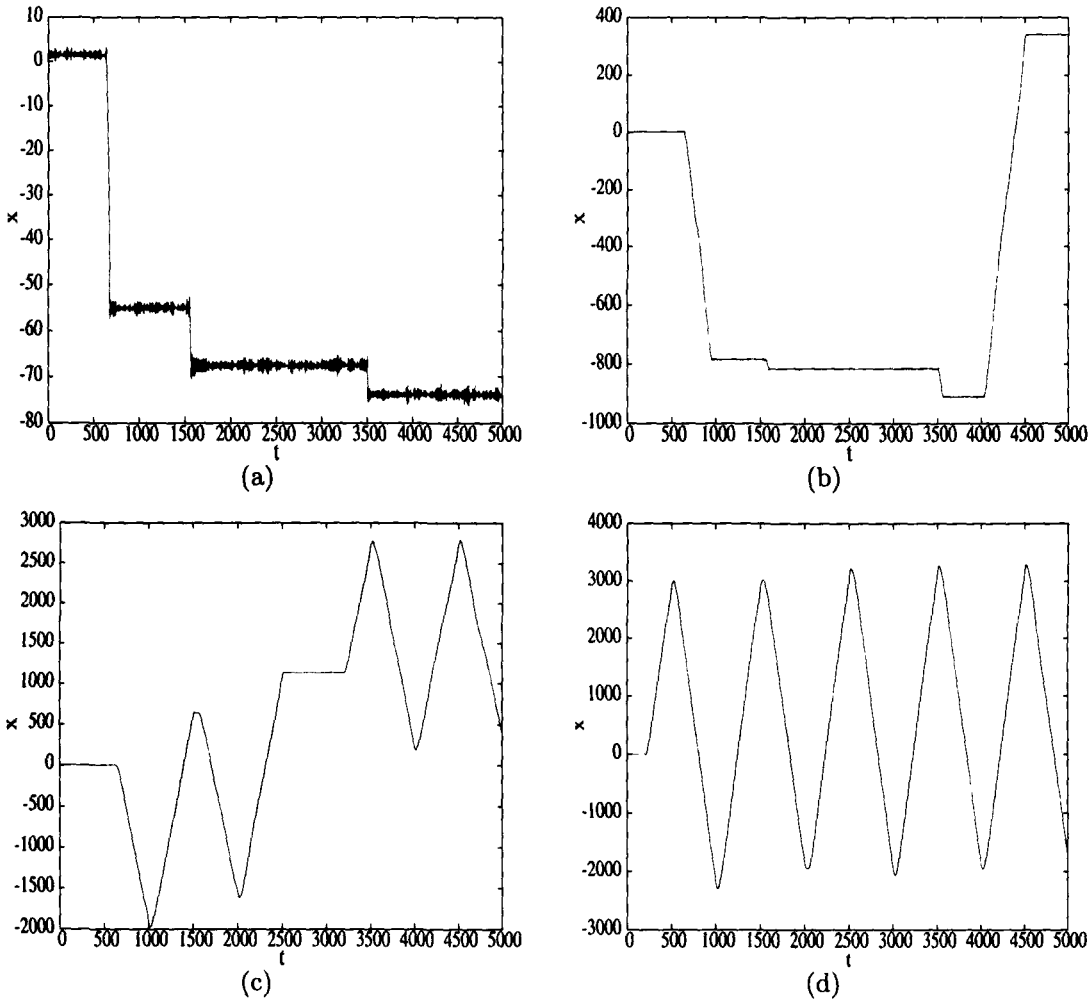

Figure 3.1: Particle trajectories for four different values of the amplitude F_0 of the, square-drive; F_0=0.05 (a), F_0=0.1(b), F_0=0.2(c), and F_0=0.4 for $T_\Omega = 500$, $\gamma = 0.035$, $\lambda = 0.9$, $\phi = 0.35$. In the scale of the figures the intrawell motion is not visible.

The nature of the particle trajectories are dependent on the various parameters governing its motion. For our work, the amplitude of external drive is F_0

is always kept less than the critical amplitude F_c, so that the particle sees a finite barrier. When inside a potential well, the particle is kicked around by the random fluctuations. It remains in this locked state till it overcomes the barrier to come out of the well, aided by the random fluctuations and goes to the running state, only to get locked in some other well after sometime (Fig. 3.1). The particle keeps on transiting between these two states. The relative amount of time that the particle spends in the locked or the running state changes with the amplitude of the drive. At higher amplitudes of drive the probability of the particle coming out of the potential wells increases (Fig. 3.1c). Beyond a particular amplitude for a constant frequency of drive, once the particle comes out of the well, it remains in te running state (Fig. 3.1d). The particle surmounts the barrier in both the positive and the negative direction. But in the asymptotic limit, the particle shows a preferential motion in a particular direction giving rise to ratchet current; the magntude and direction of which is determined b a complex interplay of the random fluctuations, non-linearity, and the symmetry properties of the problem.

3.3.2 The ratchet current

Appreciable ratchet current $\bar{v}$ (Eq. 3.3) is obtained in a small range of F_0 with a peak in an intermediate F_0 for given γ_0, T, and ϕ. The variation of $\bar{v}$ as a function of the amplitude F_0 of the applied square-wave forcing $F(t)$, with a frequency $(=\frac{1}{2T_\Omega})$ of 5×10^{-4} cycles per unit time, is shown (Fig. 3.2) for $\gamma_0 = 0.035$ and temperature $T = 0.4$. Also, for comparison the algebraic sum, $\Sigma\bar{v}(F_0)=\bar{v}(+|F_0|)+\bar{v}(-|F_0|)$ with applied forces $+|F_0|$ and $-|F_0|$, called the ratchet current in the adiabatic limit, is plotted as a function of F_0. The ratchet current in the adiabatic limit($T_\Omega \to \infty$) is calculated (by solving the Fokker-Planck equation corresponding to Eq. 3.2) using the matrix continued fraction method (continuous line in Fig. 3.2) developed by Risken and coworkers [2] and adapted in refs. [13, 14] to suit the present case. The current is also calculated

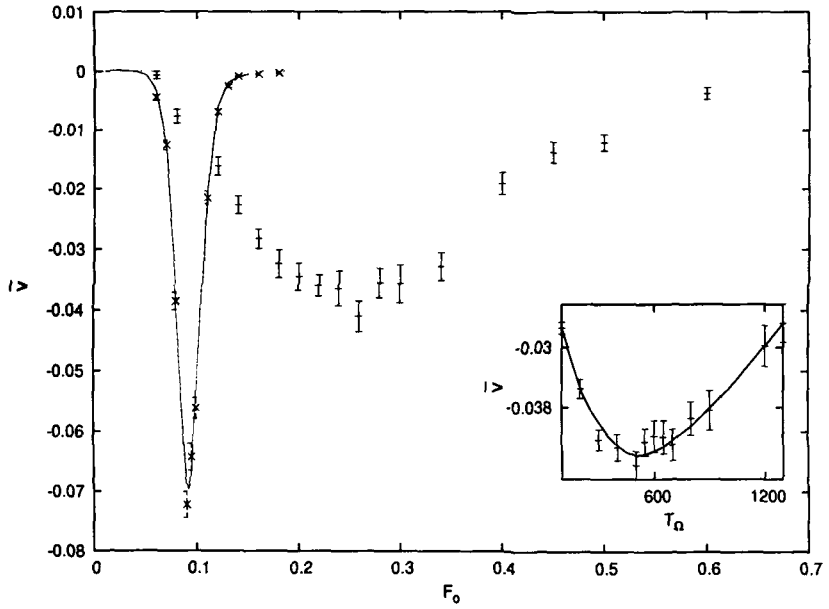

Figure 3.2: Shows the variation of $\bar{v}$ with F_0 for the adiabatic case. The results obtained by MCFM (continuous line) and simulation (crosses with errorbars) are put together for comparision. The MCFM could not be used for F_0 beyond the plotted range. The plus signs with errorbars correspond to the square drive case with parameter values $\gamma_o = 0.035$, ϕ=0.35 and $T = 0.4$ for $T_\Omega = 1000$. The zeroline is given for reference. The inset shows the variation of $\bar{v}$ with T_Ω: simulation data (points with errorbars) for F_0=0.26 and for the same γ_o, T and ϕ values. The fitted curve to the data points is given just to guide the eye.

numerically by solving the same Langevin equation (crosses with error bars in Fig. 3.2). The adiabatic current calculated by using the two methods agree quite well. The range of F_0 over which ratchet current is obtained in the square-wave drive case (using numerical methods) is much wider [$0.05 < F_0 < 0.7$] compared to the adiabatic drive condition [$0.05 < F_0 < 0.15$] and the peak current occurs at a larger F_0 value. The range, though wider, still remains well below F_c, the critical field at which the potential barrier to motion just disappears. The current is, therefore, essentially aided by thermal noise.

The ratchet current $\bar{v}$ also shows nonmonotonic behaviour as a function of the period of the drive. In the inset (Fig. 3.2) we plot the variation of $\bar{v}$ as a function of the time period of the drive for $F_0 = 0.26$, $\gamma_0 = 0.035$, and $T = 0.4$. For these parameter values the current $\bar{v}$ peaks at a value of $T_\Omega \approx 500$. For comparison of time scales, it may be noted that for an equivalent RCSJ model of Josephson junctions (with typical junction capacitance $C = 0.5 \times 10^{-12} F$ and critical current I_c=10^{-9} coul.s^{-1}) the characteristic Josephson plasma frequency ω_J turns out to be about 10^3 times larger than the drive frequency ($\frac{1}{2T_\Omega}$) corresponding to $T_\Omega = 1000$. In this sense we obtain appreciable ratchet current only for very slow drives. It should, however, be noted that in the infinitely slow adiabatic case the ratchet current is effectively zero for $F_0 > 0.15$ for γ_0=0.035 at $T = 0.4$ and $\phi = 0.35$.

The ratchet current $\bar{v}$, is also found to be dependent on the the phase difference ϕ between the periodic potential and the similarly periodic friction coefficient when he other parameters are kept fixed. In Fig. 3.3, we show the variation of $\bar{v}$ with F_0 for $\phi = 0.3$ and $\phi = 0.4$ with $\gamma_0 = 0.035$, $T_\Omega = 1000$ and $T = 0.4$. The value of $\bar{v}$ is found to be different for different values of ϕ at the same value of F_0. Also the value of F_0 at which the ratchet current $\bar{v}$ peaks, is found to be dependent on the value of ϕ.

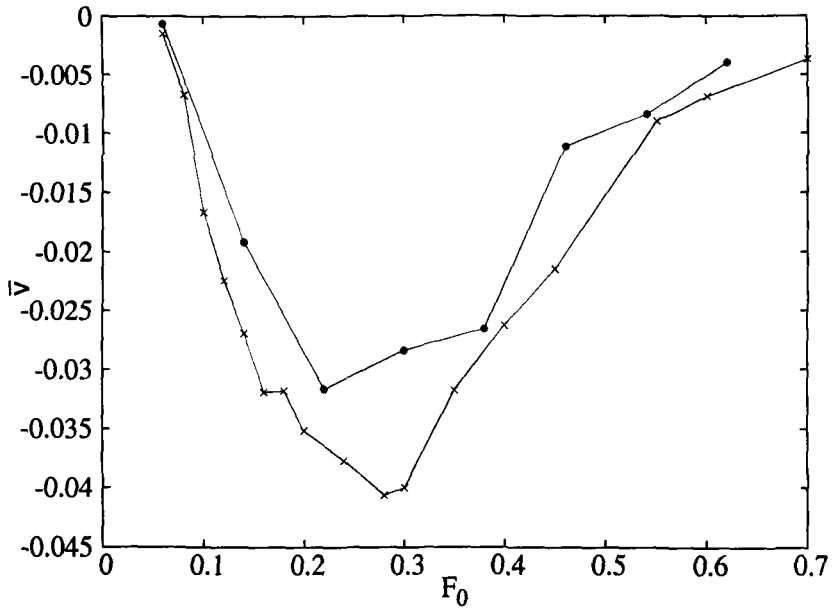

Figure 3.3: Shows the variation of $\bar{v}$ with F_0 for the square drive case for two different values of ϕ; $\phi = 0.3$ (line with circles) and $\phi = 0.4$ (line with crosses), $\gamma_o = 0.035$, ϕ=0.35, $T = 0.4$ and $T_\Omega = 1000$.

3.3.3 The steady-state dispersions

The position dispersions $\langle(\Delta x(t))^2\rangle$, where $\Delta x(t) = x(t) - \langle x(t)\rangle$ are evaluated over a large number of trajectories for various values of F_0, and $T_\Omega = 1000$. It is found that the dispersions fit nicely to

$$\log[\langle(\Delta x(t))^2\rangle] = \log(t) + \log(2D), \tag{3.4}$$

for large t, typically $t > 10^5$.

From the linear fit of the graphs we calculate the diffusion constants $D(F_0)$ and the result is shown in Fig. 3.4. The diffusion constant has a large value between $F \approx 0.15$ and 0.35. The peak height is quite large ≈ 800. As F_0 is increased D decreases sharply and becomes smaller than 50 (which is less than 10% of its peak value) for $F_0 > 0.7$. This $[0.15 \leq F_0 \leq 0.35]$ is also the region where the ratchet current $\bar{v}$ is appreciable. The Péclet number, P_e, as defined earlier, are also calculated as a function of F_0. They are plotted in the inset of

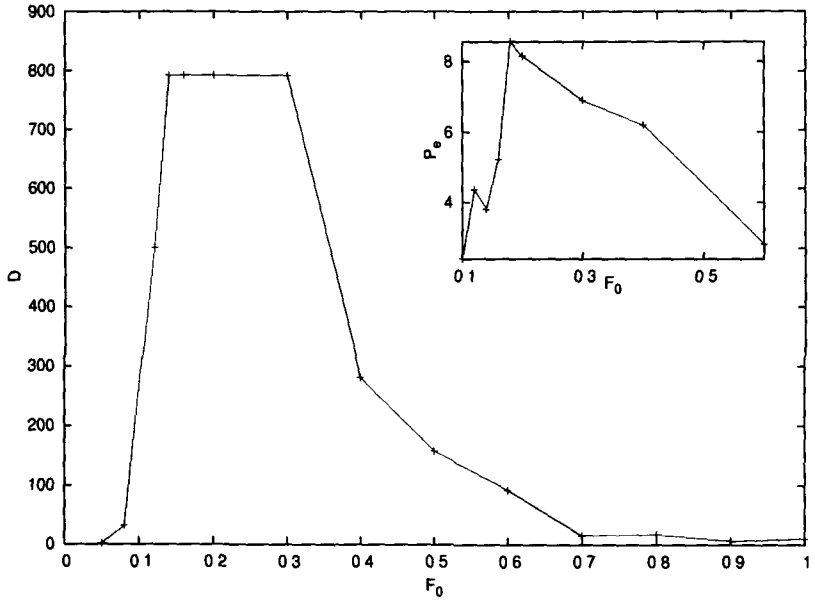

Figure 3.4: The variation of the diffussion constant D as a function of the driving amplitude F_0 for $\gamma_0 = 0.035$, $T = 0.4$, and $\phi = 0.35$ with $T_\Omega = 1000$. The inset shows the variation of the corresponding Péclet number P_e with F_0.

Fig. 3.4. It is clear from the figure that in the same region $P_e(=2(\frac{\bar{x}(t)^2}{\langle \Delta x(t)^2 \rangle})$ is also much larger than 2. This indicates that in the region $[0.15 \leq F_0 \leq 0.35]$ the particle motion is highly diffusive but concomitantly it is greatly coherent too. This is also indicated equivalently by the observation that even though the position dispersions (fluctuations) are large the relative fluctuations of position in this region are considerably low ($\frac{\sqrt{\langle \Delta x(t)^2 \rangle}}{\bar{x}(t)} < 1$). As indicated by the result in the adiabatic case (Fig.3 [13]) this range of F_0 of coherent motion is expected to shift as the value of γ_0 is changed.

Though our system is different from that of Machura, et. al. [3], at this point it would be interesting to make a comparison with their result. They observe that for their low temperature case $D_0 = 0.01$ in the vicinity of $a \approx 0.6$ the velocity fluctuation underwent a rapid change (Fig.1a of [3]). To translate this to our case [18] $a \approx 0.6$ is equivalent to $F_0 \approx 0.2$ and given their potential barrier being just about half of the value in our case one should expect the peaking of velocity dispersion to occur below $F_0 = 0.4$. Taking into consideration of

our temperature being 40 times 0.01 the phenomena should occur much below $F_0 = 0.4$. In this sense the region $[0.15 \leq F_0 \leq 0.35]$ seems quite reasonable. Also, $\bar{v}$ of Fig. 3a of Ref. [3] at $D_0 = 0.4$ make a good comparison with Fig. 3.2 in our case. However, as mentioned earlier the two systems are quite different in basics to have an exact comparison.

The velocity distribution $P(v)$ also shows interesting behaviour. In Fig. 3.5b we plot $P(v)$ for three values of F_0. A sharp peak which is almost indistinguishable from a Gaussian centred at $v = 0$ for small $F_0 = 0.05$ gets split up into three peaks for $F_0 = 0.12$, and similarly for $F_0 = 0.30$, with the central peak, gradually diminishing. This shows a behaviour, including the nearly linear growth of the variance with F_0 (inset, Fig. 3.5b), quite similar to what has been reported earlier in a different system [3]. There is, however, one difference. The side peaks of $P(v)$ in our calculation have origin in the running states of the particle. It is, perhaps, due to the low frequency square-wave drive, instead of sinusoidal drive, that for as low amplitude as $F_0 = 0.3$ we get three disjoint velocity bands and at $F_0 = 0.6$ we get just two bands, the central band being almost unpopulated. The three peaks, for example for $F_0 = 0.3$, could be fitted to a combination of three Guassians. With a cursory look, the left and right Gaussians barely show much difference. However,

$$\langle v \rangle = \int_{-\infty}^{\infty} vP(v)dv \tag{3.5}$$

gives approximately the same value as $\bar{v}$, and $\langle v \rangle(F_0)$ showing exactly the same nature as $\bar{v}(F_0)$ (Fig. 3.6). It is to be noted that the maximum ratchet current occurs (Fig. 3.2), for F_0 at which $P(v)$ shows a transition from a three peak form to a two peak one. In this transistional range the frictional asymmetry shows the maximum contrast in responding to the field. In the case where the intrawell motion dominates the ratchet current is low and again when there is only running states (at large F_0) the frictional asymmetry becomes ineffective.

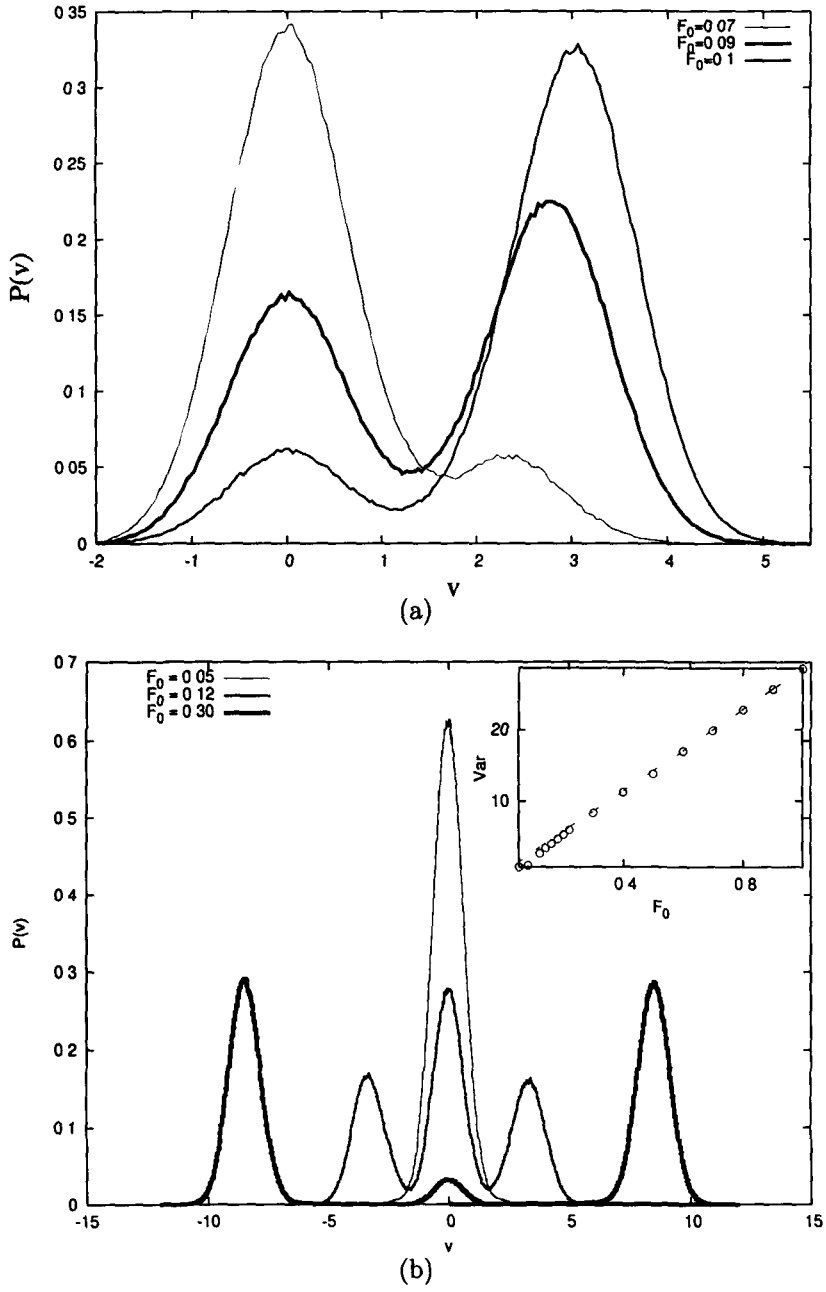

Figure 3.5: Plot of velocity distribution $P(v)$ for three values of driving amplitudes $F_0 = +0.07$, $+0.09$, and $+0.1$, in the adiabatic limit (Fig. 3.5a) and $F_0 = 0.05$, 0.12, and 0.30 and $\phi = 0.35$ for square drive (Fig. 3.5b). The figure in inset of Fig. 3.5b shows the variance of velocities as a function of F_0 fitted with a straight line to show the linear growth of variance at large F_0.

These observations are corroborated by the velocity distributions in the adiabatic case (Fig. 3.5a), where again maximum difference in current occurs at the transistional period from a two peak distribution to a single peak (running state only) distribution. For the adiabatic case the transitional range occurs at lower F_0 values (Fig. 3.5a). In the square-wave drive case, the transitional region is shifted to higher F_0, because, when the direction of F_0 is changed, the particles reverse their direction of motion too, and hence have enough chance to get locked into a potential well. This shift in F_0 is responsible for shifting of the peak of current maximum for the square drive case as shown in Fig. 3.2.

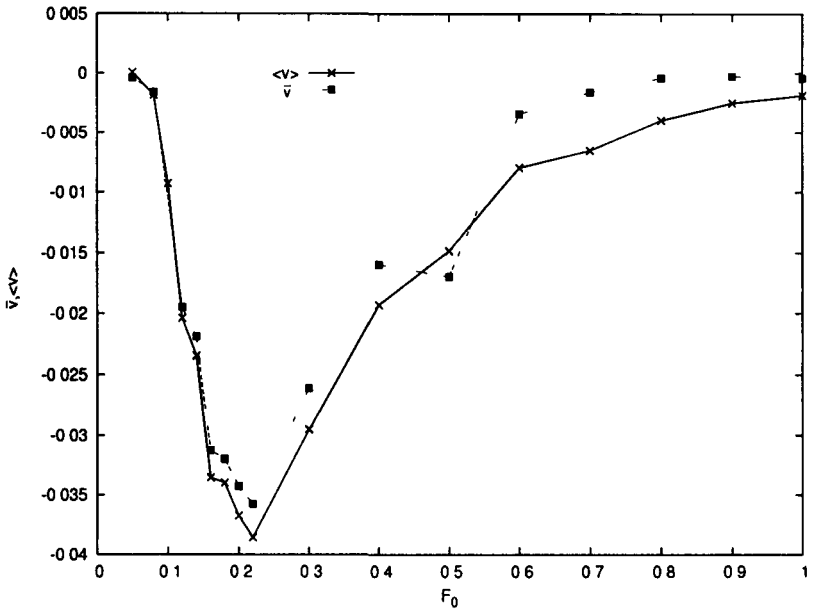

Figure 3.6: Shows the variation of the steady state mean velocity $\bar{v}$, Eq. (2.3) and $\langle v \rangle$, Eq. (3.2) for the same parameter values as in Fig.3.4.

3.3.4 The efficiency of ratchet performance

From the velocity distribution $P(v)$ we calculate the Stokes efficiency, η_S, defined as [3],

$$\eta_S = \frac{\langle v \rangle^2}{|\langle v^2 \rangle - T|}, \tag{3.6}$$

as a function of F_0. Fig. 3.7a shows that η_S is larger in the same range of F_0 where it shows larger $\bar{v}$. The peak of η_S, however, does not occur at the same position as the peak of $\bar{v}$. It is, however, to be noted that the plotted figure is calculated from averages over a small number ($\sim$ 20) of ensembles because it is computationally quite expensive to obtain results for the steady state (maximum $t = 10^7$) and hence not feasible to obtain averaging over a larger number of ensembles. Though the qualitative behaviour is encouraging the efficiencies are small $\sim 10^{-5}$. The efficiency of this symmetrically driven system can, however, be improved to a good extent by an optimal choice of these parameters.

An inertial ratchet driven by a zero mean asymmetric drive can, however, give a highly efficient performance compared to the symmetrically driven ratchet. For example, when the system is driven by a field

$$\begin{aligned} F(t) &= \pm F_0, \qquad (2nT_\Omega \leq t < (n+\alpha)2T_\Omega), \\ &= \mp\tfrac{\alpha}{(1-\alpha)}F_0, \quad ((n+\alpha)2T_\Omega \leq t < (n+1)2T_\Omega), \end{aligned}$$

with $\alpha = 0.2$ gives an efficiency of 3.8×10^{-2} compared to 6.2×10^{-5} in the symmetric-drive ($\alpha = 0$) case with $F_0 = 0.16$ and $2T_\Omega = 1000$. This is made possible because in the symmetric drive case the particles move on either direction with almost equal probability whereas in the asymmetric drive case the particle motion in one direction is practically blocked, as is evident from the corresponding velocity distributions shown in the inset of Fig.3.7a. The contribution of the system inhomogeneity for this improved performance is, however, quite insignificant.

The efficiency of the ratchet also is found to be dependent on the phase difference between ϕ between the periodic potential and the friction coefficient. In (Fig. 3.7b) the efficiencies η_S as a function of the driving amplitude F_0 are plotted for $\phi = 0.3$ and 0.4. It is seen that for a particular value of F_0, the

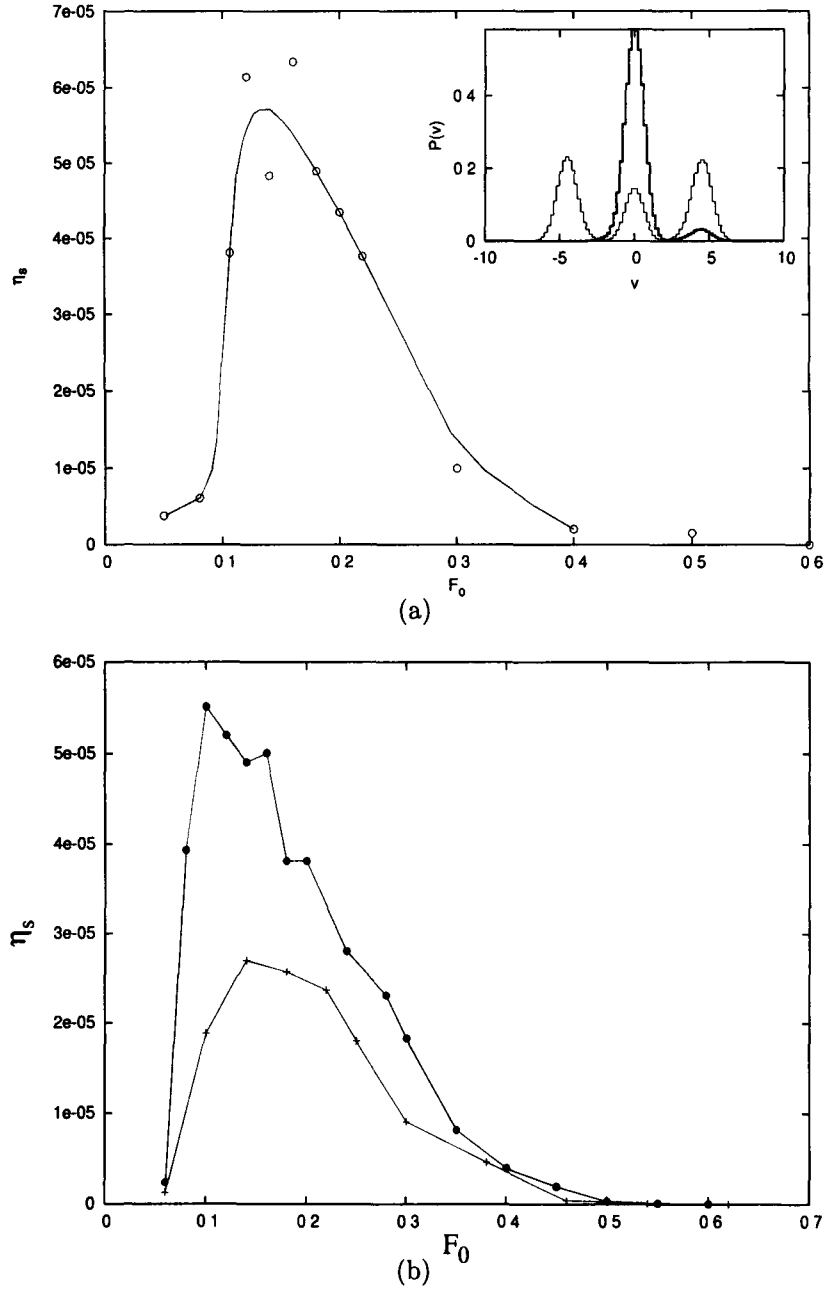

Figure 3.7: Fig. 3.7a shows Stokes efficiency, η_S as a function of F_0 for the same paramater values as in Fig. 3.4. Simulation data points (circles) fitted with a curve to guide the eye. The inset shows the difference in the velocity distribution for symmetric (three peaks) and asymmetric drive for the same value of $F_0 = 0.16$ and $\tau = 2000$ with $\alpha = 0.2$. In Fig. 3.7b, the efficiencies are shown for two other values of ϕ; $\phi = 0.3$(lines with crosses) and $\phi = 0.4$(lines with circles).

efficiency is less for $\phi = 0.3$. It is to be noted that the ratchet currents also are smaller for $\phi = 0.3$ for the same range of F_0 (Fig. 3.3). Thus we can conclude that the efficiency of the ratchet performance can be enhanced by an optimal choice of the system parameters.

3.3.5 The transient-state dispersions and the ratchet current

When a constant force F is applied to the system it shows dispersionless behaviour: $\langle(\Delta x(t))^2\rangle$ does not change with time in the intermediate time scales, roughly $[10^3 < t < 10^5]$, for around $[0.12 < F < 0.7]$ at $T = 0.4$ for $\gamma_0 = 0.035$. The result of dispersionless behaviour had originally been shown and explained [17] beautifully for constant friction γ_0 case: the position distribution moves undistorted at constant velocity $v = \frac{F}{\gamma_0}$ or equivalently, velocity distribution remains undistorted centerd at $v = \frac{F}{\gamma_0}$. The interval $[t_1 < t < t_2]$ of time during which the system shows this remarkable intermediate-time behaviour depends on the tilt force F, as should also on other parameters. t_1 is roughly of the order of but much larger than the mean Kramers passage time corresponding to the lower of the potential barriers on either side of a well. The transient-time dispersionless particle-motion behaviour is sensitive to initial conditions. In the following we specifically begin from the bottom of the well at $x \approx \frac{\pi}{2}$ with particle velocities given by Maxwell-Boltzmann distribution at temperature $T = 0.4$.

When the inhomogeneous system is driven periodically by a square-wave forcing of amplitude F_0, the dispersionless coherent nature of average motion gets interrupted depending on the value of T_Ω of the forcing (Fig. 3.8). When $t_1 < T_\Omega < t_2$, at $t = T_\Omega$ the dispersion gets a jerk and shoots up only to get flattened again to an another bout of dispersionless regime. This regime too gets a similar jolt after another T_Ω and the process continues for a large number of periods. When the direction of the applied force is changed the 'forward

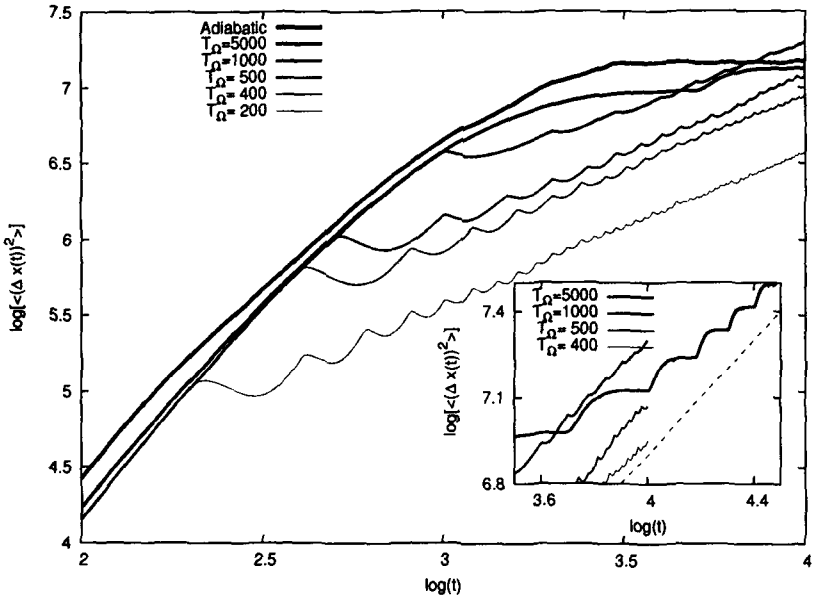

Figure 3.8: The plot of position dispersions $\langle(\Delta x(t))^2\rangle$ versus time t (in logarithmic scale) for different values of (T_Ω) of forcing with $F_0 = 0.2$, $\phi = 0.35$. The inset shows the clipped part of the plot at larger time. The dashed line in the inset is drawn just to guide the eye to compare with the diffussive regime.

moving' particles are forced individually to halt momentarily to begin moving in the new direction of the force afresh. While in the 'state of halt' particles are more likely to find themselves 'thermalized' to the bottom of some well and thus the system gets initialised as in the beginning. The system finds itself in similar situation again and again periodically with each change of force direction and continues with its unfinished dispersionless journey for a large number of periods with remarkable robustness [Inset of Fig. 3.8, T_Ω=5000]. However, when $T_\Omega < t_1$ the system never gets a chance to experience its dispersionless journey because only a fraction of the particles get the opportunity to acquire the required constant average velocity [17] of $\frac{F_0}{\gamma_0}$ and the rest keep lagging behind even by the end of constant force duration T_Ω. Instead, as soon as the direction of the force F is reversed after T_Ω, the dispersion dips after a brief climb up, as the particles get herded together briefly before getting dispersed further in the reversed direction of F_0. This can be seen very clearly in the time evolution

of the position probability distribution profile $P(x,t)$. The front of the $P(x,t)$ moves with velocity $\frac{F_0}{\gamma_0}$ while the rest lag behind it moving at a slower speed but trying to catch up with the front throughout T_Ω. This process of dispersion dipping (after a small continuing rise) and rising to a higher value after each T_Ω is repeated for several tens of periods [Fig. 3.8].

In the inset of Fig. 3.8 we have drawn a straight line with slope 1 as a guide to show that ultimately the curves should achieve that average slope at large times for various T_Ω values of drives. Even though the average slope of the curves have not yet reached the diffusive slope of *one*, the small T_Ω curves are slowly approaching that value. One can, therefore, safely infer that in the steady state situation the effective diffusion constant should increase monotonically with T_Ω for small T_Ω. The frequency of drive or equivalently T_Ω, thus, plays important role about how the particles diffuse out of their wells. For example, The population of the initial well depletes with time exponentially, $N(t) = N(0)e^{-bt}$, with $b = 0.0023$ for $T_\Omega = 250$ and $b = 0.002$ for $T_\Omega = 500$, for $\gamma_0 = 0.035$ at $T = 0.4$ that we have studied. By the time the well gets effectively exhausted the first particles would have moved farther than a thousand of potential wells. Of course, this first well itself (as all others) keeps getting repopulated all the time.

The intermediate-time dispersionless motion is not an exclusive characteristic feature of inhomogeneous systems. It is a characteristic feature of inertial washboard potential system. However, its study in the inertial inhomogeneous system provides a convincing explanation of the variation of ratchet current as a function of T_Ω [inset of Fig. 3.2] and helps in finding a criterion to improve the performance of the ratchet.

In Fig. 3.9 the displacement of particles, averaged over 1000 ensembles, as a function of time when driven by equal number of $\pm F(t)$ profiles is presented for $T_\Omega = 5000$, $\gamma_0 = 0.035$, $F_0 = 0.2$, and $T = 0.4$. This case corresponds to the repeated dispersionless motion shown in Fig. 3.8. Fig. 3.9 clearly shows that

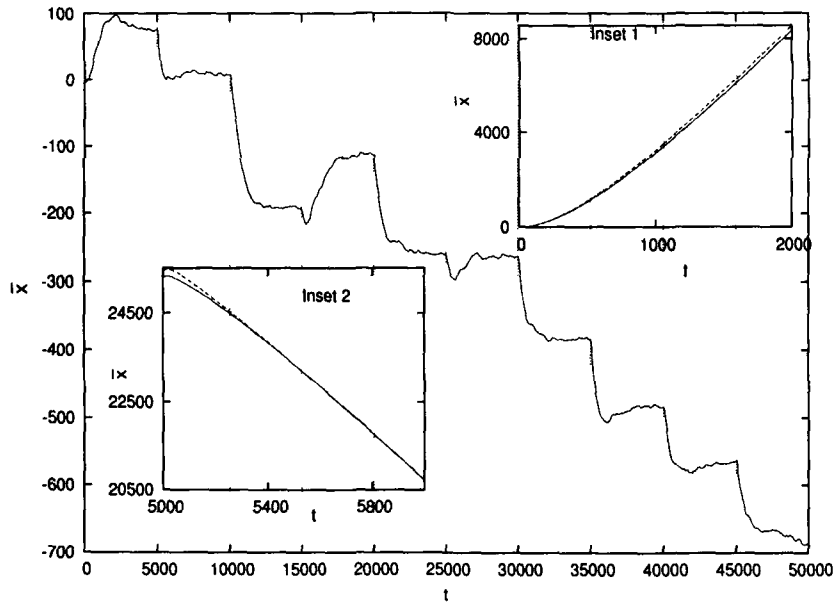

Figure 3.9: The average displacement of particles as a function of time, driven by equal number of $\pm F(t)$ profiles (or equal number of odd and even numbered trajectories) for $T_\Omega = 5000$, $\gamma_0 = 0.035$, $F_0 = 0.2$, $\phi = 0.35$ and $T = 0.4$. The insets highlight the contributions to the mean displacement of odd(dashed line, beginning with $+|F_0$) and even(solid line) numbered trajectories separately, leading to the main figure. The mean displacements for the even numbered trajectories are shown with a reversed sign.

during the dispersionless motion the average displacement of particles effectively remains constant. In other words, during the period of dispersionless motion the particles move equally in the left as well as in the right direction thereby contributing nothing to the ratchet current: while in the dispersionless motion the particles fail to see the frictional inhomogeneity of the system. All the change in the average displacement and hence all the contribution to the ratchet current comes during the dispersive period of motion. This is shown in the inset of Fig. 3.9 where for clarity the mean particle positions for $F(t)$ beginning with $F(0) = -F_0$ (even numbered trajectories) are shown as a function of time with their sign reversed. The mean particle displacements for odd and even numbered trajectories differ only during the interval just after the reversal of F_0 and before the dispersionless regime begins and the two lines of mean positions (insets of Fig. 3.9) run parallel during the dispersionless regime. This clearly indicates that in order to get a larger current an optimum choice of T_Ω needs to be made which, naturally, avoids the dispersionless regime but is not too small in order to allow the particles to leave their potential wells. This conclusion is well supported by the inset of Fig. 3.2, where the ratchet current maximises around $T_\Omega = 500$ which is well below the T_Ω showing dispersionless motion.

The velocity dispersions and position dispersions together show interesting behaviour. Fig. 3.10 shows that during the dispersionless regime when the position dispersion is constant and maximum the velocity dispersion is also constant but it has a minimum value. This minimum constant value is repeated in all the nT_Ω, $n = 1, 2, ...$ intervals whereas the value of the constant position dispersion increases in every successive nT_Ω interval as shown in Fig. 3.8 and the inset of Fig. 3.10. In the dispersive regimes the velocity dispersions are squeezed to very sharp troughs exactly where the position dispersions show sharp peaking. In the inset of Fig. 3.10 these dispersions are shown for $T_\Omega = 250$. The onward rush of the particles do not halt immediately after the direction of F_0 is changed at nT_Ω but it continues for a very short time giving a small increase in the

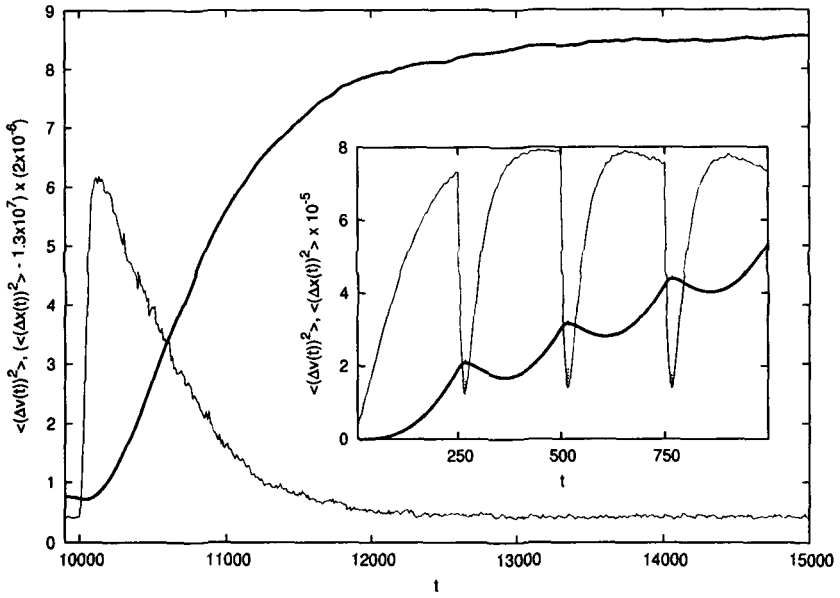

Figure 3.10: Illustration of velocity dispersions $\langle(\Delta v(t))^2\rangle$ (thin line) and position dispersions $\langle(\Delta x(t))^2\rangle$ (bold line) during a time interval for T_Ω=5000 and $\phi = 0.35$. The inset shows the corresponding plots for square drive forcing with smaller T_Ω=250 with no dispersionless regime.

spread of $P(x)$. Then a majority of particles stop, giving a sharp peak in the $P(v)$ at $v = 0$ reducing its spread drastically. At that moment the product of position and velocity distribution spread becomes a minimum. The reverse journey thereafter increases the spread of $P(v)$ but there is a slow squeezing of $P(x)$ before it begins to spread again. The maximum $P(x)$ squeezing, however, does not exactly coincide with the largest of the broad $P(v)$ but it is at a rather close range. In this case too the minimum velocity dispersion remains constant for all nT_Ω. But the wings of $P(x)$, though thin, keep spreading with time giving an average increase of dispersion as time increases. However, most of the particles remain confined roughly to a region $[-\frac{|F_0|}{\gamma_0}T_\Omega < x < +\frac{|F_0|}{\gamma_0}T_\Omega]$ for a long time.

3.4 Discussion and conclusion

The ratchet effect, in this work, is brought about just by the phase lag ϕ between the periodic potential and the nonuniform friction of the medium, without having to have an overall external bias. This is seemingly a weak cause to generate unidirectional current. The Figs. 3.2 through 3.7 refer to a square-wave forcing with $T_\Omega = 1000$. The choice of this T_Ω clearly avoids the dispersionless regime. Yet, this is not the optimum value of T_Ω. It should have been around 500 in order to get the largest possible ratchet current. This choice would have definitely enhanced the Stokes efficiency of operation. The same can also be said about other parameters, such as T, and ϕ for $\gamma_0 = 0.035$. Moreover, an optimal choice of all these parametrs may possibly help in obtaining larger ratchet current to obtain useful practical work against an applied load. However, with the help of these figures we have been able to exhibit the qualitative trends shown by the ratchet.

The dispersive behaviour for drives with $T_\Omega > t_2$ is difficult to study because it takes a very large computer time to arrive at a concrete result. However, the indications are there that for these large T_Ω also, the system show repeated dispersionless regimes, though somewhat enfeebled because the process of diffusion will dominate at these large times.

To conclude, the present detailed study gives us an interesting method of obtaining ratchet current in inertial noisy systems by exploiting the frictional inhomogeneity of the medium. Moreover, it shows that as the system is driven by a square-wave external forcing of appropriate frequency, dispersionless particle motion could be observed after each field direction change. These transient dispersionless regimes, however disappear as the frequency is increased and instead periodic variation of dispersions result. The 'moderately high frequency' dispersive regimes (where dispersions vary periodically) help in increasing the ratchet current considerably. Similarly, in these dispersive regimes, the velocity

dispersion also varies periodically, with twice the frequency of the field drive, but in exact anti-phase to the position dispersions. In the nondispersive regimes, on the other hand, when the particles move coherently, they tend not to notice the frictional inhomogeneity and do not contribute to the ratchet current. In the present work, however, the ratchet current is obtained when the amplitude of periodic rocking was small. It would be interesting to examine if one could obtain ratchet current with the help of high amplitude drive as in the case of asymmetric periodic potentials.

Bibliography

[1] S. Saikia and M. C. Mahato, J. Phys. Cond. Mat. 21, 175409 (2009).

[2] H. Risken, *The Fokker-Planck Equation*, (Springer-Verlag, Berlin), 1996; H.Risken and H.D. Vollmer, Z.Physik B **33**, 277 (1979).

[3] L. Machura, M. Kostur, F. Marchesoni, P. Talkner, P. Hänggi, and Łuczka, J. Phys. Condens. Matter 17, S3741 (2005); L. Machura, M. Kostur, P. Talkner, J. Łuczka, F. Marchesoni, and P. Hänggi, Phys. Rev. E 70, 061105 (2004).

[4] P. Reimann, Phys. Rep. 361, 57 (2002); R. P. Feynman, R. B. Leighton, and M. Sands, *The Feynman Lectures in Physics* (Publishers, year), Vol. 1, Chap. 46.

[5] L. Machura, M. Kostur, P. Talkner, J. Łuczka, and P. Hänggi, Phys. Rev. Lett. 98, 040601 (2007); M. Kostur, L. Machura, P. Talkner, P. Hänggi, and J. Łuczka, Phys. Rev. B 77, 104509 (2008).

[6] J. Nagel, D. Speer, T. Gaber, A. Sterck, R. Eichhorn, P. Reimann, K. Ilin, M. Siegel, D. Koelle, and R. Kleiner, Phys. Rev. Lett. 100, 217001 (2008).

[7] G. Wahnström, Surf. Sci. 159, 311 (1985).

[8] C. M. Falco, Am. J. Phys. 44, 733 (1976); A. Barone, and G. Paterno, *Physics and Applications of the Josephson Effect*, John Wiley, New York, 1982.

[9] R. Landauer, J. Stat. Phys. 53, 233 (1988).

[10] M. Büttiker, Z.Phys. 68, 161(1987).

[11] Ya. M. Blanter and M. Büttiker, Phys. Rev. Lett. 81, 4040 (1988).

[12] R. Benjamim and R. Kawai, Phys. Rev. E 77, 051132 (2008).

[13] W. L. Reenbohn, S. Saikia, R. Roy, and M. C. Mahato, Pramana - J. Phys. 71, 297 (2008).

[14] W. L. Reenbohn, and M. C. Mahato, J. Stat. Mec.: Theory Exp. P03011 (2009).

[15] B. Lindner, M. Kostur, and L. Schimansky-Geier, Fluct. Noise Lett. 1, R25 (2001).

[16] K. Sekimoto, J. Phys. Soc. Jpn. 66, 6335 (1997).

[17] K. Lindenberg, J. M. Sancho, A. M. Lacasta, and I. M. Sokolov, Phys. Rev. Lett. 98, 020602 (2007).

[18] The parameter scaling is different from that of Machura, et. al., where [3] the forcing amplitude a is equivalent to π times the amplitude F_0 in our case. The total potential barrier height (at $a = 0$) is ~ 1 , whereas in this work it is 2. However, the noise strength D_0 in Ref. [3] is same as the temperature T used here.

[19] W. H. Press, S. A. Teukolsky, W. T. Vetterling and B. P. Flannery, *Numerical Recipes (in Fortran): the Art of Scientific Computing*, Cambridge University Press, Cambridge, 1992; M. C. Mahato and S. R. Shenoy, J. Stat. Phys. 73, 123 (1993).

[20] B. Borromeo, G. Constantini, and F. Marchesoni, Phys. Rev. Lett. 82, 2820 (1999); M. C. Mahato, and A. M. Jayannavar, Physica A 318, 154 (2003).

Chapter 4

Dispersionless motion in a periodically rocked periodic potential

4.1 Introduction

In this chapter we study an interesting aspect of the inertial particle motion in a periodically rocked periodic potential - the intermediate time dispersionless motion [1]. This work is an extension of the previous chapter in which the presence of intermediate time dispersionless motion of particles in a periodically rocked potential was shown.

The inertial Brownian particle motion in periodic potentials [2, 3] is an important model to theoretically understand many phenomena in physical systems. For example, this model can be used to understand the current-voltage characteristics of (RCSJ model of) Josephson junctions [4], the electrical conductivity of superionic solids [5], motion of adatoms on the surface of a crystal [6], etc. [2]. Though substantial work has been done using this model, the behaviour of the model particle motion in all the parameter regimes have not been explored. A recent example being the discovery of dispersionless particle motion in a tilted

periodic potential in the intermediate time regime [7]. In this work, Lindenberg and coworkers showed (numerically) that particles moving on a cosinusoidal potential with a constant tilt, F_0, in a medium with constant friction coefficient γ_0[7] in a limited (F_0, γ_0) region, essentially move nondispersively over long intervals of time i.e during this coherent motion, the ensemble averaged position dispersion, $\Delta x(t) =< (x(t) - < x(t) >)^2 >$, remains constant.

The particles, intially in a potential well, cross the barrier because of the thermal fluctuations after a time $t = \tau_1$ ($\tau_1 > \tau_K$, the Kramers mean passage time). τ_1 is determined by the tempeature and the external forcing. After crossing the barrier they move coherently with velocity $v \approx \frac{F_0}{\gamma_0}$. During this coherent motion the thermal fluctuations have negligible influence. This coherent motion continues until normal dispersive motion sets in (at around $t = \tau_2$) and the system resumes its normal behavour. τ_1 and τ_2 are dependent on the system parameters and they are specified only as a rough guide [7].

In this work, instead of a constant tilt, we use a zero-mean square-wave external drive $F(t)$ of half period τ and amplitude F_0. We study the effect of the zero-mean square-wave external drive on the intermediate time nondispersive motion of the particle. We find that for $\tau_1 < \tau < \tau_2$, the coherent motion, naturally, gets interrupted upon reversal of direction of F at $t = \tau$. But interestingly, the coherent motion once disturbed, by reversing the field at $t = \tau$, gets reestablished around $t = \tau + \tau_1$ in almost the same form as it was during $\tau_1 < t < \tau_2$ in the constant tilt case. This loss and subsequent recovery of coherent motion continues for a large number of reversals of $F(t)$. The dispersion $\Delta x(t)$, however, increases rapidly during $\tau < t < \tau + \tau_1$. (During $0 < t < \tau_1$, $\Delta x(t) \sim t^\alpha$, $\alpha \approx 2$).

4.2 The model

For this work, we use the same model as in the previous chapter. We consider the motion of a Brownian particle of mass m moving in a potential $V(x) = -V_0 \sin(kx)$ in a medium with friction coefficient [8] $\gamma(x) = \gamma_0(1 - \lambda \sin(kx + \phi))$ at temperature T (in units of k_B) and subjected to an external force field $F(t)$. The corresponding Langevin equation is written [9] as in the previous chapter in terms of dimensionless variables for convenience. The applied square-wave force $F(t)$ is taken as $F(t) = \pm F_0$ for $(2n\tau \leq t < (2n+1)\tau)$ and $F(t) = \mp F_0$ for $((2n+1)\tau \leq t < (2n+2)\tau)$ with $n = 0, 1, 2, ...$

4.3 Numerical results

For constant applied force $F(t) = F_0$ (for all t) the Langevin's equation can be solved using the matrix continued fraction method and also numerically, supporting each other quantitatively [2, 10, 11, 12, 13]. However, for finite τ, the corresponding Langevin equation is solved numerically. using the 4^{th} order Runge-Kutta method [15], by taking time steps of $\Delta t = .001$. Throughout our calculations, we take $\gamma_0 = 0.035$, $\lambda = 0.9$ and $\phi = 0.35$. $\gamma_0 = 0.035$ is the value of friction where the system exhibits hysteresis [14]. $\lambda \neq 0$, however, is relevant only while discussing ratchet current at the end. In fact, except for this minor point, all the results discussed in the following qualitatively remain same for the simpler case of $\lambda = 0$. Averaging is done over an ensemble of particles having initial position distribution as as $\delta(x - \frac{\pi}{2})$ and the initial velocity from a Maxwell distribution corresponding to a temperature $T = 0.4$.

For the constant tilt case, for $F_0 = 0.2$, the particles exhibit coherent motion in the potential $V(x) = -\sin(x) - xF_0$, in the intermediate times roughly in the range $[\tau_1(\approx 2 \times 10^3) < t < \tau_2(\approx 3 \times 10^4)]$, for $F_0 = 0.2$ (Fig. 4.1). Therefore, for our calculations we take the amplitude of the zero-mean square-wave driving field $F(t)$ as $F_0 = 0.2$. Also in most cases, if not stated otherwise, we take

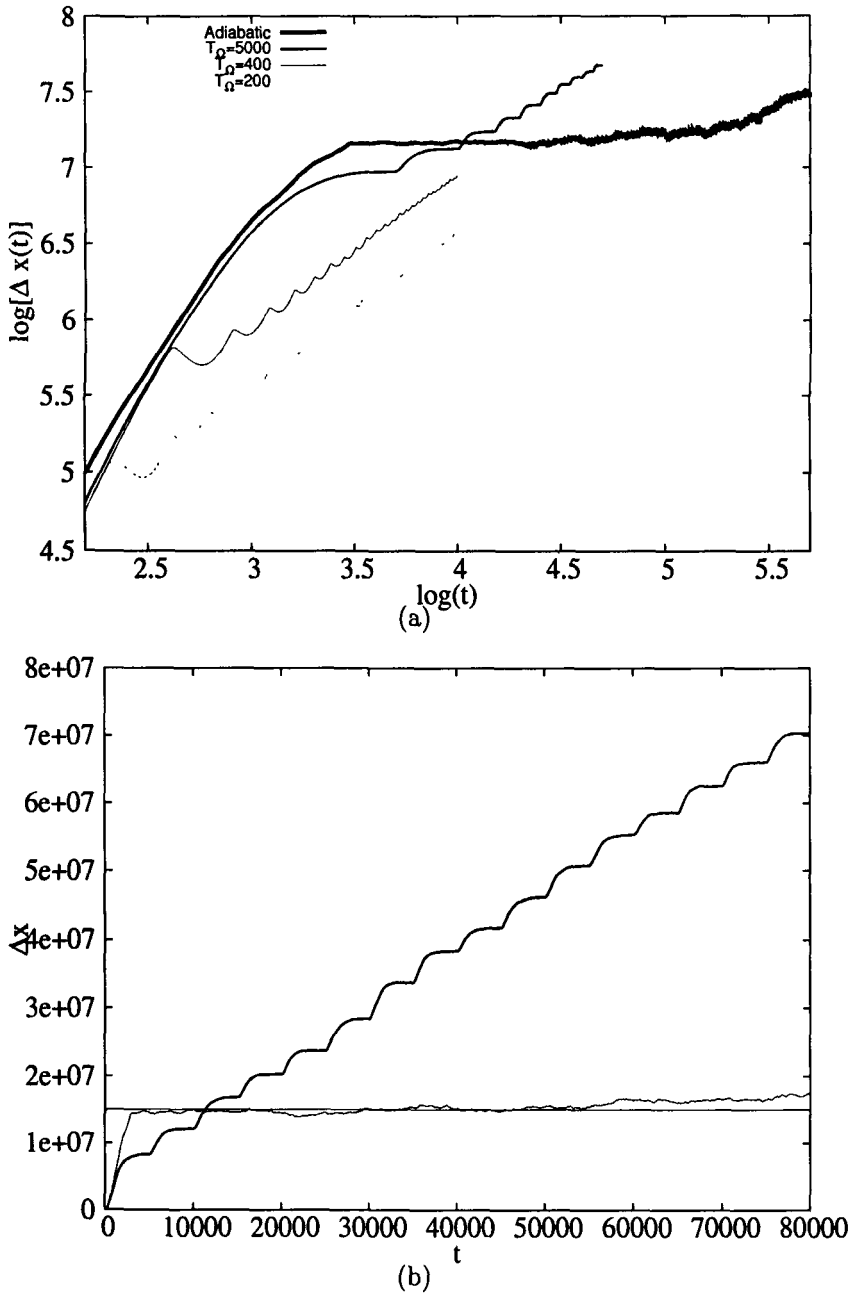

Figure 4.1: The position dispersion $\Delta x(t)$ for the adiabatic limit (constant tilt), $\tau = 5000$, 400, and 200 versus time (logarithmic scale) are plotted (Fig4.1a). In Fig4.1b the plot for $\tau = 5000$ is extended to 16 half periods together with the plot for the constant tilt case. The dotted horizontal line is drawn to guide the eye. Note that $t_2 < 60000$.

the half period of the drive to be $\tau = 5000$ which is well within the range $[\tau_1, \tau_2]$. Naturally, in the first half period ($0 < t \leq \tau$) the motion is same as in the constant tilt case. In the zero-mean square-wave driven case, the periodic potential gets tilted in the reverse direction after every half period τ as a result of field reversal.

4.3.1 Particle motion in intermediate time regimes

It is observed that for $\tau = 5000$ of the external forcing $F(t)$, the particle exhibits a repetitive sequence of coherent motion in each half period of the drive during which the position dispersion $\Delta x(t)$ remains constant (Fig. 4.1). The coherent motion in each half period is preceded by a length of dispersive particle motion. As a result $\Delta x(t)$ grows, in discrete steps, with time, as the number n of half periods increases. The generation of coherent motion continues for many ($n >> 8$) half periods ($\tau = 5000$) of $F(t)$, Fig. 4.1b. Thus, as an important consequence, of the zero-mean square-wave drive $F(t)$, the cumulative duration ($\approx n(\tau - \tau_1)$) of coherent motion is made much larger than the duration, $\tau_2(\approx= 60000) - \tau_1$, achievable in the constant tilt case as shown in the inset of Fig. 4.1b.

We also study the variation of Δx with time t corresponding to the half periods τ =400, and 200 (Fig4.1a). The important feature to be noticed in the figure is that, for $\tau = 400, 200 < \tau_K, \tau_1$, Δx dips immediately after the field is reversed before it rises. This behaviour of dispersion dipping and subsequent rise becomes most pronounced at a small but intermediate τ. It continues for many periods of $F(t)$.

Fig.4.2, summarizes the main results of this work. It shows many interesting effects of taking few initial half periods of $F(t)$ of smaller duration, $\tau = 400$ (curve (b)), and $\tau = 200$ (curves (c-d)) and then making its later half periods $\tau = 5000$ or larger (e.g., 10000, curve (d)). The curves (b-c) show that, in this case too, during the later half periods $\tau = 5000$ of $F(t)$, a similar sequence of trains of coherent motion, as in Fig. 4.1b, (or curve (a)), can be obtained. It also

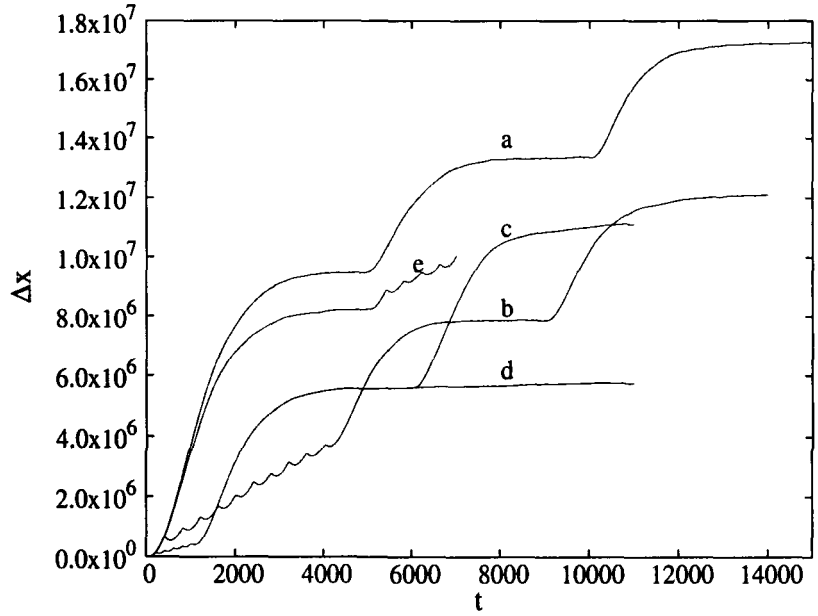

Figure 4.2: $\Delta x(t)$ for three $\tau = 5000$ (a) ten $\tau = 400$ and two $\tau = 5000$ (b), five $\tau = 200$ and two $\tau = 5000$ (c), five $\tau = 200$ and one $\tau = 10000$ (d), and one $\tau = 5000$ and five $\tau = 400$ (e) half periods are plotted.

allows to postpone (curve (b)) the appearance of coherent motion beyond $t = \tau_1$. Moreover, it is possible to obtain coherent motion with lower constant dispersion (curves (c,d)) than in the constant tilt case (i.e., lower than the constant Δx in the first half period in the curve (a)) too. Curve (e) shows that the curves (b-d) can be repeated, using the same customized procedure, many times over again.

4.3.2 Velocity distribution of particles

The results of Fig. 4.1 and 4.2 can be understood by analyzing the time evolution of velocity distribution, $P(v)$. Fig. 4.3a shows the velocity distributions for various values of t for $\tau = 5000$. It is seen that the velocity distributions invariably assume almost a Gaussian form of same width and centred at a fixed $v \approx \pm\frac{F_0}{\gamma_0}$ at $t = n\tau$ for $\tau = 5000$. The plot of the mean velocity $\bar{v}(t)$ and velocity dispersion $\Delta v(t)$ (Fig. 4.3b), supports this observation. However, the velocity distributions $P(v)$, for $\tau = 1000$, at $t = n \times 1000$, has two peaks one centred at

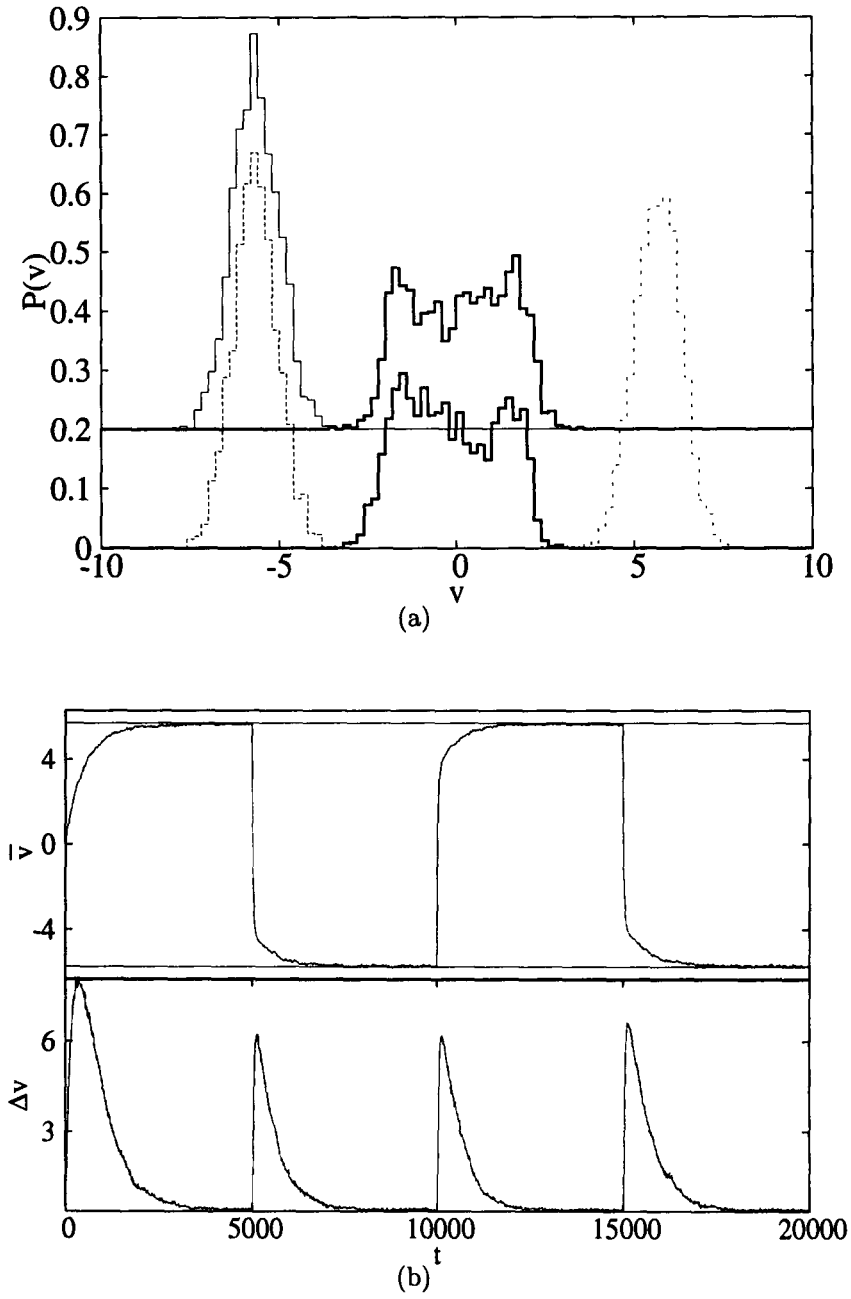

Figure 4.3: Fig. a shows velocity distributions for $\tau = 5000$ at $t = 10000$ (left peak, dashed) , 10015.5 (central peak, bold), 15000 (right peak, dot-dash), 15015.5 (central peak, bold shifted by 0.2) and 20000 (left peak shifted by 0.2). In Fig. b, $\bar{v}(t)$ and $\Delta v(t)$ are plotted for $\tau = 5000$. $\bar{v} = \pm\frac{F_0}{\gamma_0}$ lines are drawn for reference.

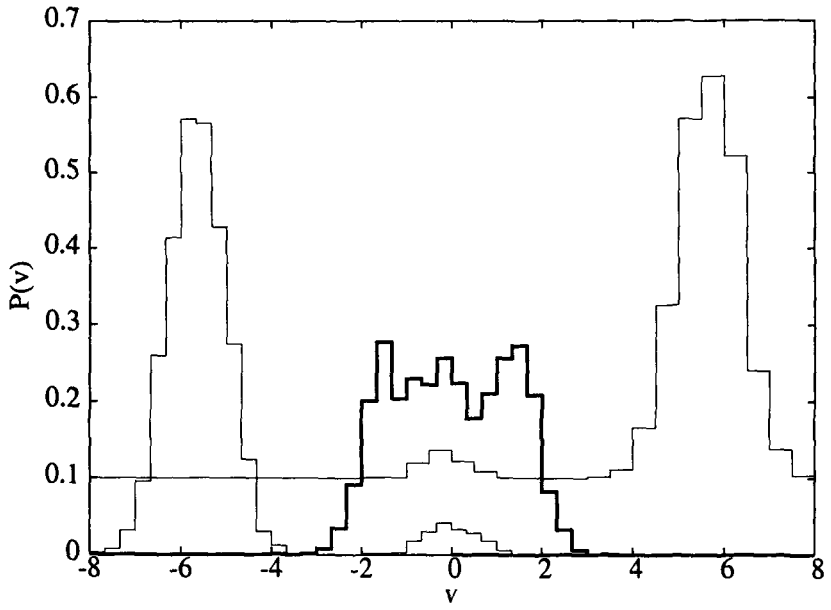

Figure 4.4: Velocity distributions at different t for $\tau = 1000$; $t = 2000$(bimodal with higher left peak), $t = 2016$ (bold line), and $t = 3000$ (bimodal, shifted by 0.1).

$v \approx \pm\frac{F_0}{\gamma_0}$ and the other at $v = 0$ (Fig. 4.4). The $P(v)$ peak at $v = 0$ shows that at $t = n\tau$, for $\tau < \tau_1$, implies that some particles are left behind in the locked state in one or some other wells. The peak in $P(v)$ at $n\tau$ centred at $v = 0$ is more prominent for lesser values of τ. These locked particles try to gravitate to their respective well bottoms and, being slower, even succeed in shrinking the position distribution $P(x)$ more effectively than the much faster particles in the running state on the front. Thus, for smaller $\tau < \tau_1$, the bimodal nature of $P(v)$ helps appreciable Δx dipping immediately after field reversal, Fig. 4.1a.

At $t = n\tau + t_0$, $15 < t_0 < 16$, $\bar{v}$ becomes zero for all τ, and n. (It turns out, $2t_0 \approx \frac{1}{\gamma_0}$, the frictional relaxation time.) The corresponding $P(v)$ are also shown in Fig. 4.3a. For $\tau = 5000$, $P(v)$ at $t = n\tau + t_0$ is like a sum of two "Gaussians" centred on either side of $v = 0$. But for $\tau = 1000$ (Fig. 4.4), the surviving $P(v)$ peak at $v = 0$ at $t = n\tau$, contributes an additional one centred at $v = 0$, making $\bar{v} = 0$ at the same delay time τ_0.

Due to the tilt direction reversal the particles, in the running state, are

forced to reverse their direction of motion and hence each of them necessarily go through zero velocity at least once momentarily. Thus, the entire system passes approximately through a "thermal" state at $t = n\tau + \tau_0$. Hence, after every field reversal at $t = n\tau$ the particles begin their subsequent journey in the reversed direction with almost the same delayed initial condition (at $t = n\tau + \tau_0$) of thermalized $P(v)$. Therefore, Δx are expected to behave similarly after every $n\tau$.

As discussed above, it is just the reversal of field which leads $P(v)$ to the required form at $t = n\tau + t_0$, irrespective of the form of $P(v)$ at $t = n\tau$ for any value of $\tau >> \tau_0 \approx 16$. It shows that in order to obtain coherent motion neither an exact initial Gaussian velocity distribution is necessary nor all the particles are required to be intially confined sharply to a single well bottom of the periodic potential. Also, a mere switching the field alternately *on* ($F_0 \neq 0$) for duration τ and *off* ($F_0 = 0$) for the same duration τ, fails to yield results like Figs. 4.1 and 4.2. This indicates that a reversal of the field direction is essential because this alone ensures a "thermalized" $P(v)$.

Also in the constant tilt case the average particle displacement is large, $\approx \frac{\tau_2 F_0}{\gamma_0}$ by the end of its coherent motion whereas in the zero-mean square-wave case it is zero, for $\lambda = 0$, and small and finite for $\lambda \neq 0$ and $\phi \neq 0, \pi$ after any large time $t = 2n\tau$. This is an added practical advantage over the constant tilt case for, in the zero-mean square-wave case, most of the particles on the average remain confined to a finite region of space despite periodically showing coherence of motion for a long time.

The dimensionless values of parameters used (e.g., $\gamma_0 = 0.035, T = 0.4, \tau = 5000$, and $F_0 = 0.2$) and other derived quantities when restored to their usual units are presented in Table 4.1 for three illustrative cases: (i) The motion of an Ag ion in AgI crystal [16], (ii) the motion of a macromolecule (kinesin) along a polymer fibre (microtubule) [17], and (iii) diffusion of Cooper pairs across a Josephson junction [4]. Notice that $\omega(= \frac{\gamma_0}{m}) << \omega_0$, in the particle

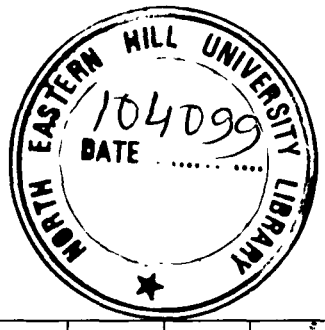

System	m	V_0	T	k	ω_0	γ_0	$\omega(=\frac{\gamma_0}{m})$	F_0	τ	$\bar{v}=\frac{\dot{F}_0}{\gamma_0}$
	C	I_1		$\frac{2e}{\hbar}$	ω_P	G	$(=\frac{G}{C})$	I_0		$\bar{V}=\frac{I_0}{G}$
Ag on *AgI*	1.792	0.15	348	0.5π	4.07	2.55	1.42	5.03	1.23	1.48
	$\times 10^{-25}$			$\times 10^{10}$	$\times 10^{12}$	$\times 10^{-14}$	$\times 10^{11}$	$\times 10^{-10}$	$\times 10^{-9}$	$\times 10^{3}$
	Kg	eV	K	m^{-1}	s^{-1}	Kg s^{-1}	s^{-1}	N	s	ms^{-1}
Macro-	3.321	0.129	300	2.5π	6.202	7.209	2.17	3.253	8.062	4.512
molecule on	$\times 10^{-22}$			$\times 10^{8}$	$\times 10^{9}$	$\times 10^{-14}$	$\times 10^{8}$	$\times 10^{-13}$	$\times 10^{-7}$	
Polymers	Kg	eV	K	m^{-1}	s^{-1}	Kg s^{-1}	s^{-1}	N	s	ms^{-1}
Josephson	0.5	1.0	9.53	3.0385	2.465	4.314	8.63	2.0	2.028	4.636
Junction		$\times 10^{-9}$		$\times 10^{15}$	$\times 10^{9}$	$\times 10^{-5}$	$\times 10^{7}$	$\times 10^{-8}$	$\times 10^{-6}$	$\times 10^{-4}$
	pF	Amp	mK	$Volt^{-1}s^{-1}$	s^{-1}	Ohm^{-1}	s^{-1}	Amp	s	Volt

Table 4.1: The systems considered are: (1) Ag: Ag on AgI lattice, (2) Mm: a macromolecule along a polymer, and (3) JJ: Josephson junction. The symbols have their usual meaning. The RCSJ-model JJ equation equivalent to Eq.(3.1 of chapter 3) is[4]:
$\frac{\hbar C}{2e}\frac{d^2\theta}{dt^2}+\frac{\hbar}{2e}G(1+\lambda\cos(\theta+\phi))\frac{d\theta}{dt}+I_1\sin(\theta)=I(t)+\sqrt{2TG(1+\lambda\cos(\theta+\phi))}\xi(t)$.
(Add $-\frac{\pi}{2}$ to θ for exact correspondence.)

motion case, and $\omega << \omega_P$, the Josephson plasma frequency ($= \frac{2eI_1}{\hbar C}$), showing that the systems considered are, indeed, underdamped. The last column of the table gives the magnitude of mean velocity (mean voltage) attained during the coherent state when the initial value of the drive field $F(t)$ ($I(t)$) is fixed either at $+|F_0|$ ($+|I_0|$) or with their sign reversed and not an equal mixture of both. Also, during the half period τ the particles move to an average distance (the product of quanties in the last two columns) of the order of a micron (μ) which will get retraced in the next half period. This gives a rough idea of the sample size one would need to take in a zero-mean square-wave case. Also, $\frac{2\pi}{\tau} << \omega_0(\omega_P)$ (by about two orders of magnitude).

The calculated average velocities $\bar{v}$ and velocity dispersions Δv are plotted, in Fig. 4.3b. An equal mixture of $F(t=0) = \pm|F_0|$ makes $\bar{v}$ close to zero during coherent motion. It is exactly zero for $\lambda = 0$ at all t and hence even in the limit $t \to \infty$ $\bar{v}$ remains zero. However, for $\lambda \neq 0$ and $\phi \neq 0, \pi$ a nonzero finite mean (steady state) velocity is obtained [11, 13, 12] earlier. The contribution of coherent particle motion being insignificant, the dispersive motion alone contributes to this *ratchet* current of particles.

The diffusion constant, D, defined as $\lim_{t\to\infty} \Delta x(t) = 2Dt$, is hard to calculate for a constant tilt F_0 [7]. The asymptotic limit barely reaches even by $t = 10^7$. However, for zero-mean square-wave this limit is readily reached by $t = 10^7$ (Fig. 4.5). It may be noted that for each curve in Figs. 4.1 and 4.2 we have averaged over 2000 realizations but in Fig. 4.5 we could average over number of realizations ranging only between 18 and 60. The nature of $\Delta x(t)$ so clear in Fig. 4.1 appears less convincing in Fig. 4.5. Therefore, it is hard to conclude that the same nature of Δx, as in Fig. 4.1, will continue till the asymptotic time regime. However, from the "thermalized" $P(v)$ argument given earlier, there is a fair likelyhood that the nature of $\Delta x(t)$ shown in Fig.4.1 will extend to a large number of half periods of $F(t)$ provided a large number of particles are considered for averaging.

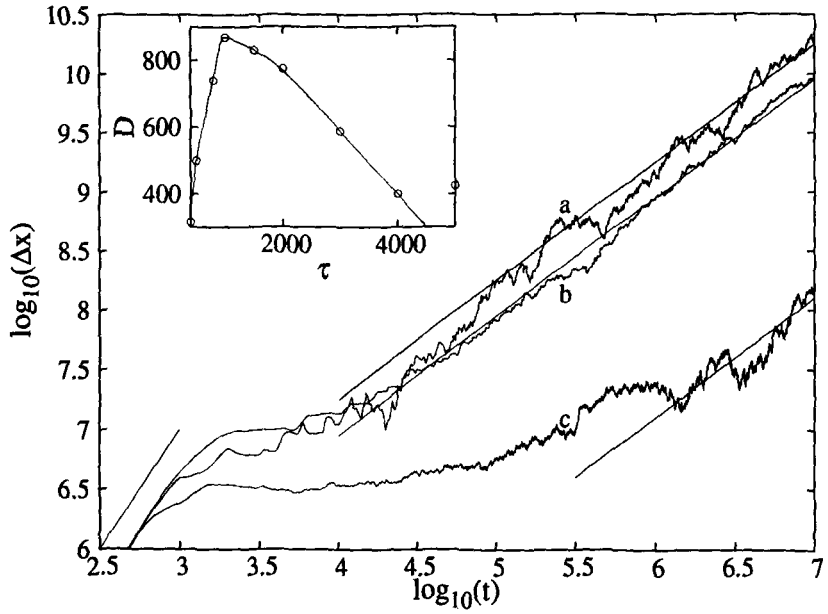

Figure 4.5: $\Delta x(t)$ for $\tau = 1000$ (a), 5000 (b), and for the case of CT $F_0 = 0.2$ (c) averaged over, respectively, 20, 60, and 18 ensembles are plotted. Lines of slope 1 are fitted to the curves. The short line at the lower left corner indicates $\Delta x \sim t^{\alpha}, \alpha \approx 2$. The inset shows variation of D with τ.

The nature of $\Delta x(t)$ shown by the curves in Figs.4.1 and 4.2 is in no finite region close to $\Delta x(t) \sim t$. It remains, therefore, open to explain why a large number of repeatedly same diverse combinations of dispersions such as ones ranging from $\Delta x(t) \sim t^2$ to $\Delta x(t) \sim t^0$, when averaged over a large number of realizations, yields the same nature of dispersion, $lim_{t\to\infty}\Delta x(t) \sim t$, for all τ, Fig.4.5.

$D(\tau)$, plotted in the Inset of Fig. 4.5, are rough estimates as the averagings are done only over a small number of realizations. However, the overall qualitative trend of $D(\tau)$ remains valid. $D(\tau)$ shows a peak around $\tau = \tau_1$. For $\tau > \tau_1$, the closer τ is to τ_1 smaller is the constant Δx region and hence larger is the fraction of sharply rising Δx region. Naturally total Δx will be larger as $\tau \to \tau_1$. However, the nature of $D(\tau)$ as $\tau \to \tau_2$ is not clear from the available data. In the range $\tau < \tau_1$, Δx rises only after an appreciable dipping, Fig. 4.1a. Therefore, the initial rise of Δx is slower as τ is decreased from τ_1 resulting in

a smaller total $\Delta x(t)$ as $t \to \infty$ and hence smaller D.

From the *rms* spread ($\sqrt{\Delta x}$) point of view the advantage of zero-mean square-wave $F(t)$ over constant tilt, except in cases like curve (d) in Fig. 4.2, quickly evaporates as t increases. Whereas for the constant tilt case at $t = 10\tau = 5 \times 10^4$, the mean displacement $\bar{x}$ is 2.8×10^5 and $\sqrt{\Delta x}$ is 0.22×10^5, and at $t = 2000\tau = 10^7$, $\bar{x} = 5.7 \times 10^7$ and $\sqrt{\Delta x} = 0.012 \times 10^7$, for the zero-mean square-wave case, at $t = 10\tau$, $\bar{x} \approx 0$, and $\sqrt{\Delta x} = 0.06 \times 10^7$, and at $t = 10^7$ $\bar{x} \approx 0$, and $\sqrt{\Delta x} = 0.095 \times 10^7$. Perhaps in the zero-mean square-wave case, the particles left behind during a τ get pushed father away during the next τ, make the $\sqrt{\Delta x(t)}$ increase faster as t increases.

Coherent motion is observed only in the negative slope region of $D(\tau)$. However, for this same system it is shown in Ref. [13] that ratchet current is maximum for a value of $\tau \simeq 500$, i.e., in the rising $D(\tau)$ region and becomes significantly small for larger $\tau \geq \tau_1$ and almost zero at $\tau = 5000$. The peak of the $D(\tau)$, thus, roughly divides τ into two regions: (i) small τ giving ratchet current, and (ii) larger τ showing coherent motion.

4.4 Conclusion

To summarise, the dispersionless (coherent) motion discovered earlier, to occur for a brief but finite duration in the intermediate time regime, on a constant tilt sinusoidal potential, was extended to the case of periodically reversing constant tilts. We have shown the possibility of obtaining coherent particle motion interspersed by dispersive motion over many periods of an external zero-mean square-wave field. The cumulative duration of coherent motion can, thus, be extended to a substantial fraction of the total journey time, of course, at a cost of making the system several times more diffusive.

Bibliography

[1] S. Saikia and Mangal C. Mahato, Phys. Rev. E 80, 062102 (2009).

[2] H. Risken, *The Fokker-Planck Equation*, (Springer-Verlag, Berlin), 1996.

[3] P. Reimann, Phys. Rep. 361, 57 (2002); R.P. Feynman, R.B. Leighton, and M. Sands, *The Feynman Lectures in Physics* (Publishers, year), Vol. 1, Chap. 46.

[4] C.M. Falco, Am. J. Phys. 44, 733 (1976); A. Barone, and G. Paterno, *Physics and Applications of the Josephson Effect*, John Wiley, New York, 1982.

[5] P. Fulde, L. Pieternero, W.R. Schneider, and S. Strässler, Phys. Rev. Lett. 35, 1776 (1975).

[6] A.M. Lacasta, J.M. Sancho, A.H. Romero, I.M. Sokolov, and K. Lindenberg, Phys. Rev. 70, 051104 (2004).

[7] K. Lindenberg, J.M. Sancho, A.M. Lacasta, and I.M. Sokolov, Phys. Rev. Lett. 98, 020602 (2007).

[8] G. Wahnström, Surf. Sci. 159, 311 (1985).

[9] A.M. Jayannavar, and M.C. Mahato, Pramana-J. Phys. 45 369 (1995); M.C. Mahato, T.P. Pareek, and A.M. Jayannavar, Int. J. Mod. Phys. B 10, 3857 (1996).

[10] H. Risken, and H.D. Volmer, Z. Physik B 33, 297 (1979).

[11] W.L. Reenbohn, S. Saikia, R. Roy, and M.C. Mahato, Pramana J. Phys. 71, 297 (2008).

[12] W.L. Reenbohn, and M.C. Mahato, J. Stat. Mech: Theor. Exp. P03011 (2009).

[13] S. Saikia, and M.C. Mahato, J. Phys.: Condens. Matter 21, 175409 (2009).

[14] B. Borromeo, G. Constantini, and F. Marchesoni, Phys. Rev. Lett. 82, 2820 (1999); M.C. Mahato, and A.M. Jayannavar, Physica A 318, 154 (2003).

[15] W.H. Press, S.A. Teukolsky, W.T. Vetterling, and B.P. Flannery, *Numerical Recipes (in Fortran): the Art of Scientific Computing*, Cambridge University Press, Cambridge, 1992; M.C. Mahato, and S.R. Shenoy, J. Stat. Phys. 73, 123 (1993).

[16] M. Hayana, A. Hatate, and M. Oguni, J. Phys.: Condens. Matter 15, 3867 (2003).

[17] R.D. Astumian, and M. Bier, Phys. Rev. Lett. 72, 1766 (1994).

Chapter 5

Stochastic resonance in a driven double well system

5.1 Introduction

In this chapter, the results of our work on the phenomenon of stochastic resonance in a driven double well system is presented [1].

Stochastic resonance (SR) refers to the enhanced response of a system to a small deterministic periodic forcing in the presence of an optimal amount of noise [2]. It often occurs in bistable and excitable systems with subthreshold inputs. Noise plays a constructive role in this phenomenon. This is due to a cooperative interplay between nonlinearity of the system, input signal and noise. Thus the power from the whole spectrum is pumped into a single mode that is coherent with the external driving force. Because of its generic nature, this phenomenon, has varied applications in almost all areas of natural sciences. Different quantifiers of SR have been discussed [3, 4, 5, 6, 7] as regards to its validity as a bonafide resonance, i.e., the resonance phenomena as a function of noise strength as well as the driving frequency. Hysteresis loop area [3], input energy or the work done on the system per cycle [4, 5] and area under the first peak in the residence time distribution [11] have turned out to be good

quantifiers characterizing SR as a bonafide resonance. Recently it has been shown that the different quantifiers of SR are mathematically related to each other [6].

The work presented in this chapter is organised in the two parts.

5.2 Part one

In the first part of the work, we study the phenomenon of SR in a driven bistable potential by using the average input energy per period of the external drive and the hysteresis loop area as quantifiers. Earlier studies on the work done in a periodically driven bistable system by an external agent has established that the average work peaks around the resonance, as expected [4, 5]. In our present work [1], apart from the average input energy per period of drive, we also calculate the hysteresis loop area and compare it with the input energy. We show that the area of the hysteresis loops too can be used as a quantifier for SR. We also study the fluctuations and nature of the probability distributions of work done over a period in a driven double-well system in the time asymptotic regime (where all averaged quantities become periodic in time with a period of the external drive). Our study of input energy fluctuations also reveal that the relative variance is larger than one across SR indicating that fluctuations dominate the mean value.

5.2.1 The model

We consider overdamped particle motion in a double well potential $V(x) = \frac{x^4}{4} - \frac{x^2}{2}$ (Fig. 5.1). The system is driven by an external forcing $F(t) = A\sin\omega t$. The corresponding Langevin equation is given by [9]

$$\frac{dx}{dt} = -\frac{\partial V(x)}{\partial x} + F(t) + \xi(t), \tag{5.1}$$

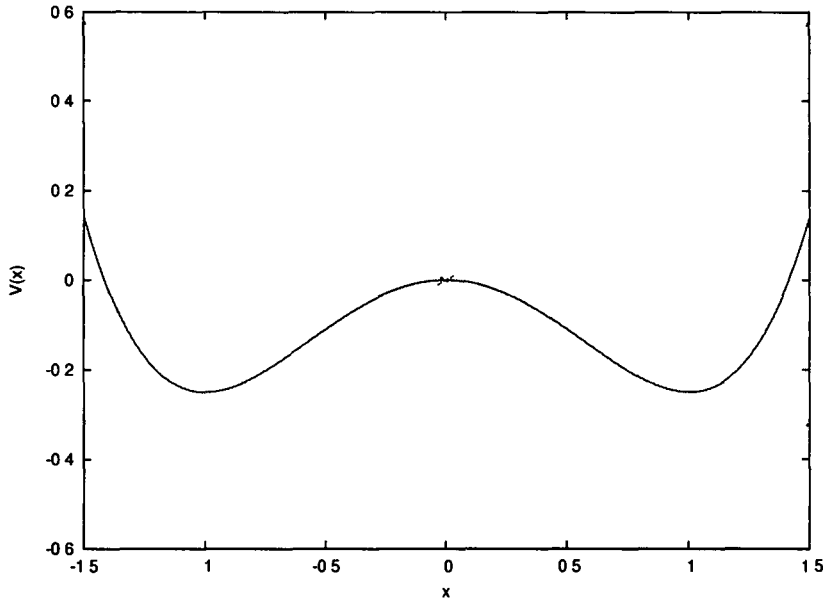

Figure 5.1: Plot of the bistable potential $\frac{x^4}{4}$-$\frac{x^2}{2}$ and its driven state.

where the random force field $\xi(t)$ is a zero mean Gaussian white noise, i.e,

$$\langle \xi(t)\xi(t') \rangle = D_0 \delta(t - t'). \tag{5.2}$$

where $D_0 = 2k_BT$ is the strength of the noise. The static double-well potential $V(x) = \dfrac{x^4}{4} - \dfrac{x^2}{2}$, has a barrier height $\Delta V = 0.25$ between the two symmetrical wells (minima) located at distances $x_m = \pm 1$. We consider the case of weak forcing $A|x_m| < \Delta V$. All the physical quantities are taken in dimensionless units [4, 5].

The work done by the external drive on the system or the input energy $\left(\tau_\omega = \dfrac{2\pi}{\omega}\right)$ is defined as [4, 5]

$$\begin{aligned} W_p &= \int_{t_0}^{t_0+\tau_\omega} \frac{\partial U(x,t)}{\partial t}\, dt, \\ &= -A\omega \int_{t_0}^{t_0+\tau_\omega} x(t) \cos \omega t\, dt \end{aligned} \tag{5.3}$$

where $U(x,t) = V(x) - xF(t)$ This follows from the stochastic energetics

formalism developed by Sekimoto [12].

Numerical simulation of this model was carried out by using Huen's method [13]. To calculate the work done we first evolve the system and neglect initial transients and then work done over a period (W_p) is calculated (Eq.5.3). The values of W_p are different for different cycles. To get better statistics we have calculated W_p for 100000 different (sometimes even more) cycles.

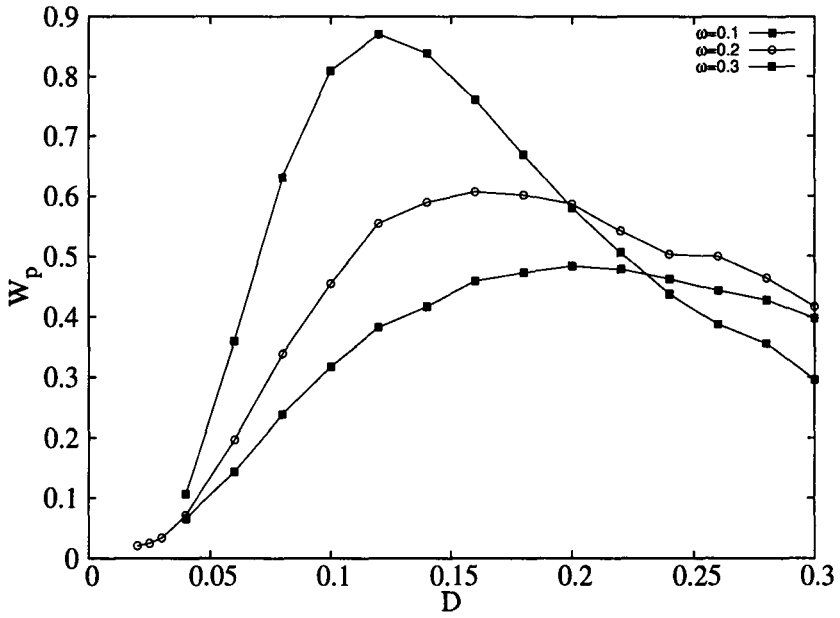

Figure 5.2: Figure shows the variation of average work W_p done per period with temperature D for different values of ω for A=0.1.

5.2.2 Numerical results

In Fig. 5.2 we plot the average work done (W_p) over a single period (in the time asymptotic regime) as a function of noise strength D($= kT = \frac{1}{\beta}$, in dimensionless units) for low amplitude driving of strength $A = 0.1$ and for three values of frequency $\omega = 0.1$, 0.2 and 0.3. We clearly see that input energy exhibits a peak as a function of D. This peaking of input energy is because of the synchronized escape of the particle from the potential well with the external periodic drive. We reproduce exactly the same figure as in reference [5], which has been obtained using a different numerical method.

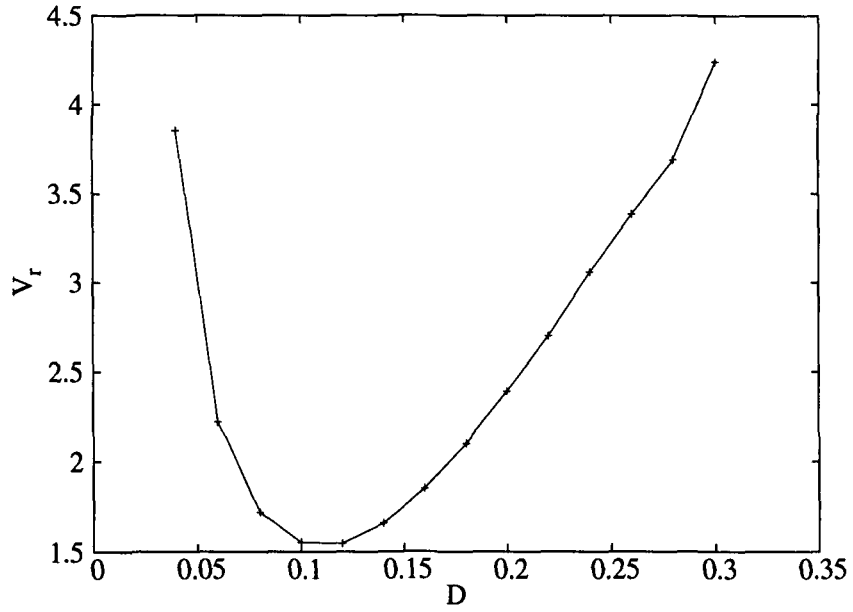

Figure 5.3: Figure shows the relative variance of the average work W_p done per period with temperature D $\omega = 0.1$ and A=0.1.

When the temperature is small, the particle remains in one of the potential wells for a longer time(intrawell motion dominates) with an occassional random jump to another well (Kramers' escape over the barrier) as a function of time (Fig. 5.4a). When the noise is very strong a large number of interwell random switches occur for each period of the sinusoid and the systems response is again random (interwell motion dominates) (Fig. 5.4d). In between these two conditions, surprisingly, there exists an optimal value of the noise that cooperatively concurs with the periodic forcing to make almost exactly one switch per period. Hence interwell motion will be in synchrony with the input signal. Quantitatively this condition is determined by the matching of the two time scales [2, 5], namely, the period of the input signal and the Kramers' escape rate r_k, $\left(\frac{1}{r_k} = \frac{\tau_\omega}{2} \rightarrow \frac{\omega}{\pi} = r_k, \text{with } r_k = \frac{1}{\sqrt{2\pi}} e^{-(\frac{0.25}{D})}\right)$. At the optimal value of noise the input energy is maximum. From the position time plot alongwith the driving force (Fig. 5.4), with $A = 0.1$ and $\omega = 0.1$, it can be seen that best synchronisation of the particle with the driving force occurs at $D = 0.12$. This is the value of D where there is a peak in the input energy for these parameters

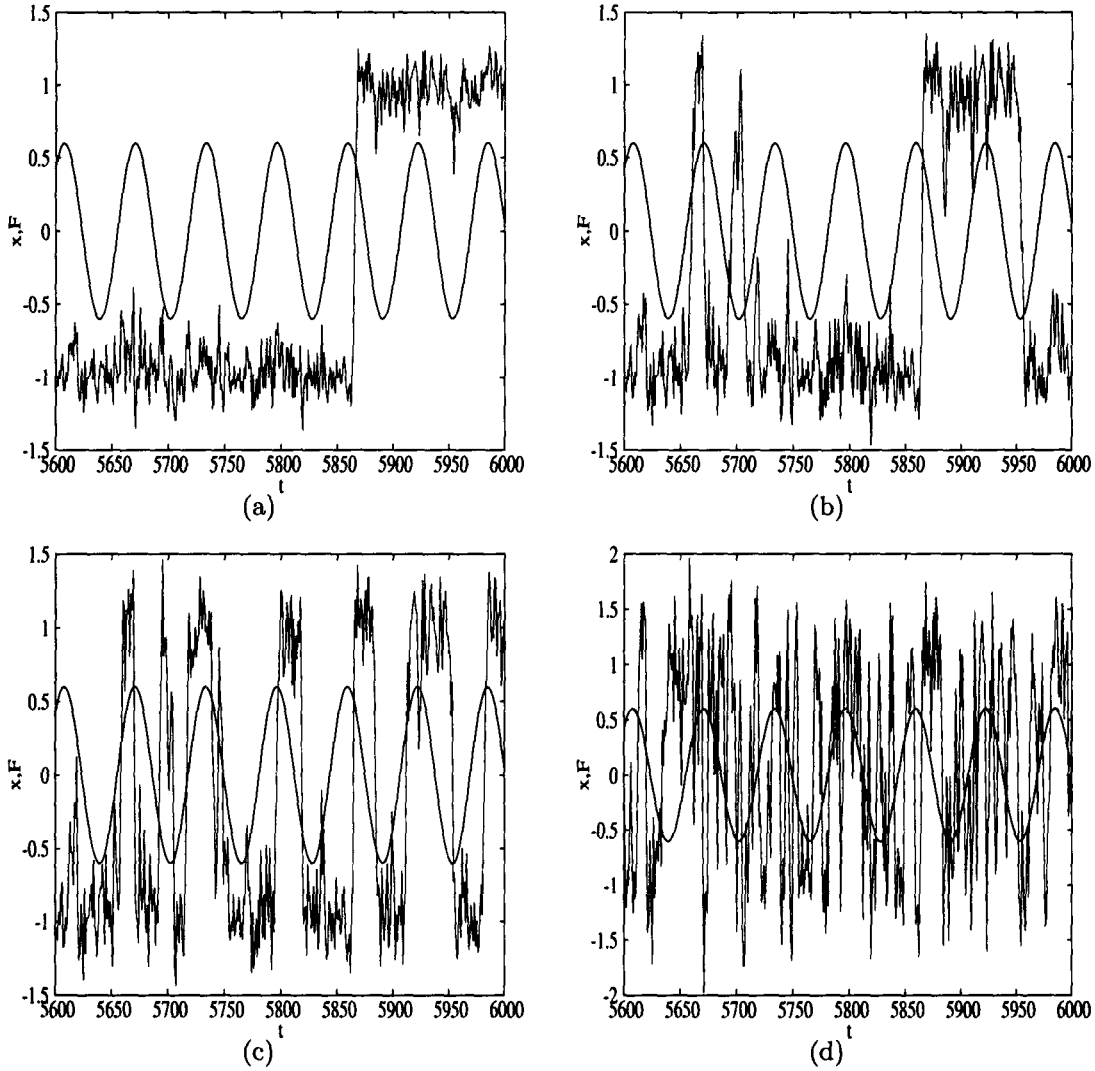

Figure 5.4: Plot of $x(t)$ and $F(t)$, for $D = 0.04$ (a), 0.08 (b), 0.12 (c) and 0.5 (d); $\omega = 0.1$, $A = 0.1$.

(Fig. 5.2).

The shifting of the peak at higher frequencies of drive (Fig. 5.2) can be understood from the fact that the particles when driven at higher frequencies needs stronger fluctuations to get over the barrier. This is because the particles get very less time to absorb energy from the fluctuations and cross over the barrier when the barrier height is minimum which is the most favorable condition for barrier crossing.

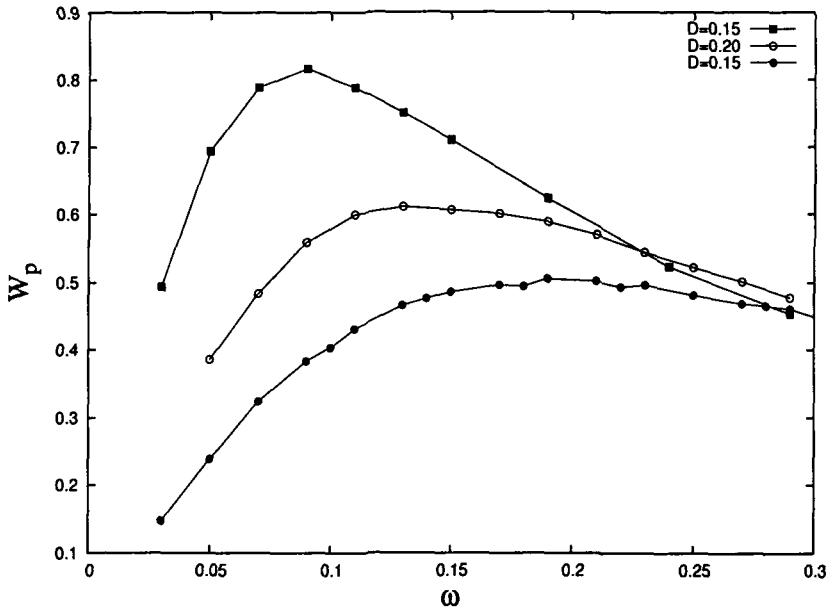

Figure 5.5: Figure shows the variation of average work W_p done per period with ω for different values of D for A=0.1.

The input energy also shows a peaking with the frequency ω of drive (Fig. 5.5) which shows that the SR observed with input energy as a quantifier is a bonafide resonance [5]. In Fig. 5.3 the relative variance $V_r = \sqrt{\frac{\langle {W_p}^2 \rangle - \langle W_p \rangle^2}{\langle W_p \rangle^2}}$ of work done W_p over a period as a function of noise strength is plotted. We see that $V_r > 1$ in the parameter range we have chosen. This shows that fluctuations dominate the mean value. V_r exhibits a minimum near the value of D at which SR occurs for $\omega = 0.1$ and $A = 0.1$, V_r shows a similar behaviour with D for $\omega = 0.2$ and $\omega = 0.3$. As because $V_r > 1$ in the range of D under our consideration, a study of the distributions of W_p becomes necessary.

In the time periodic state the average work done or the input energy into the system is dissipated as heat. Thus one can identify $\langle W_p \rangle$ as a hysteresis loss in the medium. We plot the hysteresis loops (Fig. 5.6a) and calculate the hysteresis loop area(Fig. 5.6b). The hysteresis loop areas for different values of D, exactly match the values of input energy. However, it may be noted that fluctuations of work done cannot be identified with heat fluctuations [8, 9].

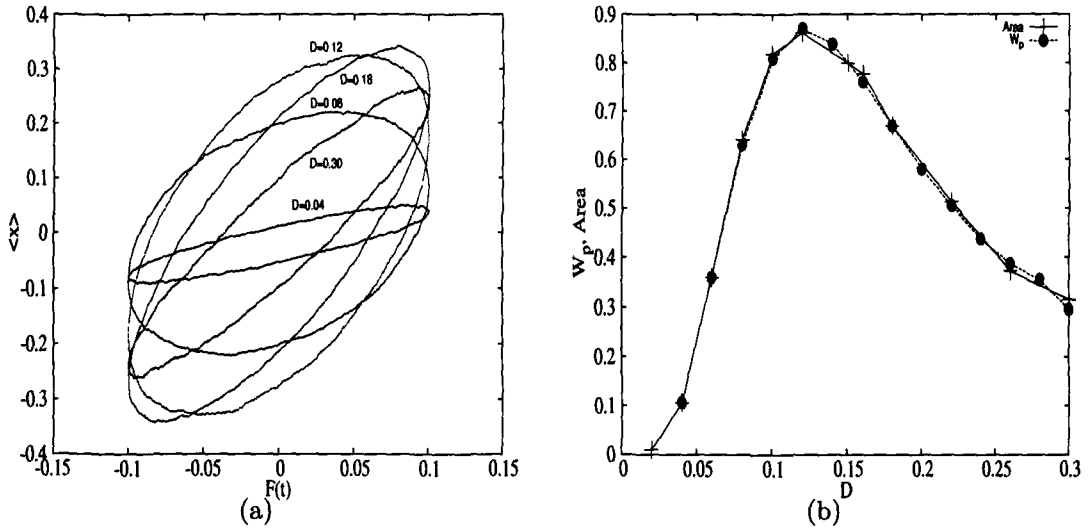

Figure 5.6: Plot of the hysteresis loops for different values of D (a) and the corresponding loop areas, plotted together with average work done per period W_p versus D (b); $\omega = 0.1$, $A = 0.1$.

Now we will turn to the understanding of the nature of probability distribution $P(W_p)$ of W_p for various values of noise strength D across SR peak. For this we have plotted $P(W_p)$ as a function of W_p in Figs. 5.7a and 5.7b for various values of D for $A = 0.1$ and $\omega = 0.1$. For low values of D (~ 0.02) particle dynamics is mostly confined to a small amplitude intrawell oscillatory motion. Hence the distribution is closer to the Gaussian. For slightly higHer values of D ($\simeq 0.04$ and 0.06) the particle makes occassional random excursions into the other well as a function of time Fig. 5.4a). This is clearly reflected as a small asymmetry and a hump (interwell motion) in the plot of $P(W_p)$. It is interesting to note that there is substantial weight towards negative values of W_p. As we

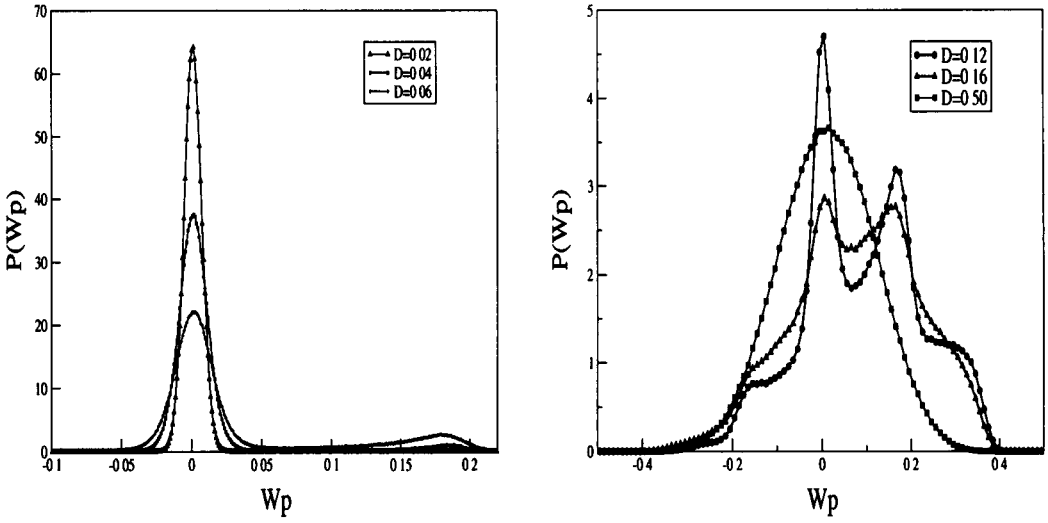

(a) (b)

Figure 5.7: Plot of the probability distributions $P(W_p)$, for various values of D; $\omega = 0.1$, $A = 0.1$.

increase D further the interwell dynamics starts playing a prominent role. It is interesting to note that position of the first and the second peak does not shift much, however, its width increases. The weight of the probability distribution towards higher negative values of W_p increases. The distributions $P(W_p)$ are most asymmetric for $D = 0.12$. That is the value of D at which there is SR. On further increasing D (Fig.5.7b) finally a single peak structure appears. The shape of the single peak structure is closer to a Gaussian at high D(~ 0.5). For such high values of D particle makes several random excursions between the two wells during a single time period of an external drive (Fig.5.4d). Hence total work can be treated as an addition of independent increments of work. Then the central limit theorem leads us to expect that the distribution of work will be approximately Gaussian. This is indeed the case. The parameter range for which we have explored the distributions are broad and the variance of fluctuations dominate over the average values (Fig. 5.3).

5.3 Part two

In the second part of our work we study the role of the confining strength of a bistable potential on the phenomenon of stochastic resonance exhibited by such a system.

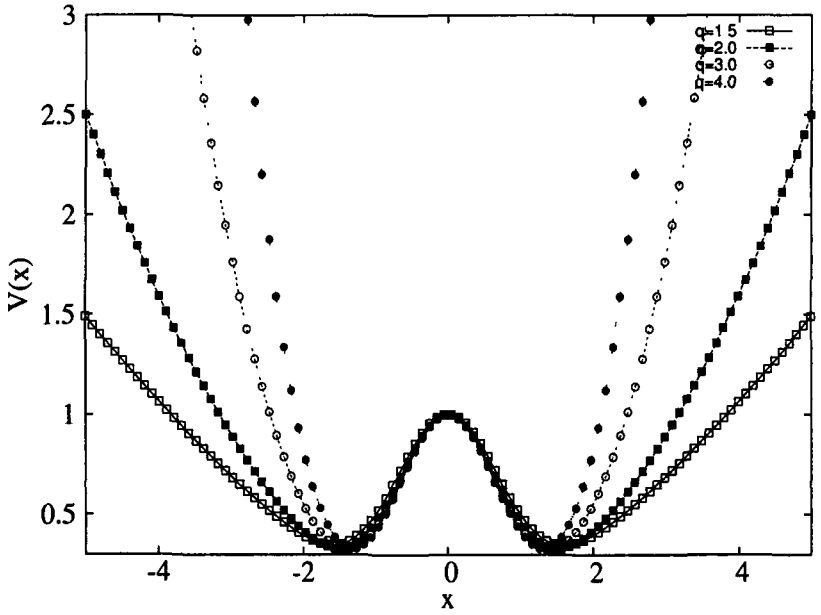

Figure 5.8: The rescaled potential (Eq. 5.8) with $k = 0.2$ and different values of the parameter q. It is to be noted that the confining strength of the potential increases with increase of q.

For most of the studies on SR in a bistable potential, the potential $V(x)$ used was one which diverged as $V(x) \sim x^4$ for $x \sim \infty$ (as the one we used in the first part of this work) [2, 11]. For this kind of a potential, the confining action of the potential on the particle motion was quite strong. However recently it was shown that the nature of the particle dynamics in a one dimensional bistable potential $V(x)$ is strongly dependent on the divergence of $V(x)$ as $|x| \to \infty$ [10]. Using the amplitude of the interwell motion as a quantifier for SR it was shown that the confining strength of the potential had a role to play on the phenomenon of SR. It was shown that bistability is a necessary but not a sufficient condition for SR to occur. Potentials with lesser confining strength did not exhibit SR [10]. We report similar results by using the average input energy per period of

external drive as a quantifier for SR, that has been effectively used in the first part of our work. Also we study the distributions of input energy for various confining strengths of the potential. The nature of these distributions explain the role played by the confining strength of a bistable potential on SR.

5.3.1 The model

We consider overdamped motion of a Brownian particle in a potential of the form [10]

$$V(x) = V_0 exp(-x^2/{L_0}^2) + k|x|^q/q \tag{5.4}$$

which is a superposition of a Gaussian repulsive barrier of height V_0 and width L_0 to a power-law well. The system is driven by an external periodic forcing $F(t) = a\cos\omega t)$ ($\omega = 2\pi\nu$. The corresponding Langevin equation is given by

$$\gamma\frac{dx}{dt} = -\frac{\partial V(x)}{\partial x} + F(t) + \xi(t), \tag{5.5}$$

The random force field $\xi(t)$ is a zero mean Gaussian white noise, i.e,

$$\langle\xi(t)\xi(t')\rangle = D_0\delta(t-t'), \tag{5.6}$$

where $D_0 = 2\gamma k_B T$ is the strength of the noise, γ is the friction coefficient. The dimensionless form of the Langevin equation is written by setting $\gamma = 1$, $V_0 = 1$ and $L_0 = 1$ as

$$\frac{dx}{dt} = -\frac{\partial V(x)}{\partial x} + F(t) + \sqrt{T}\xi(t), \tag{5.7}$$

where $\langle \xi(t) \rangle = 0$ and $\langle \xi(t)\xi(t') \rangle = 2\delta(t - t')$. The rescaled potential (Fig.5.8) then becomes,

$$V(x) = exp(-x^2) + k|x|^q/q, \tag{5.8}$$

which has minina at $x = \pm 1.3$. The parameter q determines the confining strength of the potential. The minima of the potential and the barrier height changes very little with the parameter q (Fig. 5.8). As in the preceding part, following the stochastic energetics formalism developed by Sekimoto [12], the work done by the external drive on the system per period or the input energy per period $\left(\tau_\omega = \frac{2\pi}{\omega}\right)$ is defined as [4, 5]

$$\begin{aligned} W_p &= \int_{t_0}^{t_0+\tau_\omega} \frac{\partial U(x,t)}{\partial t}\, dt, \\ &= A\omega \int_{t_0}^{t_0+\tau_\omega} x(t) \sin \omega t\, dt, \end{aligned} \tag{5.9}$$

where $U(x,t) = V(x) - xF(t)$.

We solve the dimensionless Langevin equation (Eq. 5.7) by numerical simulation by using Huen's method [13]. The work done per period of external drive (W_p) is calculated (Eq. 5.9) by allowing the system to evolve and by removing initial transients. The values of W_p are different for different cycles. W_p is averaged over 100000 different (sometimes even more) cycles.

5.3.2 Numerical results

In Fig. 5.9, we plot the average work done per period (W_p) or the average input energy per period as a function of noise strength D (in dimensionless units) for different values of the confinement parameter q is plotted. W_p shows a peaking with D as expected from the results of part one of our work, but only for values

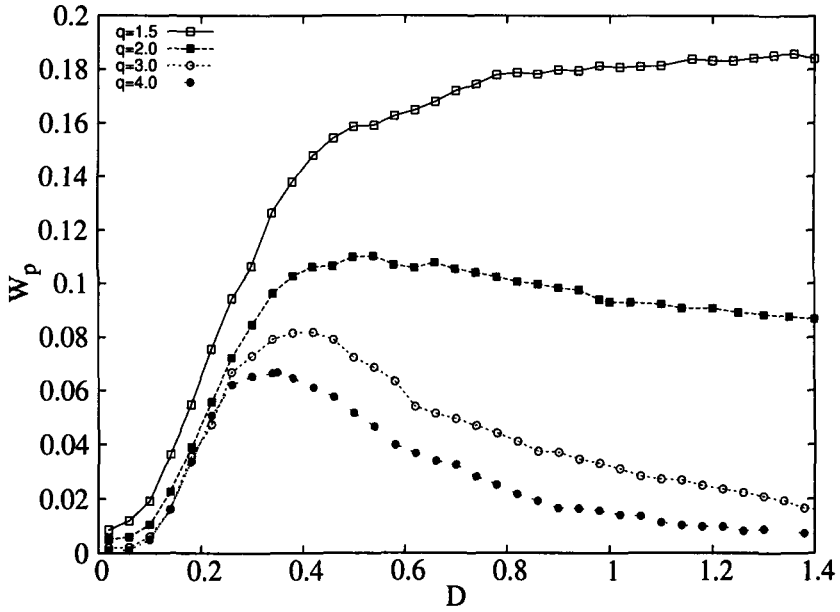

Figure 5.9: Plot of W_p as a function of D for different values of q; $k = 0.2$, $\nu(= \frac{2\pi}{\omega}) = 0.02$.

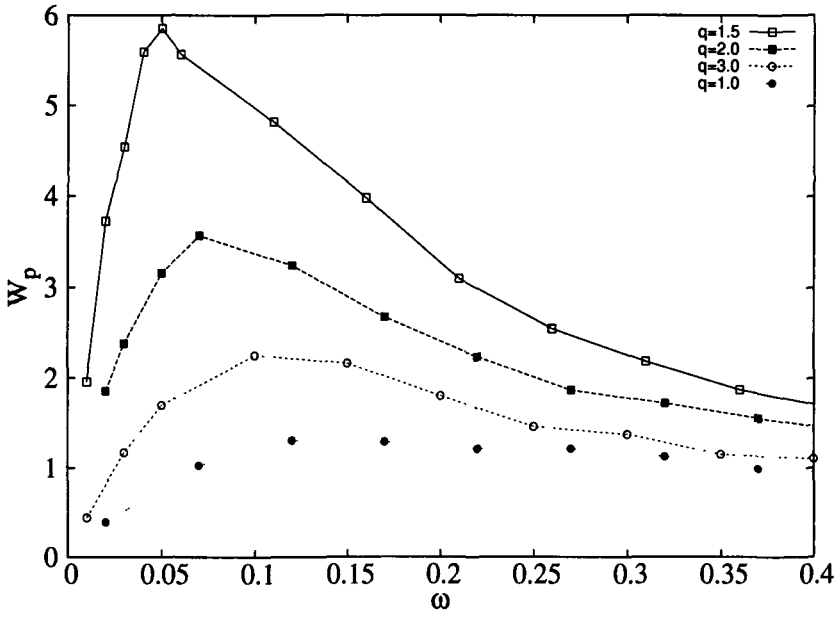

Figure 5.10: Plot of W_p as a function of ω for different values of q; $k = 0.2$, $D = 0.4$.

of $q \geq 2$. With W_p as a quantifier for SR, we are able to reproduce the results of [10].

In Fig. 5.10, W_p is plotted as a function of ω for various values of q keeping D fixed. W_p also shows a resonance as a function of ω. But the resonant frequency changes with the value of q.

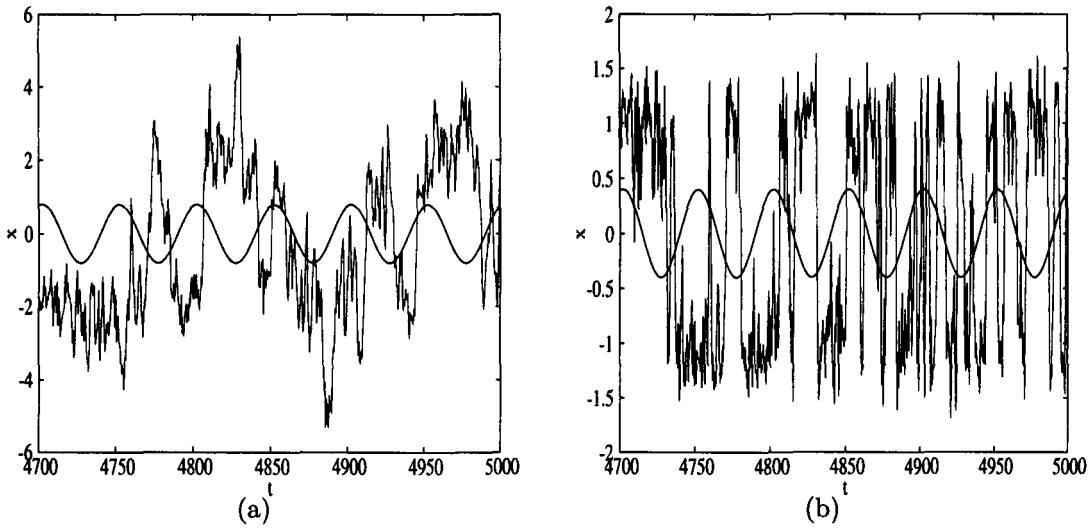

Figure 5.11: Plot of $x(t)$ and $F(t)$ for $q = 1.5$ (a) and $q = 8.0$ (b) with $D = 0.4$, $k = 0.2$, $\nu = 0.02$.

Stochastic resonance occurs when the particles make a synchronised hopping between the two wells of a bistable potential, with the external drive, as has been discussed in part one of this chapter. From the particle trajectories (Fig. 5.11) we see that, when the confining strength of the potential is less (Fig.5. 11a) (lesser q), the particle after crossing over from one well to another well, travels appreciable distance away from the bottom of the well. This is because the particle is driven up the walls of the potential in response by the external forcing $F(t)$[10]. So when external field direction reverses, it fails to cross back in synchrony with the drive. With the increase of the confining strength (larger q), however, the chances of the particle making synchronised hoppings between the wells increases (Fig.5.11b). So SR can be observed only for values of q greater than a particlular minimum.

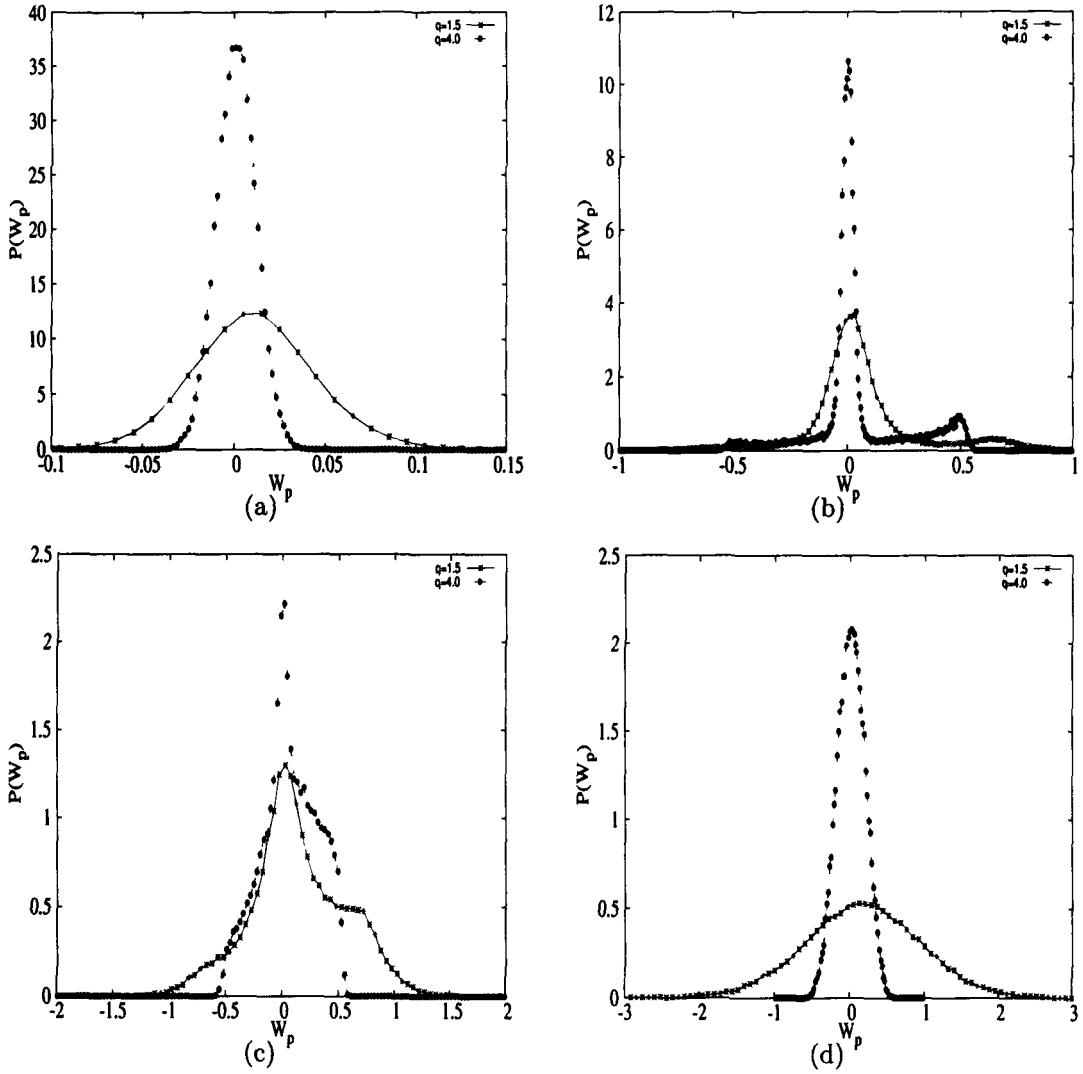

Figure 5.12: Plot of $P(W_p)$ for $D = 0.05$ (a), $D = 0.2$ (b), $D = 0.4$ (c) and $D = 1.2$ (d) for $q = 1.5$ and $q = 4.0$; $k = 0.2$, $\nu = 0.02$, $A = 0.1$.

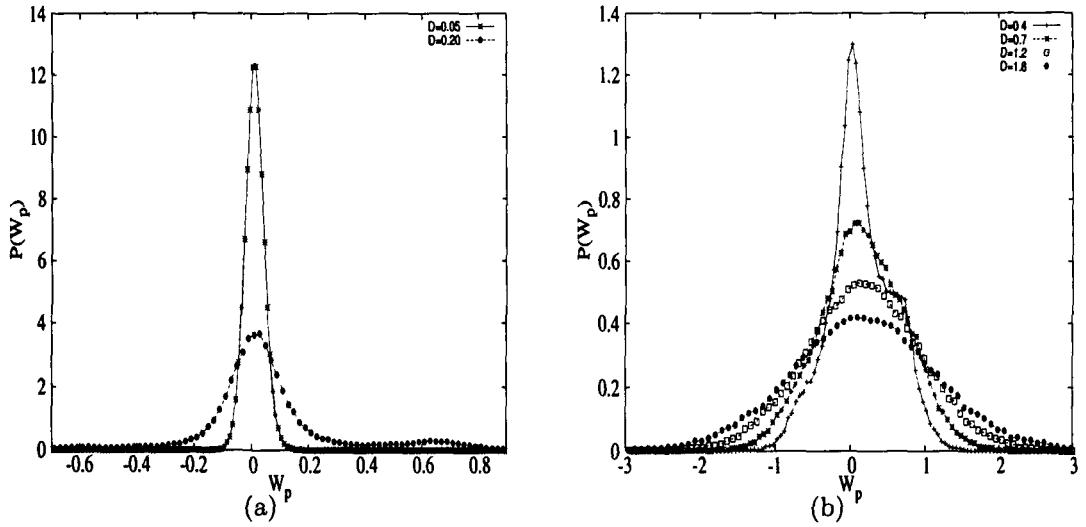

Figure 5.13: Plot of $P(W_p)$ for various values of D for $q = 1.5$, $\nu = 0.02$, $k = 0.2$ and $A = 0.1$.

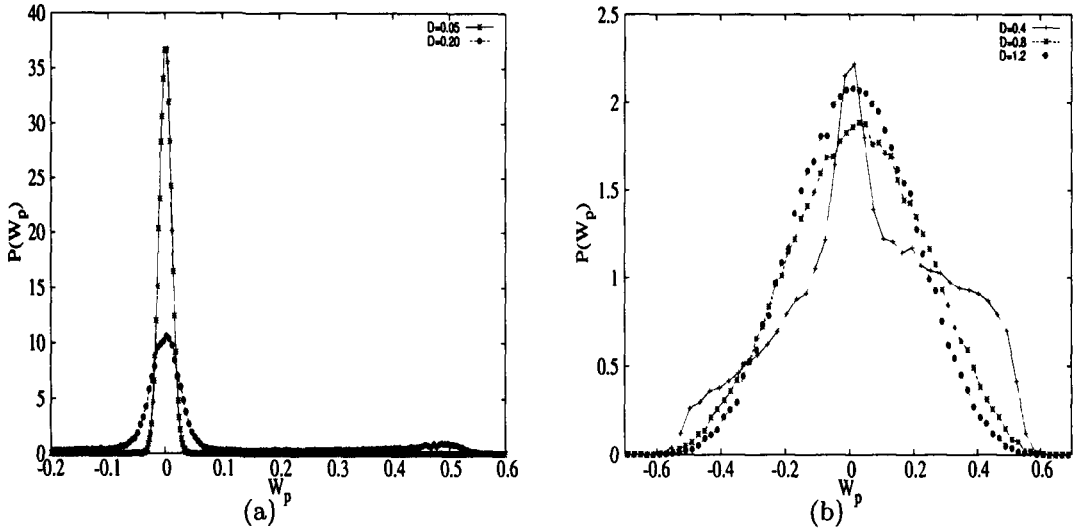

Figure 5.14: Plot of $P(W_p)$ for various values of D for $q = 4.0$, $\nu = 0.02$, $k = 0.2$ and $A = 0.1$.

The very fact that the particle can be driven up the potential walls by the external drive, leads to higher amplitudes of intrawell motion at lower values of D or interwell motion at higher values of D. Thus the the work done per period of drive W_p increases with the decrease of q irrespective of the value of D as can be seen from Fig. 5.9. The distributions of W_p also reflects this (Fig. 5.12). For different values of D, the distributions for $q = 1.5$ are much broader than those for $q = 4.0$. There is substantial weight towards negative values of W_p which reflects the presence of transient second law violating trajectories. But for lesser q values, the weight of the probability distributions towards higher negative values of W_p are more.

In Fig. 5.13 and 5.14, the distributions in W_p are plotted for different values of D for $q = 1.5$ (Fig. 5.13) and $q = 4.0$ (Fig. 5.14). At lesser values of D where intrawell oscillatory motion is dominant, the distributions are closer to gaussian. At very high values of D, the particle does not see the barrier between the two wells and in this limit also the distributions approach a gaussian nature. But at intermediate temperatures ($D = 0.4$ shown in the figure), for $q = 4.0$ the asymmetry in the distribution is maximum. This corresponds to the temperature at which the SR peak occurs. This is in agreement with the results of part one of this work. However, for $q = 1.5$, there is no marked asymmetry even at intermediate temperatures. This is reflected in the absence of the peaking of W_p with D.

5.4 Conclusion:

We have studied the phenomenon of SR occuring in a driven bistable potential, using the input energy per period of drive or the work done as a quantifier for SR. The system exhibits hyteretic behaviour. We have shown that the hysteresis loop area can also be a quantifier of SR and compared it with the input energy. We have also studied the work fluctuations. We have shown that across SR

fluctuations of work calculated over a single period in the asymptotic time region dominates the mean value. The distributions exhibit significant weight towards negative values of work indicating transient second law violating trajectories. We have also studied the role played by the confining strength of a bistable potential on the nature of SR using the the input energy per period of drive as a quantifier for SR. We have found that, for the phenomenon of SR to occur in a bistable potential, it should have a a certain minimum confining strength. For different confining strengths of the potential we have studied the nature of the input energy or the work fluctuations.

Bibliography

[1] S. Saikia, R. Roy and A. M. Jayannavar, Phys. Lett. A 369, 367 (2007).

[2] L. Gammaitoni, P. Hanggi, P. Jung and F. Marchesoni, Rev. Mod. Phys. 70, 223 (1998); R. Benzi, G. Parisi, A. Sutera and A. Vulpiani, Tellus 34, 10 (1982).

[3] M. C. Mahato and S. R. Shenoy, Phys. Rev. E 50, 2503 (1994); M. C. Mahato and A. M. Jayannavar, Phys. Rev. E 55, 6266 (1997); M.C. Mahato and A. M. Jayannavar, Mod. Phys. Lett. B 11, 815 (1997); M.C. Mahato and A. M. Jayannavar, Physica A 248, 138 (1998); J. C. Phillips and K. Schulten, Phys. Rev. E 52, 2473 (1994); M. Thorwart and P. Jung, Phys. Rev. Lett. 78, 2503 (1997); S. W. Sides, P. A. Rikvold and M. A. Novotny, Phys. Rev. Lett. 81, 834 (1997); S. W. Sides, P. A. Rikvold and M. A. Novotny, Phys. Rev. E 57, 6512 (1998); M. Thorwart,P. Reimann,P. Jung and R. F. Fox, Chem.Phys. 235, 61 (1998); J. S. Lim, M. Y. Choi and B. J. Kim, Phys. Rev. B 68, 012501 (2003);

[4] T. Iwai, Physica A 300, 350 (2001); T. Iwai, J.Phys. Soc. Jpn. 70, 353 (2001).

[5] D. Dan and A. M. Jayannavar, Physica A 345, 404 (2005).

[6] M. Evstigneev, P. Riemann and C. Bechinger, J.Phys. C 17, S3795 (2005).

[7] V. Berdichevsky and M. Gitterman, Physica A 249, 88 (1998).

[8] A. M. Jayannavar, M. Sahoo, Phys. Rev. E 75, 032102 (2007).

[9] R. van Zon, E. G. D. Cohen, Phys. Rev. E 67, 046102 (2003).

[10] E. Heinsalu, M. Patriarca and F. Marchesoni, Eur. Phys. J. B 69, 19 (2009).

[11] L. Gammaitoni, F. Marchesoni and S. Santucci, Phys. Rev. Lett 74, 1052 (1995); M. H. Choi, R. F. Fox and P. Jung, Phys. Rev. E 57, 6335 (1998); G. Giacomelli, F. Marin, and I. Rabbiosi, Phys. Rev. Lett. 82, 675 (1999); F. Marchesoni, L. Gammaitoni, F. Apostolico and S. Santucci, Phys. Rev. E 62, 146L (2000); L. Gammaitoni, F. Marchesoni, E. Menichella-Saetta, and S. Santucci, Phys. Rev. Lett. 62, 349 (1989).

[12] K. Sekimoto, J. Phys. Soc. Jpn. 66, 6335 (1997).

[13] R. Mannella, Stochastic Processes in Physics, Chemistry, and Biology, J. A. Freund and T. Pöschel, Lecture Notes in Physics, vol. 557, 353 (2000).

[14] R. Marathe and A. Dhar, Phys. Rev. E 71, 036126 (2005).

Chapter 6

Stochastic resonance in periodic systems

6.1 Introduction

This chapter is based on the results of our investigations on the phenomenon of Stochastic Resonance in a periodic system [1].

Stochastic resonance (SR) was discovered theoretically about three decades ago[2]. Since then SR has been investigated with fervour and many notable reviews have appeared, for instance [3, 4]. Physical systems are always subject to internal or external (thermal or otherwise) fluctuations (noise). The optimal periodic response of a system to an external periodic drive as a function of noise strength is termed as stochastic resonance. It has been experimentally found to occur, to just mention a few, in electronic circuits [5, 6, 7], two-mode ring lasers [8], nanomechanical systems [9], neuronal systems [10, 11, 12, 13], etc. Its main attraction lies in its practical utility of selecting and enhancing a signal of a particular frequency out of a host of signals by tuning the noise strength. Presumably, biological systems use SR to their advantage [14]. It has the potential to be utilized to control kinetically the pathways of a biochemical reaction [15].

SR has been predicted and shown to occur mostly in bistable systems [3, 16]. However, there has been some notable investigations of SR in monostable and periodic potential systems as well [17, 18]. In the monostable systems, SR is shown to occur in the high frequency regime close to the natural frequency of oscillation at the bottom of the potential. However, the occurrence of SR in periodic potentials have not been conclusive [19, 20, 21].

Dykman and coworkers [18] use an interesting model in which a single-well Duffing oscillator with additive noise is driven at a frequency close to the natural frequency of the oscillator. The model is used under linear response theory formalism to study fluctuation phenomena associated with two coexisting periodic attractors. A weak Gaussian noise causes transition between these two attractors. The population of these two attractors become equal at a particular noise strength where the response becomes maximum. This is considered as a genuine signature of a (nonconventional) stochastic resonance. The theoretical result was supported by an analog electronic circuit experiment. A similar result was obtained in an underdamped superconducting quantum interference device [23].

The same resonance behaviour as Dykman et. al. [18] in the frequency dependent mobility was obtained in a periodic potential using linear response theory by Kim and Sung [19] in the high frequency range of the external periodic drive. However, these authors ascribe this resonant behaviour as simply a noise assisted standard dynamical resonance as the transitions involve only intrawell motion. Also, in the interwell-hopping (low) frequency regime the frequency dependent mobility shows monotonic behaviour as a function of noise strength thereby discounting the possibility of occurrence of SR in periodic structures. However, the authors show that SR can occur if the driven system has a tilted periodic potential so that the passages are allowed only in one direction.

Moreover, recently, it was observed that in a bistable potential, $V(x) = V_0 e^{-ax^2} + b|x|^q/q$, the confinement parameter q plays an important role in de-

ciding whether the system will show SR or not [24]. For $q \geq 2$ the system shows SR whereas for $q < 2$ it does not (please see Chapter 5). In addition, we find the input energy expended per period of the external field on the system by the field acts as a good quantifier of SR. This input energy is ultimately dissipated into the thermal bath. This is naturally a measure of the hysteresis loop area in position(x)-force(F) space. Although the input energy and hysteresis loop area are exactly the same in magnitude, the latter is an average quantity, whereas input energy has a well defined distribution. The input energy distribution provides useful information about stochastic resonance behaviour. In particular, the distribution shows a maximum asymmetry at stochastic resonance, which is a characteristic of SR [25, 26, 27]. On the other hand, hysteresis loops carry important information about phase relationship between x and F which have also been of interest to SR [28, 29].

In the present work we explore the possibility of occurrence of SR in a periodic sinusoidal potential using input energy and hysteresis loop area as quantifiers which have been found to be good quantifiers for SR in double well systems. We find that the periodic sinusoidal potential does not show SR when driven by a low frequency field corresponding to Kramers rates across the maxima of the potential or at a lower frequency. We also find that in the high frequency range the input energy behaves exactly similarly as the response function in the works of Dykman and coworkers [18] and as the frequency dependent mobility does in the work of Kim and Sung [19]. However, our work shows that the input energy or the work done also peaks as a function of noise strength. This is an indication of SR, as in the case of bistable systems, arising due to a competition between two dynamical states of particle trajectories. Though the trajectories are intrawell in nature close to SR the transition between these two states are also aided by interwell passages of particles across the potential maxima. These two dynamical states are distinctly identified by the phase difference ϕ between the periodic forcing $F = F_0 \cos(\omega t)$ and the trajectory $x(t) = x_0 \cos(\omega t + \phi)$;

one having a fixed phase lag ϕ_1 and the other ϕ_2. These phase lags effectively do not vary with the noise strength. Moreover, the distribution of input energy shows very similar behaviour across the input energy peak as in case of SR in a bistable system thus affirming the genuineness of SR in the present periodic potential system.

We consider two model systems for our study. In one case the medium is considered to have a uniform friction whereas in the other case the friction is considered to be nonuniform. Since the potential is symmetric and periodic the former system do not show any average mobility. The nonuniform system, however, shows average current when driven by a sinusoidal forcing. Interestingly, for the uniform system and the nonuniform case, ϕ_1 and ϕ_2 are different. In either case the the trajectories have distributions of these two phases depending on the noise strength. This is reflected in the form of the $(x - F)$ hysteresis loops.

6.2 The model

In this chapter, we consider the underdamped motion of a particle in a periodic potential $V(x) = -V_0 \sin(kx)$ which is symmetric in space (about $kx = (2n + 1)\pi/2$, $n = 0, \pm 1, \pm 2, ...$). The system is driven periodically by an external forcing $F(t)=F_0 \cos(\omega t)$. We study the system under two approximations - when the friction coefficient $\gamma(x)$ is uniform ($=\gamma_0$) (system is homogeneous) and when the friction coefficient is space dependent $\gamma(x) = \gamma_0(1 - \lambda \sin(kx + \theta))$ (system is inhomogeneous). In the latter case, the friction is periodic with the same periodicity as the potential but has a phase difference θ with it ($\theta \neq 0, \pi$). λ ($0 \leq \lambda < 1$) determines the degree of inhomogeneity of the system ($\lambda = 0$ corresponds to the homogeneous system).

A particle of mass m moving in a periodic potential $V(x) = -V_0 sin(kx)$ in a medium with friction coefficient $\gamma(x)$ and subjected to an external periodic

forcing $F(t)$ is described by the Langevin equation,

$$m\frac{d^2x}{dt^2} = -\gamma(x)\frac{dx}{dt} - \frac{\partial V(x)}{\partial x} + F(t) + \sqrt{\gamma(x)T}\xi(t). \tag{6.1}$$

$$m\frac{d^2x}{dt^2} = -\gamma_0\frac{dx}{dt} - \frac{\partial V(x)}{\partial x} + F(t) + \sqrt{\gamma_0 T}\xi(t). \tag{6.2}$$

Eq. 6.1 is for the inhomogeneous system and Eq. 6.2 for the homogeneous system. The temperature T is in units of the Boltzmann constant k_B. The inherent random fluctuations in the system are represented by $\xi(t)$ which satisfy the statistics: $< \xi(t) >= 0$, and $< \xi(t)\xi(t') >= 2\delta(t - t')$. The equations are written in dimensionless units by setting $m = 1$, $V_0 = 1$, $k = 1$. The Langevin equation, with reduced variables denoted again now by the same symbols corresponding to Eq. 6.1 and 6.2 is written as

$$\frac{d^2x}{dt^2} = -\gamma(x)\frac{dx}{dt} + cosx + F(t) + \sqrt{\gamma(x)T}\xi(t), \tag{6.3}$$

$$\frac{d^2x}{dt^2} = -\gamma_0\frac{dx}{dt} + cosx + F(t) + \sqrt{\gamma_0 T}\xi(t), \tag{6.4}$$

The potential barrier between any two consecutive wells of $V(x)$ disappears at the critical field value $F_0 = F_c = 1$. The noise variable, in the same symbol ξ, satisfies exactly similar statistics as earlier.

6.3 Numerical results

We solve Eq. 6.3 numerically using Heun's method [30] for solving stochastic differential equations, to obtain the trajectory $x(t)$ of the particle for a given initial condition and different values of the parameters F_0, γ_0, T and τ_ω $(= \frac{2\pi}{\omega})$.

The work done by the external drive on the system or the input energy is

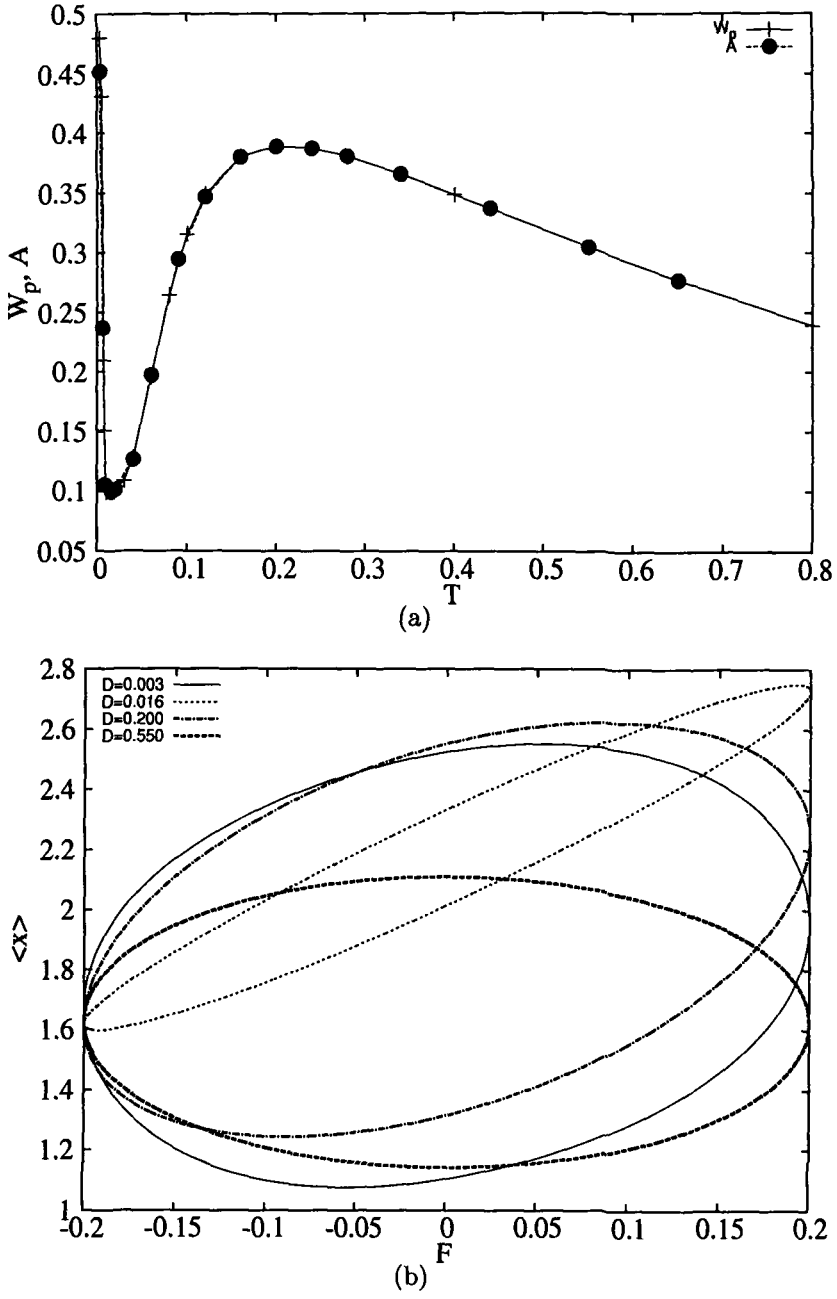

Figure 6.1: Plot of average work done per period of drive, W_p and the corresponding average $(x - F)$ hysteresis loop area A as a function of temperature T for the homogeneous system (a). Fig.6.1b shows the ensemble averaged $(x - F)$ hysteresis loops for a few D values; τ_ω=8, $F_0 = 0.2$, $\gamma_0 = 0.12$.

F

defined as[31, 32],

$$\begin{aligned} W_p &= \int_{t_0}^{t_0+\tau_\omega} \frac{\partial U(x,t)}{\partial t}\, dt, \\ &= F_0\omega \int_{t_0}^{t_0+\tau_\omega} x(t) \sin\omega t\, dt \end{aligned} \tag{6.5}$$

This follows from the stochastic energetics formalism developed by Sekimoto [33].

To obtain physically relevant quantities, independent of the initial conditions, the system is allowed to evolve for time of the order of $t = 10^5$ to $t = 10^7$ in steps of $\Delta t = 0.001$. The averaging is done over an ensemble of 100 particles, each starting from an initial position taken from a uniform grid between the two maxima at $x = -\frac{\pi}{2}$ and $\frac{3\pi}{2}$ of the potential. The initial velocity of the particles is kept fixed at $v(0) = 0$.

To calculate the average work done per period of the external drive, W_p is calculated (eqn.(6.3)), after removing the initial transients, for 100000 periods for each of the 100 initial conditions. The values of W_p are different for different periods. Averaging is done over all the 100×100000 periods of drive. We study the distributions of W_p which are initial condition independent. The ensemble averaged $x(t) - F(t)$ hysteresis loops are plotted and the area of these loops are calculated for comparison with W_p.

Throughout our work, we keep $\tau_\omega = 8.0$ (unless stated otherwise), which is close to the natural frequency of the intrawell particle oscillations [18, 19] in our periodic system.

6.3.1 Homogeneous system

In Fig. 6.1a, the variation of the average work done (input energy) per period by the external drive, W_p, and also the area of the corresponding $(x - F)$ hysteresis loops (Fig. 6.1b) are shown as a function of the temperature T, for the homo-

geneous system. W_p and the area of the hysteresis loops match exactly. This proves that all the input energy to the system is dissipated. As T is increased from the deterministic limit (very small T), W_p decreases attaining a minimum at an intermediate value of T. With further increase of T, W_p shows a peaking as a function of T which bears the signature of Stochastic Resonance in the periodic system under our consideration. Earlier, input energy (and equivalently hyteresis loop area) has been proved to be a good quantifier for SR in bistable systems [31, 32, 25] (please see, chapter 5). Similar resonance behaviour has been observed earlier in the frequency dependent mobility of the particles in a driven periodic potential system [19].

A look at the particle trajectories (Fig. 6.2 a and b), clearly shows that the particles can have two kinds of trajectories corresponding to two different phases, ϕ_1 (out of phase) and ϕ_2(in phase) with respect to the external driving force. The corresponding hyteresis loops (Fig. 6.2 c and d) reflect the presence of the two phases. The out of phase loop (Fig. 6.2c) is a superposition of the the periodic forcing $F = 0.2\cos(\omega t)$ and the response $x(t) = 1.94\cos(\omega t + 0.6\pi)$ while the in-phase loop (Fig.6.2d) is a superposition of $F = 0.2\cos(\omega t)$ and $x(t) = 0.56\cos(\omega t + 0.1\pi)$. Thus $\phi_1 = 0.6\pi$ and $\phi_2 = 0.1\pi$. The out of phase trajectories have higher amplitudes compared to the in phase trajectories. Also, the area of the hysteresis loops and hence correspondingly W_p for the out of phase trajectories are more than those of the in-phase ones. The presence of phase lag between the external periodic forcing and the response $x(t)$ and its role in SR has been investigated earlier for a different system [28, 29].

The presence of the two different trajectories correspond to two distinct dynamical energy states.

This is reflected in (Fig. 6.4a) where W_p for trajectories starting with 100 initial conditions are plotted. For trajectories with some initial conditions, the particle is out of phase giving higher $W_p = 1.17$ (equal to the out of phase loop area (Fig. 6.2c)), while others are in phase having $W_p = 0.09$ (equal to the in-

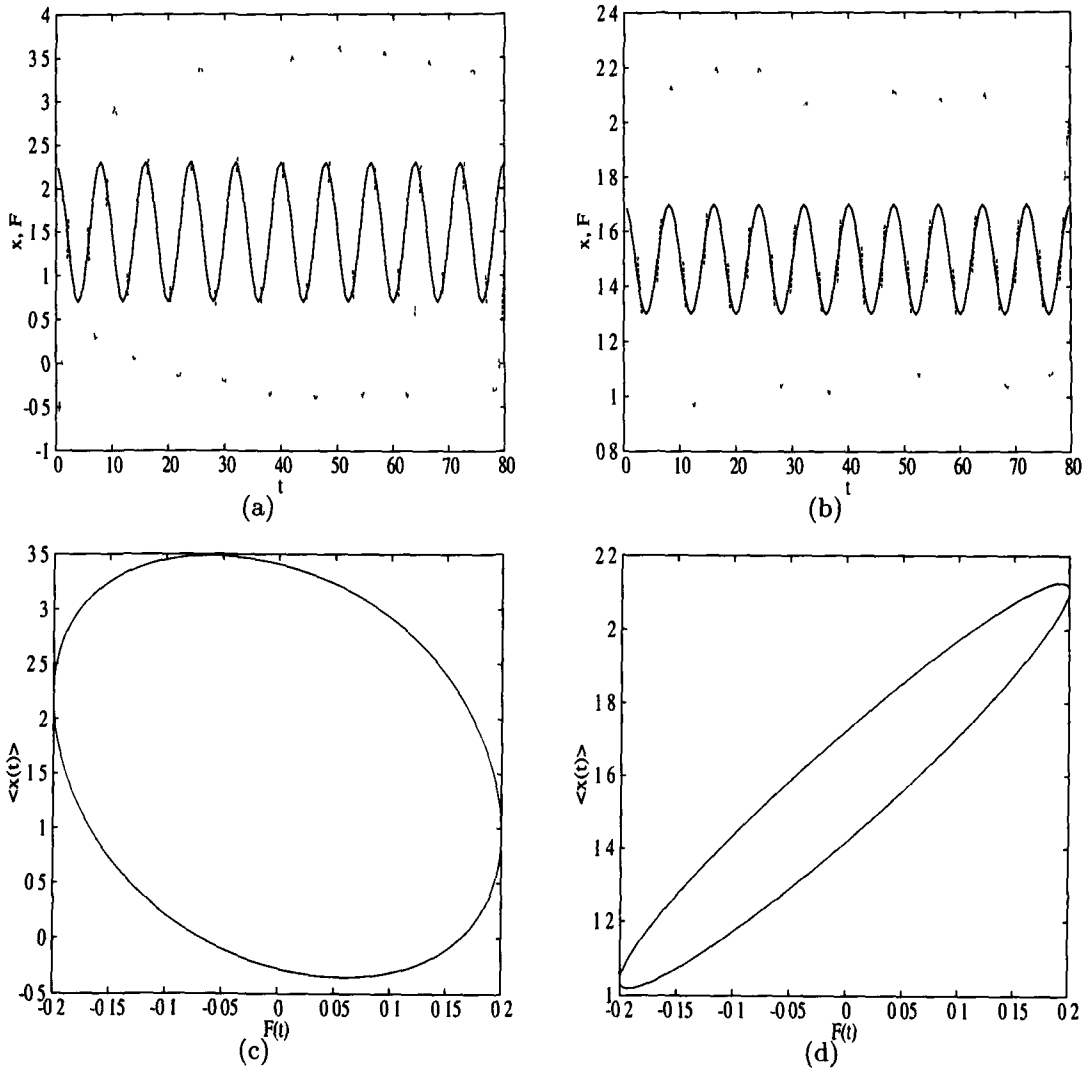

Figure 6.2: Plot of $x(t)$ and $F(t)$ for $x(0) = -0.68$ (a) and $x(0) = 2.0$ (b) and the corresponding $(x - F)$ hysteresis loops (c and d); $T = 0.003$, $\tau_\omega = 8$, $F_0 = 0.2$, $\gamma_0 = 0.12$.

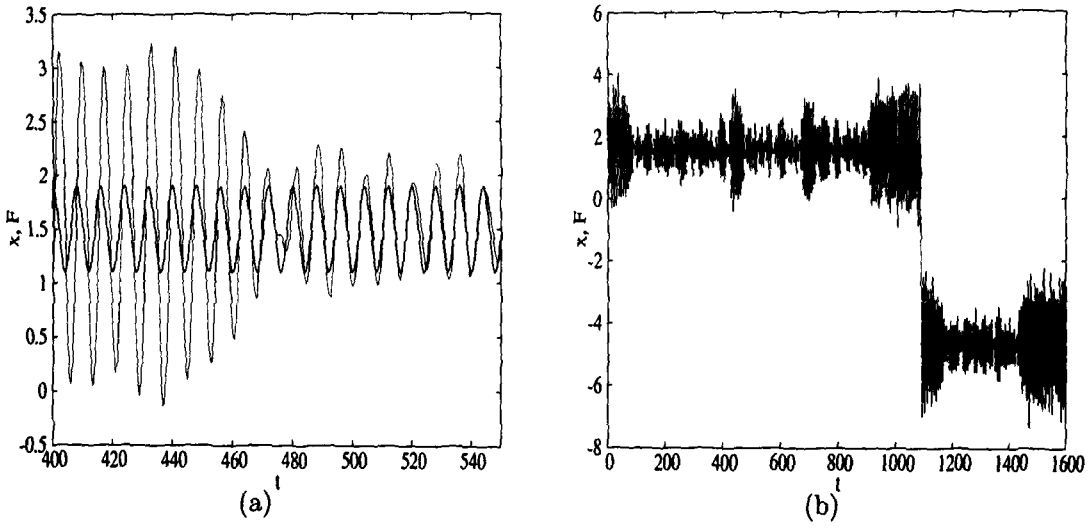

Figure 6.3: Plot of $x(t)$ and $F(t)$ for $T = 0.015$ (Fig. a) . Fig. b shows the particle trajectory for a higher temperature $T = 0.1$ with $x(0) = -0.68$. It reflects the interwell motion as also the presence of the two phases of motion; $\tau_\omega = 8$, $F_0 = 0.2$, $\gamma_0 = 0.12$.

phase loop area (Fig. 6.2d). Clearly, the in-phase state has lesser energy than the out of phase state. The nature of the trajectories at very low temperatures (deterministic limit) are very sensitive to initial conditions. So depending on the initial condition, the particle may go to either of these dynamical states, and remains in that state throughtout its evolution (Fig. 6.4a). When averaged over an ensemble, the relative abundance of the two states determines the final value of W_p. The ensemble averaged hysteresis loop Fig. 6.1b (and correspondingly the average response $\langle x \rangle$) naturally has a phase different from that of individual particles of the ensemble.

As the temperature increases, transistions start occuring at intermediate times from out of phase state to in phase state (Fig.6.4b). At the temperature corresponding to the minimum ($T = 0.015$), all the trajectories go to the in phase state, whatever initial phase they start with (Fig. 6.3a and Fig. 6.4c). Till this temperature, intrawell dynamics determines the system behaviour. As the temperature increases further, the particles start making random jumps out of the wells (Fig. 6.3b) interspaced by periods of intrawell motion. Alongwith

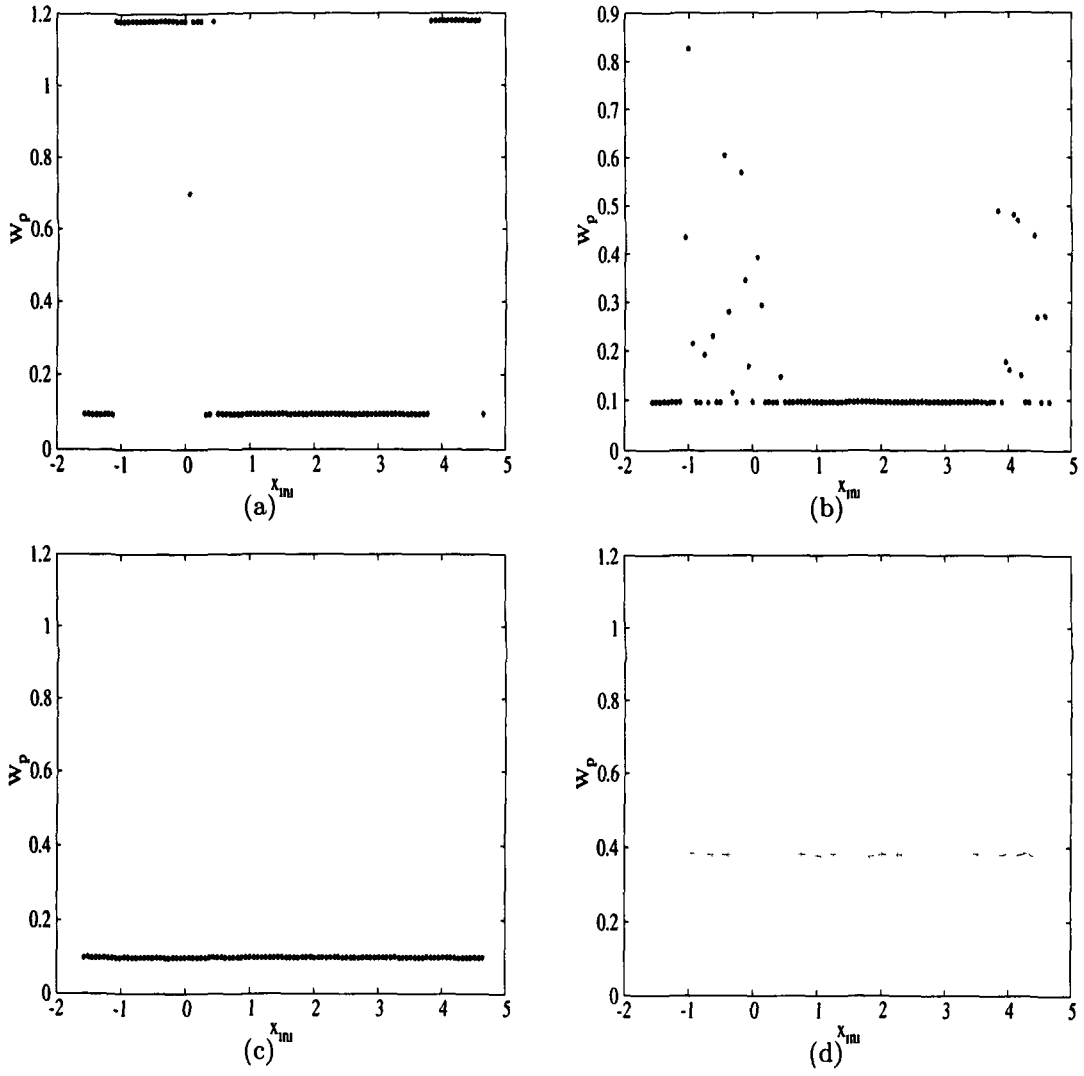

Figure 6.4: Plot of average work done per period (along y-axis) with the different initial conditions $x(0)$ along x-axis (corresponding to different trajectories) for $T = 0.003$ (a), $T = 0.008$ (b), $T = 0.015$ (c) and $T = 0.16$(d), $\tau_\omega = 8$, $F_0 = 0.2$, $\gamma_0 = 0.12$. At low temperature (a), particle trajectories are either in phase or out of phase depending on the initial conditions.

this, transitions start occurring between the two dynamical states of the particle. This is reflected in Fig. 6.3b where the presence of higher amplitude (out of phase) and lower amplitude (in phase) trajectories can be seen with transistions from one to the other. In Fig.6.3a, a transition from out of phase to in phase state of the particle is shown. It can be seen that at the point of transition, the amplitude of particle motion becomes very less.

With the increase of temperature above that of the minima, therefore, competition occurs between the two dynamical states of the particle. At an optimum value of temperature ($T = 0.2$), this competition leads to a peaking of the input energy W_p. It is to be noted that, around the temperature where W_p peaks, interwell motion also aids the switching between the two states. At higher temperatures, the switching between these two states becomes too frequent, in every single realisation, leading to a decrease of overall amplitude of the particle motion and hence a lesser value of W_p for each realisation (Fig. 6.4d) and also the ensemble averaged W_p (Fig. 6.1). The peaking of W_p as a result of competition between two dynamical states of the particle at an optimum temperature also aided by random interwell hoppings makes it a bonafide Stochastic Resonance. A similar phenomenon of SR due to noise assisted synchronised switching between two coexisting periodic attractors in a driven monostable system had been reported earlier [18].

Fig. 6.5 shows the distributions $P(W_p)$ for different values of T. For lesser values of T, two distinct peaks are seen in the plot for $P(W_p)$, which reflects the existence of the two dynamical energy states. At an intermediate temperature where there is a minimum in W_p, $P(W_p)$ shows a single peak. Around the temperature where there is a peak in W_p ($T = 0.2$), the distribution becomes broad and also the asymmetry in $P(W_p)$ is maximum, exhibiting a characteristic (bimodal) hump as in the case of the double well system ([25] and chapter 5). The distributions show tails towards the negative energies reflecting the presence of transient second law violating trajectory segments.

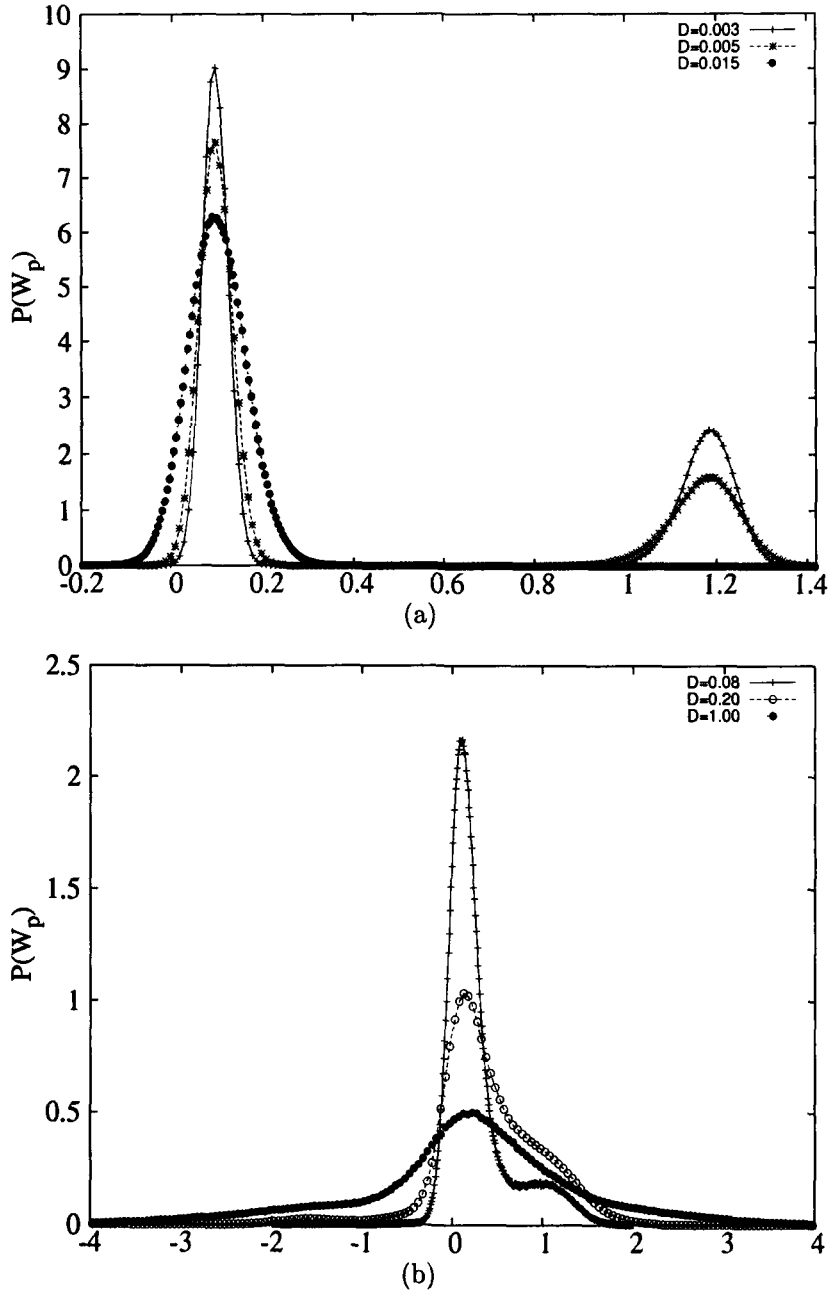

Figure 6.5: Plot of $P(W_p)$ for different values of T for the homogeneous system; $\tau_\omega = 8$, $F_0 = 0.2$, $\gamma_0 = 0.12$.

6.3.2 Inhomogeneous system

We made similar investigations as in the previous section for an inhomogeneous system using a space dependent friction coefficient $\gamma(x) = \gamma_0(1 - \lambda \sin(kx + \theta))$, as discussed earlier, with $\lambda = 0.9$.

The variation of W_p and the $(x - F)$ hysteresis loop area shows a similar variation as in the homogeneous case, exhibiting SR (Fig.6.6).

However for the inhomogeneous system, the peaking is much sharper and the peak in W_p occurs at a much lower temperature than in the homogeneous system. Also the initial dip in W_p at lower temperatures is less prominent. For inhomogeneous case also, there exists two dynamical energy states corresponding to particles which are out of phase (Fig. 6.7a and Fig. 6.7c) and in phase (Fig. 6.7b and Fig. 6.7d) with the external drive $F(t)$. The out of phase loop (Fig. 6.7c) in this case is a superposition of the the periodic forcing $F = 0.2\cos(\omega t)$ and the response $x(t) = 2.1\cos(\omega t + 0.83\pi)$ while the in-phase loop (Fig. 6.7d) is a superposition of $F = 0.2\cos(\omega t)$ and $x(t) = 0.59\cos(\omega t + 0.02\pi)$. Thus for the inhomogeneous system, $\phi_1 = 0.83\pi$ and $\phi_2 = 0.02\pi$ which are interestingly, different from those of the homogeneous system. The explanation for the nature of variation of W_p with T in the homogeneous system holds for the inhomogeneous system too.

However, because of the presence of inhomogeneity in the system, the particle has more probability to go for random excursions out of the potential wells (interwell motion) at a lower temperatures in the inhomogeneous system than for the homogeneous one (Fig6.8). This interwell hopping, assists the particle in making transistions from one dynamical state to the other. So the peaking of W_p is observed at a lower T value for the inhomogeneous system.

In Fig. 6.9, the distributions of W_p are plotted for various T in the ihomogeneous system. Comparing with the distributions in the homogeneous system, one can see that at lower temperatures, the weight towards the out of phase states in the inhomogeneous system is more than in the homogeneous system.

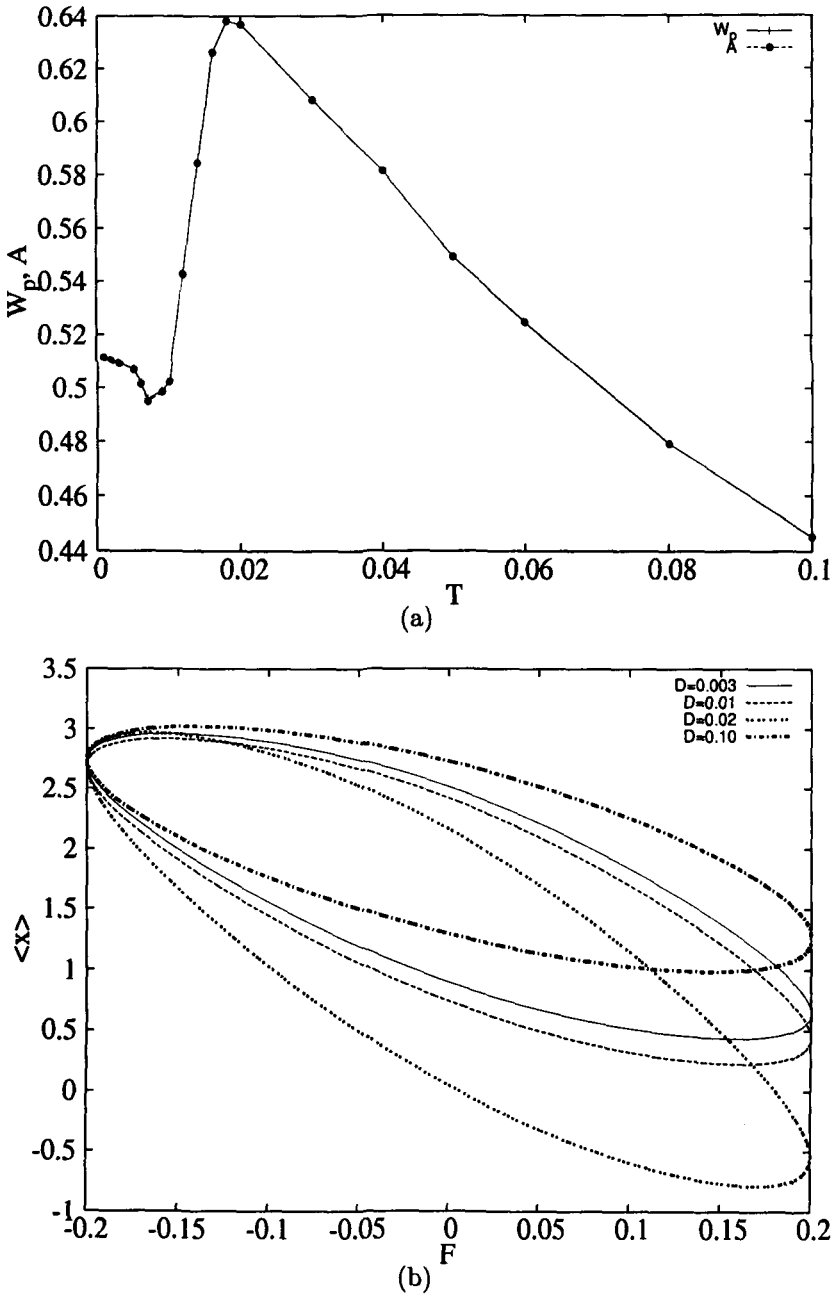

Figure 6.6: Plot of average work done per period of drive, W_p and the corresponding average $(x - F)$ hysteresis loop area A as a function of temperature T for the inhomogeneous system (a) and the corresponding ensemble averaged $(x - F)$ hysteresis loops (b);$\tau_\omega = 8$, $F_0 = 0.2$, $\gamma_0 = 0.12$.

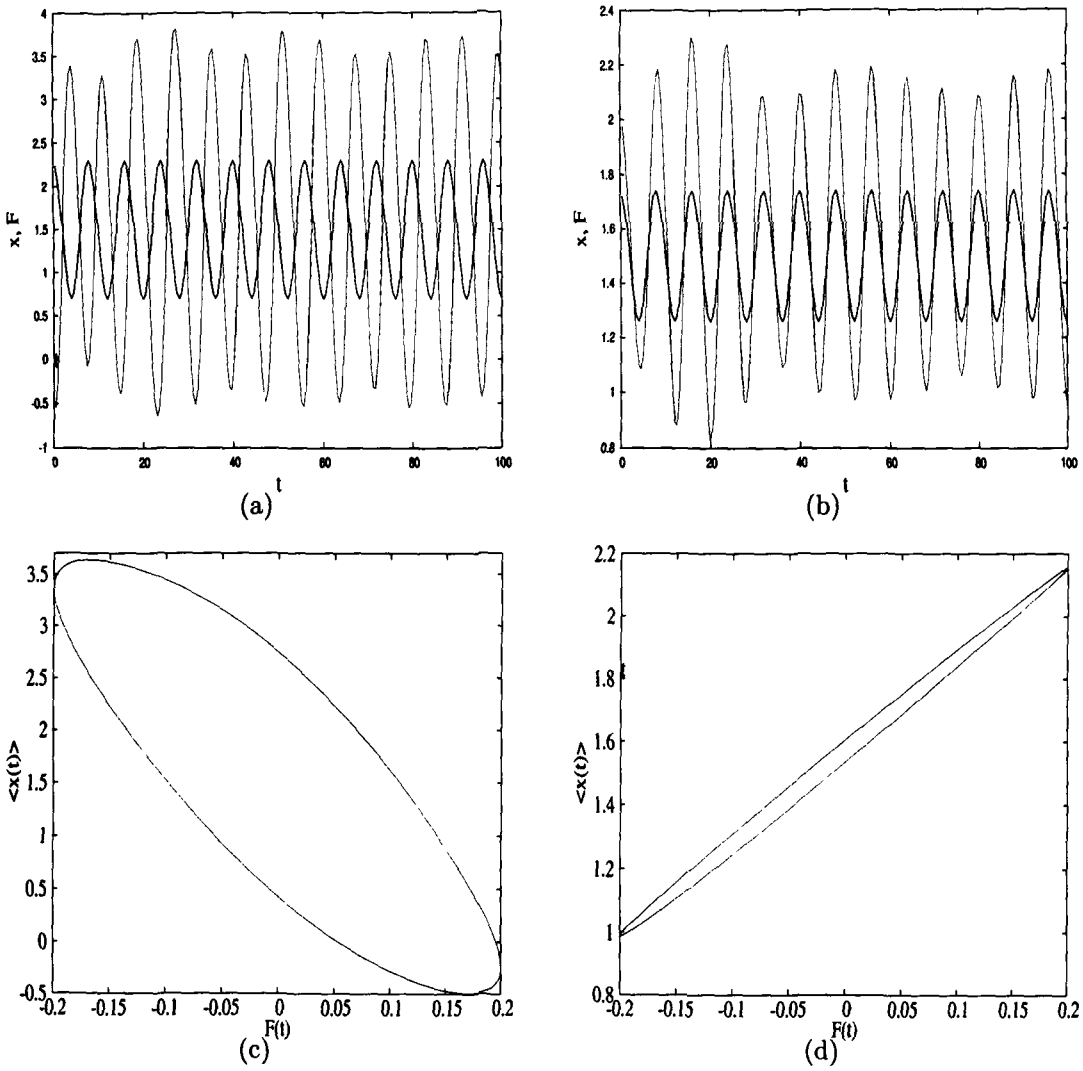

Figure 6.7: Plot of $x(t)$ and $F(t)$ for $x(0) = -0.68$ (a) and $x(0) = 2.0$(b) and the corresponding $(x - F)$ hysteresis loops (c and d); $T = 0.003$, $\lambda = 0.9$, $\tau_\omega = 8$, $F_0 = 0.2$, $\gamma_0 = 0.12$.

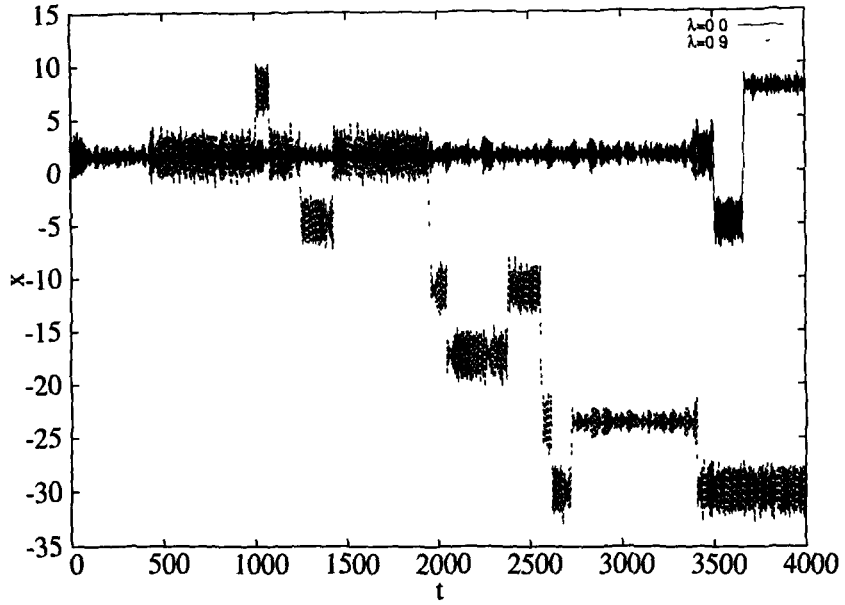

Figure 6.8: Plot of $x(t)$ for the homogeneous system ($\lambda = 0$) and the inhomogeneous system ($\lambda = 0.9$) for temperature $T = 0.08$; $x(0) = 2.0, \tau_\omega = 8$, $F_0 = 0.2$, $\gamma_0 = 0.12$.

In this case too there is sufficient weight towards negative energies which shows the existence of transient second law violating trajectory segments.

Variation of particle velocity

The presence of a space dependent friction coefficient $\gamma(x) = \gamma_0(1 - \lambda \sin(kx + \theta))$ in a periodic and symmetric potential system can generate ratchet current (please see chapter 2 and 3). We calculated the ensemble averaged velocity $\langle v \rangle$ for the inhomogeneous system in the range of T values where W_p shows a peaking. As expected, for such low temperatures, particle velocity is very low (Fig. 6.10). Also, it does not show any peaking behaviour in that range of T values.

However, we checked the particle velocity behaviour with temperature in a low frequency regime, with $\tau_\omega = 140$. It is seen that, $\langle v \rangle$ exhibited a nice peak with temperature (Fig. 6.11). The ensemble averaged velocity $\langle v \rangle$ also is found to show a peaking with the time period (analogously the frequency) of

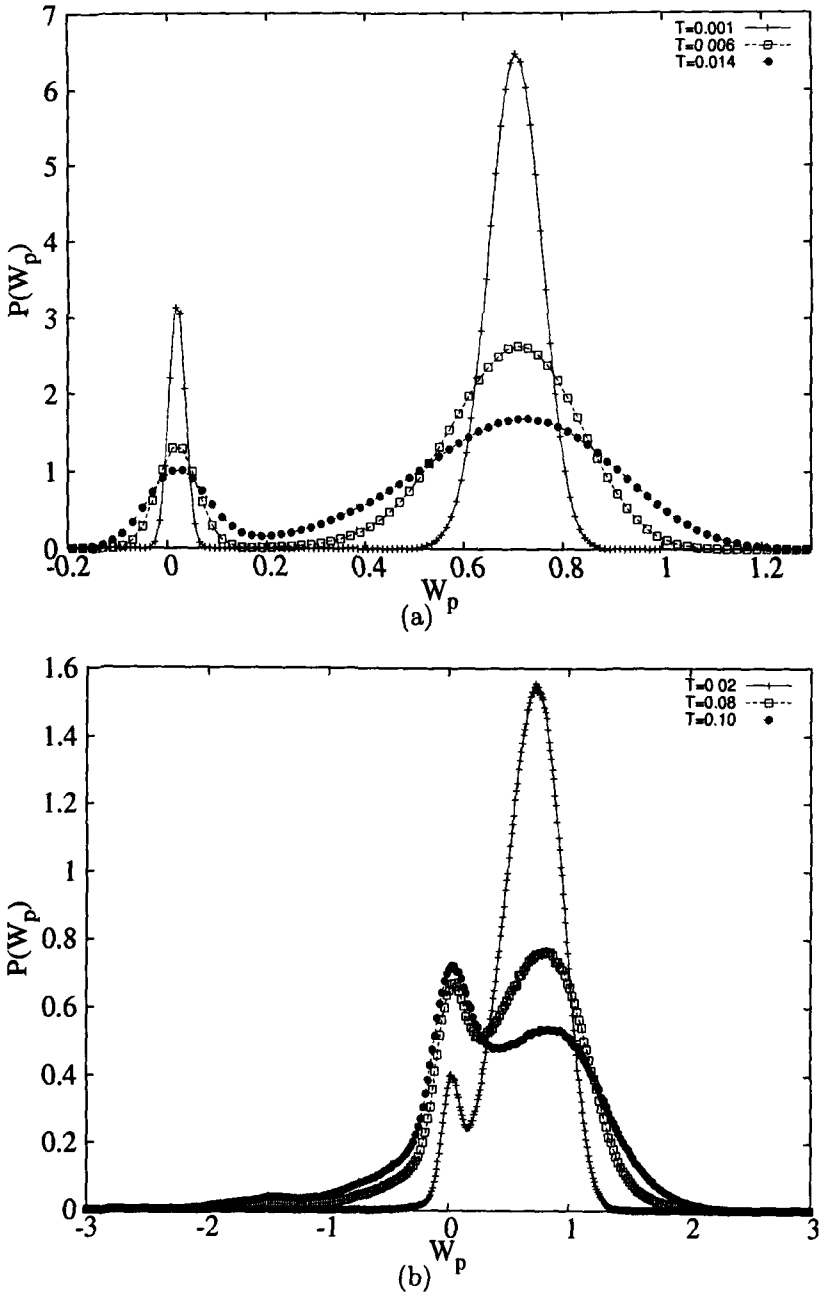

Figure 6.9: Plot of $P(W_p)$ for different values of temperature T for the inhomogeneous system; $\tau_\omega = 8$, $F_0 = 0.2$, $\gamma_0 = 0.12$.

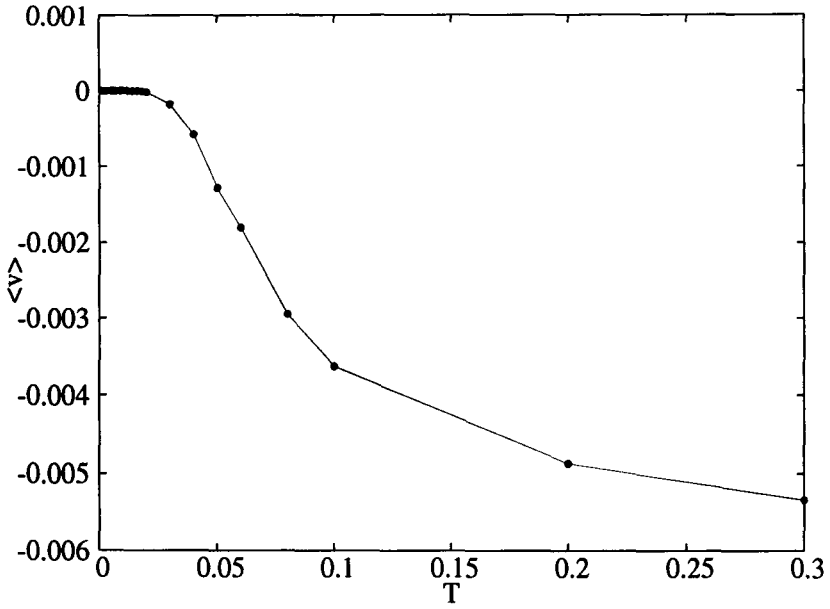

Figure 6.10: Plot of ensemble averaged velocity $\langle v \rangle$ with T, for the inhomogeneous system ($\lambda = 0.9$); $\tau_\omega = 8$, $F_0 = 0.2$, $\gamma_0 = 0.12$.

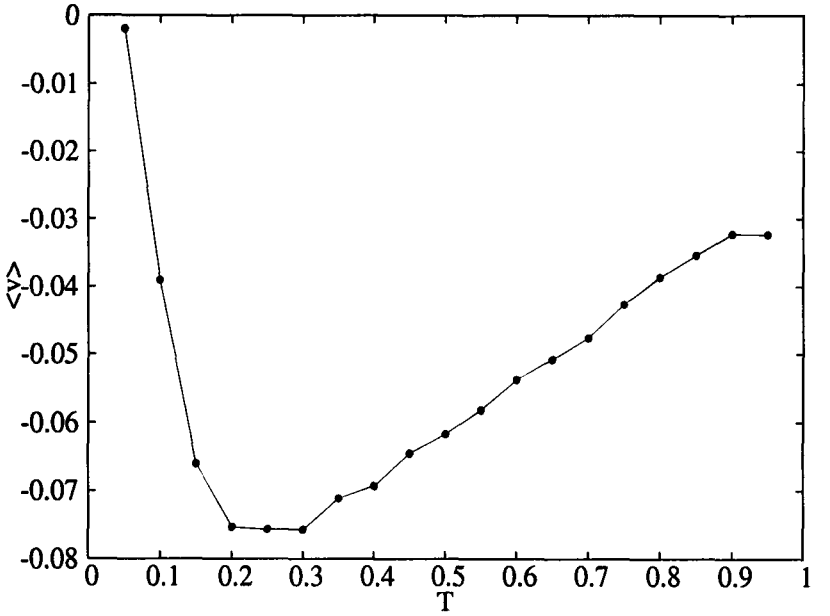

Figure 6.11: Plot of ensemble averaged velocity $\langle v \rangle$ versus T, for the inhomogeneous system ($\lambda = 0.9$); $\tau_\omega = 140$, $F_0 = 0.7$, $\gamma_0 = 0.12$.

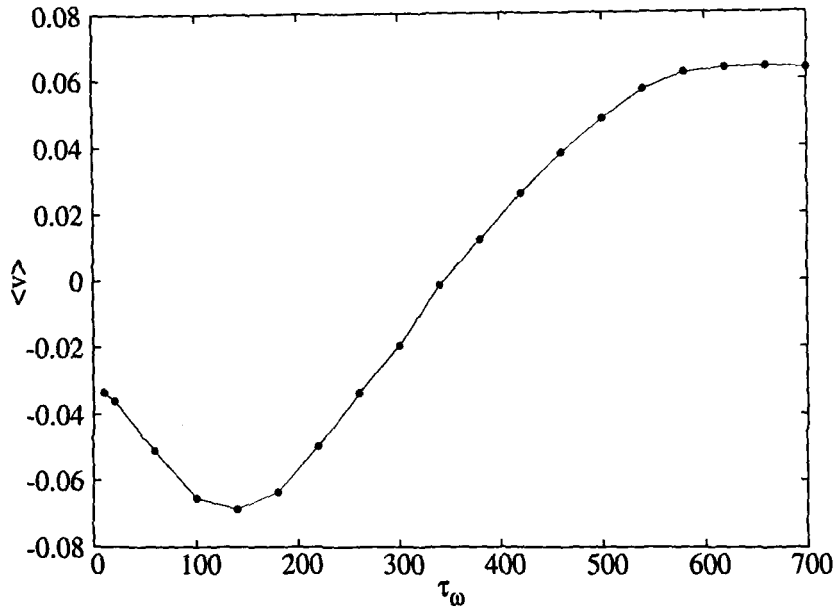

Figure 6.12: Plot of ensemble averaged velocity $\langle v \rangle$ versus τ_ω, for the inhomogeneous system ($\lambda = 0.9$); $T = 0.4$,$F_0 = 0.7$, $\gamma_0 = 0.12$.

the external periodic drive (Fig. 6.12).

In an earlier work SR was observed in the mobility of an overdamped Brownian particle in a tilted periodic potential (without the presence of an oscillating field) but in the presence of space dependent periodic friction coefficient. Though in our case of the inhomogeneous system in the underdamped regime, we are seeing a peaking of $\langle v \rangle$ with T, we don't see any synchronisation of the system's response to the external periodic drive giving rise to this peak, unlike in the case of the peaking of W_p and $(x - F)$ hysteresis loop area with temperature. Hence this peaking of $\langle v \rangle$ with T is not SR in our underdamped periodic system.

6.3.3 Variation of response amplitude and phase across SR

The existence of the two dynamical states of the particle $x(t) = x_0 \cos(\omega t + \phi_1)$ and $x(t) = x_0 \cos(\omega t + \phi_2)$ characterised by their phase difference with the external drive $F(t) = F_0 \cos(\omega t)$ in both the homogeneous and the inhomogeneous

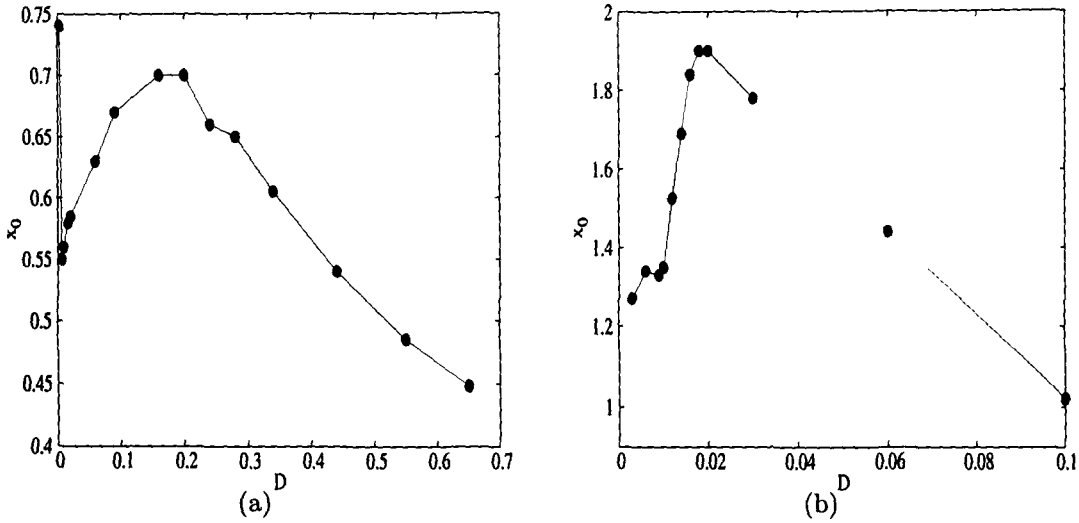

Figure 6.13: Plot of the response amplitude x_0 versus T for homogeneous (a) and inhomogeneous system (b); $\tau_\omega = 8$, $F_0 = 0.2$, $\gamma_0 = 0.12$.

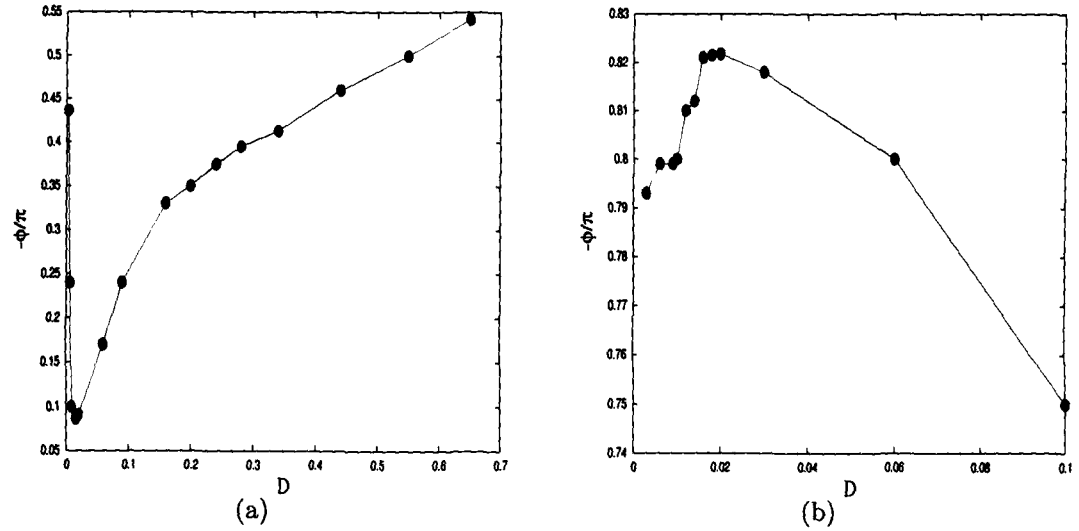

Figure 6.14: Plot of the phase diference ϕ of the response function $\langle x(t) \rangle$ as a function of the temperature T for the homogeneous (a) and the inhomogeneous (b) system; $\tau_\omega = 8$, $F_0 = 0.2$, $\gamma_0 = 0.12$.

system has been discussed in the previous sections. From the ensemble averaged hysteresis loops (Fig. 6.1b and 6.6b), we calculate the average response function $\langle x(t) \rangle$ of the system and study the nature of the variation of its phase and amplitude across the SR peak.

Fig. 6.13 shows the variation of the response amplitude x_0 as a function of the temperature for both the homogeneous and the inhomogeneous system. Fig. 6.14 shows the variation of the corresponding phases with temperature. The response amplitude, in both the homogeneous and inhomogeneous system shows a peak with temperature. This is analogous to the peaking of work done W_p and the hysteresis loop area and hence is again an indication of SR in the periodic system. A similar measure of SR in a different system has been experimentally demonstrated by Gammatoni et. al. [28].

From Fig. 6.14a, it is obvious that the temperature $T = 0.2$ at which the SR peak occurs (Fig. 6.1a) for the homogeneous system under our consideration, is an inflection point in the ϕ vs T curve. A similar behaviour was earlier reported in a bistable EPR system [28]. For the inhomogeneous system also (Fig. 6.14b), the ϕ vs T curve shows a peaking at the T value where the SR peak occurs (Fig. 6.6a) [29]. The difference in behaviour of the homogeneous and the inhomogeneous system is rooted in the fact that the presence of inhomogeneity in the system under our consideration, introduces an asymmetry in the system which changes the nature of the particle dynamics.

The SR phenomenon observed by us in periodic systems is thus consistent with the existing analysis of SR in bistable systems with respect to the response amplitude and phase.

6.4 Discussion and Conclusion

Stochastic Resonance in periodic systems has been a widely debated topic over the past few years [19, 20, 21, 22]. Also different quantifiers of SR has been used

to study this phenomena.

Using work done per period of external drive W_p (or equivalently the input energy) and the loop area A of the corresponding $(x - F)$ hysteresis loops as quantifiers, we have shown that conventional SR, (due to hopping between two stable states, synchronised with the external drive) does occur in a periodic system. This is manifested as a peak in W_p and A as a function of noise strength.

We have found that the particle in a driven periodic system (both homogeneous and inhomogeneous) has two distinct possible dynamical states which are characterised by their phase and energy. This phase difference between the external driving force $F(t)$ particle response $x(t)$ has been shown to play an important role in SR [28, 29].

The SR in a driven periodic system that we observe as a peaking in W_p and A with the temperature T, occurs in the high frequency regime where the frequency of external driving is near about the natural frequency of the system. Also, it occurs in a range of temperature where intrawell particle oscillations are dominant with occasional interwell hoppings. This resonant behaviour is similar to that of the response function of Dykman et.al. [18] and the frequency dependent mobility of Kim et.al. [19]. Kim et.al. opined that the peaking of mobility observed by them in a periodic system as a function of noise strength, in the high frequency regime is not SR but just a dynamical resonance. Their conclusion was based on the reasoning that this resonance is not due to hopping between two states synchronised with the external drive, which is a pre-requisite for conventional SR. Also they observed that the particle motion is dominated by intrawell oscillations which is as good as the particle being in a monostable system.

However from our numerical analysis, we have shown that, though in these parameter regimes particle motion is dominantly intrawell, two distinct dynamical states are available for the particle in the driven periodic system (as discussed earlier). The particle can make noise facilitated transitions between these two

states. We have found that the peaking of W_P and A with T is due to a competition between the particle occupancy in these two states. This counters the argument of Kim et.al. proving that the resonance we observe is indeed conventional SR. Also we observe that at temperatures around the SR peak, random interwell particle hopping sets in, which assists the particle transistions between the two states. Thus the SR we have observed is not solely because of intrawell particle motion as argued by Kim et.al. That interwell motion plays a role, is strengthened by our observation that, with inhomogeneity in the system, a sharper SR peak is observed at a lower temperature. This is because, with inhomogeneity, interwell hopping of the particles become more probable even at lower temperatures.

We studied the distributions of W_p across the SR peak. They are found to exhibit similar behaviour as the distribtions in the case of bistable systems [25, 26, 27], where the phenomenon of SR has been established beyond doubt.

We further analyse the response amplitude and phase difference of the response with the driving force. We find that they too show signatures of SR as had been reported earlier for bistable systems [28, 29].

The study of the work distributions and also that of the response amplitude and phase, further supports the occurrence of SR in periodic potentials.

Bibliography

[1] S. Saikia, A. M. Jayannavar and M. C. Mahato, Unpublished.

[2] R. Benzi, A. Sutera, and A. Vulpiani J. Phys. A 14, L453 (1981).

[3] L. Gammaitoni, P. Hänggi, P. Jung and F. Marchesoni, Rev. Mod. Phys. 70, 223 (1998).

[4] T. Wellens, V. Shatokhin and A. Buchleitner, Rep. Prog. Phys. 67, 45 (2004).

[5] S. Fauve and F. Heslot, Phys. Lett. A 97, 5 (1983).

[6] R. N. Mantegna and B. Spagnolo, Phys. Rev. E 49, R1792 (1994).

[7] K. Murali, S. Sinha, W.L. Ditto and A. R. Bulsara, Phys. Rev. Lett. 102, 104101 (2009).

[8] B. McNamara, K. Wiesenfeld and R. Roy, Phys. Rev. Lett. 60, 2626 (1988).

[9] R. L. Badzey and P. Mohanty, Nature 437, 995 (2005).

[10] J. K. Douglass, L. Wilkens, E. Pantazelou and F. Moss, Nature 365, 337 (1993).

[11] J. J. Collins, T.T. Imhoff and P. Grigg, J. Neurophysiology 76, 642 (1996).

[12] B. J. Gluckman, T. I. Netoff, E. J. Neel, W. L. Ditto, M. L. Spano and S. J. Schiff, Phys. Rev. Lett. 77, 4098 (1996).

[13] E. Simonotto, M. Riani, C. Seife, M. Roberts, J. Twitty and F. Moss, Phys. Rev. Lett. 78, 1186 (1997).

[14] K. Wiesenfeld and F. Moss, Nature 373, 33 (1995).

[15] P. K. Ghosh, B. C. Bag and D. S. Ray, Phys. Rev. E 75, 032101 (2007).

[16] B. McNamara and K. Wiesenfeld, Phys. Rev. A 39, 4854 (1989).

[17] N. G. Stocks, P. V. E. McClintock and S. M. Soskin, Europhys. Lett. 21, 395 (1993); N. G. Stocks, N. D. Stein and P. V. E. McClintock, J. Phys. A: Math. Gen. 26, L385 (1993).

[18] M. I. Dykman, D. G. Luchinsky, R. Mannella, P. V. E. McClintock, N. D. Stein and N. G. Stocks J. Stat. Phys. 70, 479 (1993).

[19] Y. W. Kim and W. Sung, Phys. Rev. E 57, R6237 (1998).

[20] G. Hu. Phys. Lett. A 174, 247 (1993).

[21] M. Gitterman, I. B. Khalfin and B. Ya. Shapiro, Phys. Lett. A 184, 339 (1994); J. M. Cassado et. al. Phys. Lett. A 297, 365 (1994); F. Marchesoni, Phys. Lett. A 231, 61 (1994).

[22] D. Dan, M. C.Mahato and A. M. Jayannavar, Phys. Lett. A 258, 217 (1999), *ibid* Phys. Rev. E. 60, 6421 (1999).

[23] I. Kh. Kaufman, D. G. Luchinsky, P. V. E. McClintock, S. M. Soskin and N. D. Stein, Phys. Lett. A 220, 219 (1996).

[24] E. Heinsalu, M. Patriarca and F. Marchesoni, Eur. Phys. J. B 69, 19 (2009).

[25] S. Saikia, R. Roy and A.M. Jayannavar, Phys. Lett. A 369, 367 (2007).

[26] M. Sahoo, S. Saikia, M.C. Mahato and A.M. Jayannavar, Physica A 387, 6284 (2008).

[27] P. Jop, A. Petrosyan and S. Ciliberto, EPL 81, 50005 (2008).

[28] L. Gammaitoni, F. Marchesoni, M. Martinelli, L. Pardi, and S. Santucci, Phys. Lett. A 158, 449 (1991).

[29] M. I. Dykman, R. Mannella, P. V. E. McClintock and N. G. Stocks, Phys. Rev. Lett. 68, 2985 (1992); L. Gammaitoni, and F. Marchesoni, Phys. Rev. Lett. 70, 873 (1993); M. I. Dykman, R. Mannella, P.V.E. McClintock and N.G. Stocks, Phys. Rev. Lett. 70, 874 (1993).

[30] R. Mannella, in Stochastic Processes in Physics, Chemistry, and Biology, Lecture Notes in Physics, vol. 557, 353, edited by J. A. Freund and T. Pöschel (Springer-Verlag, Berlin, 2000).

[31] T. Iwai, Physica A 300, 350 (2001); T. Iwai, J. Phys. Soc. Jpn. 70, 353 (2001).

[32] D. Dan and A. M. Jayannavar, Physica A 345, 404 (2005).

[33] K. Sekimoto, J. Phys. Soc. Jpn. 66, 6335 (1997).

Chapter 7

Summary and Conclusion

The counterintuitive and constructive role played by noise in many physical and biological systems in the microscopic regime, is an active field of research. Many noise assisted non-equilibrium phenomena like ratchet effect, stochastic resonance, noise enhanced stability of states etc. have been discovered in systems, where the presence of an optimal amount of noise concurs constructively with the system parameters to give rise to these phenomena. In most of these phenomena, noise activated barrier crossing play a central role.

Ratchet effect is one such phenomenon in which Brownian particles moving in a periodic potential system, driven far away from equilibrium, show a net directed transport in the presence of a optimal amount of noise, even in the absence of any obvious external bias. Such particle motion in periodic potentials has relevance in various physical and biological systems. For example in Josephson junctions, motion of an ad-atom on a crystal surface, superionic conductors, motion of motor proteins like kinesin and dyenin along microtubules for intracellular transport etc. Various models of ratchet has been used to study the phenomenon of ratchet effect. Inhomogeneous ratchet is one such model where the particle experiences a space dependent diffusion coefficient either due to a space dependent temperature or a friction coefficient.

One of the primary emphasis of this thesis, was to study the underdamped

particle motion in a driven symmetric and periodic potential system with a space dependent friction coefficient in the deterministic regime as well as in the presence of noise. The friction coefficient is similarly periodic as the potential, but has a phase difference with it.

From our studies in the deterministic regime, we show that even with a perfectly symmetric potential, we get all the qualitative behaviour of deterministic ratchets like particle current, chaotic dynamics etc. that had been obtained with asymmetric potentials in most of the earlier works, just by having a space dependent friction. The role of by the various parameters of the system like external drive frequency and degree of asymmetry in shaping the nature of the particle dynamics was investigated. We found that at lower values of asymmetry, there is a need of averaging over initial phase of the external drive to obtain pysically relevant particle currents. At low amplitude and low frequency driving, noise plays a crucial role in generating particle current.

With the addition of noise into the system, using a square-wave drive, we obtained appreciable and steady ensemble averaged particle current in our inhomogeneous ratchet system, even with a symmetric potential. We studied the effect of the various parameters of the system like the frequency of drive and the phase difference between the potential and the friction coeficient on the nature and magnitude of the particle current. We characterised the ratchet performance by calculating the efficiency, diffusion coefficient and the Péclet number. We found that for efficient performance of these ratchets, an optimal choice of the various parameters is of utmost necessity. We studied another important penomenon of underdamped particle transport in tilted periodic systems, in which the particles undergo dispersionless motion in intermediate time regimes even in the presence of fluctuations. Using square-wave drive, we showed that the cumulative duration of the coherent motion of the particles can be increased manifold over that of a constant tilt case, which was investigated earlier. Also we show the possibility of tuning the system to make the particles move coherently

when required.

Another focus area of this thesis was on the phenomenon of Stochastic resonance (SR)- a phenomenon in which a system shows an enhanced periodic response to an external periodic forcing in the presence of noise. We show that a particle in a driven double well system exhibits SR by using input energy per period of external drive as a quantifier which shows a peaking with the strength of noise in the system. The system is found to exibit hysteretic behaviour. We calculated the hysteresis loop areas and they are found to show exact matching with the input energy or the work done. This implies that all the energy supplied to the system is dissipated as heat (whose measure is given by the hysteresis loop area). Using the same quantifier of SR, we also study the role played by the confining strength of the bistable potential on the phenomenon of SR. Using input energy as a quantifier too, we show that for SR to occur, the confining strength of the bistable potential should be greater than a threshold value. This was earlier shown using the amplitude of particle motion as a quantifier. We also study the distributions of the work done per period on the system for various values of temperature across the SR peak and their change in their nature with the confining strength of the potential. Interestingly, the input energy distributions show substantial weight towards the negative energy values, which hints to the fact that in non equilibrium systems, certain transient second law violating trajectories occur.

Lastly we examine the occurrence of SR in periodic systems. We show that using the work done (or equivalently the input energy) per period of drive and the hysteresis loop area in a driven periodic system, SR can indeed be observed in periodic systems. This SR is manifested as a peaking of the work done per period as a function of noise strength, which is due to the competition between the particles to occupy the two dynamical states that they can be in. These states are characterised by the phases and energy. We also studied the SR phenomenon with respect to the response amplitude and phase and found our

results to be consistent with earlier works on bistable systems.

The thesis is thus an effort to contribute to the understanding of a few aspects of noise assisted phenomenon that are prevalent in various systems.

BIODATA

Name: Shantu Saikia

Date of birth: 20 January 1977

Permanent Address: Krishnanagar, Sarbaibandha,Jorhat, Assam-785001

Present occupation: Lecturer in the Dept. of Physics,St. Anthony's College, Shillong.

Email: shantusaikia@yahoo.com

Education

- HSLC in 1993, from Don Bosco High School, Jorhat, Assam with 76% marks.
- HSSLC in 1995, from J.B. College, Jorhat, Assam with 76.2% marks.
- BSc in 1998, from Cotton College, Guwahati, Assam with 76.4% marks.
- MSc in 2001, from Delhi University, Delhi in 2001 with 73.9% marks.
- Qualified JRF(NET)UGC conducted by UGC-CSIR in December, 2001.

Lists of publications

1. Deterministic inhomogeneous inertia ratchets, S. Saikia and M.C.Mahato, Physica A 389, 4052 (2010).

2. Dispersionless motion in periodically rocked periodic potential, S.Saikia and M. C. Mahato, Phys. Rev. E 80, 062102 (2009).

3. Dispersionless motion and ratchet effect in a square-wave driven inertial periodic system, S. Saikia and M. C. Mahato, Journal of Physics: Condensed Matter 21, 175409 (2009).

4. Work fluctuations and stochastic resonance, S. Saikia, R. Roy and A. M. Jayannavar, Phys. Lett. A 369, 367 (2007).

5. Stochastic resonance and heat fluctuations in a driven double-well system, M. Sahoo, S. Saikia, M. C. Mahato and A. M. Jayannavar, Physica A 387, 6284 (2008).

6. Motional dispersions and ratchet effect in inertial systems, W.L.Reehnbohn, S. Saikia, R. Roy and M. C. Mahato, Pramana - Journal of Physics 71, 297 (2008).

7. Stochastic resonance in periodic potentials, S. Saikia, A. M. Jayannavar and M. C. Mahato, Unpublished